

## CURRICULUM VITAE

---

### Etat civil :

Vahid ASNAFI

Né le 29 Mai 1968, à Téhéran (Iran), Marié 2 enfants

Nationalité Française

### Coordonnées personnelles :

5 rue Robert Branchard 95870 Bezons

Téléphone portable : 06.24.31.08.85

Email : [vahid.asnafi@gmail.com](mailto:vahid.asnafi@gmail.com)

### Coordonnées professionnelles :

Hôpital Necker-Enfants Malades

Laboratoire d'Onco-hématologie – Tour Pasteur 2<sup>ème</sup> étage

149 rue de sèvres

75015 Paris

Téléphone : +33 1 44 49 49 14 (direct) / 42 (secrétariat).

Fax : +33 1 44 38 17 45

Email : [vahid.asnafi@nck.aphp.fr](mailto:vahid.asnafi@nck.aphp.fr)

### Diplômes :

1986-1987 :

Baccalauréat série C –Mention AB- Académie de Créteil

1988-1993 :

Premier et Deuxième cycles des études médicales (Faculté Necker-Enfants Malades)

1994-1999 :

**DES de biologie médicale**

Maîtrise de sciences biologiques et médicales (1996)

**DEA** : Biologie des cellules sanguines (1997)

2000-2003 :

**Thèse de sciences** soutenue en Novembre 2003 : Ecole doctorale BC2T Paris 7 (Pr E. Macintyre). "*Apport de l'étude des LAL-T dans la compréhension de l'ontogénie et de l'oncogenèse T humaines*"

2003-2005 :

**Contrat d'accueil INSERM pour post-doctorant** (CIML, Marseille-génopole Dr P. Ferrier. "*Contrôles épigénétiques des processus de réarrangements V(D)J et de différenciation des cellules lymphoïdes*"

2008 : **Habilitation à diriger les recherches (HDR).**

## Fonctions hospitalières et universitaires :

1993-1999 : **Internat de Biologie Médicale.**

2000-2003 : **Assistant Hospitalo-Universitaire (AHU)** au laboratoire d'hématologie de l'hôpital Necker Enfants Malades (Pr E.Macintyre).

2004-2005 : **Poste d'accueil INSERM** pour post doctorant au laboratoire du Dr Pierre Ferrier au Centre d'Immunologie Marseille Luminy (CIML)

2005-2012 : **Maître de Conférences Universitaires - Praticien Hospitalier (MCU-PH)** au laboratoire d'hématologie de l'hôpital Necker Enfants Malades (Pr E.Macintyre).

Depuis 2012 : **Professeur des Universitaires - Praticien Hospitalier (PU-PH)** au laboratoire d'hématologie de l'hôpital Necker Enfants Malades  
Responsable médical du laboratoire onco-hématologie et **co-directeur de l'équipe 10** (lymphopoïèse normale et pathologique) de l'institut Necker-Enfant Malades (INEM) UMR INSERM 1151.

## Enseignements :

### **Premier et Second cycle des études médicales :**

Deuxième année (PCEM2) Hématopoïèse et sémiologie (3h)

Cinquième année (DCEM3) enseignement d'hématologie (26h)

### **Troisième cycle des études médicales :**

DES de biologie médicale : hématopoïèse et oncogenèse lymphoïde (4h)

### **Masters :**

M2 de Cancérologie Ecole Doctorale de Cancérologie 0418 (2h)

## Brevet et activités de valorisation :

Brevet Européen "Euroflow antibody panel" P88556EP00 (2009).

Membre des conseils scientifiques et administratif du protocole GRAALL.

Membre du conseil scientifique du protocole CAL\_01

Membre du conseil scientifique du groupe ALFA.

Membre de la société française d'hématologie.

### 2-1 Sélection Publications (20 meilleurs 2003-2015, \* **corresponding author**)

1- Site- and allele-specific polycomb dysregulation in T-cell leukaemia.

**Nat Commun. Jan 23;6:6094 (2015).**

Navarro JM, Touzart A, Pradel LC, Loosveld M, Koubi M, Fenouil R, Le Noir S, Maqbool MA, Morgado E, Gregoire C, Jaeger S, Mamessier E, Pignon C, Hacein-Bey-Abina S, Malissen B, Gut M, Gut IG, Dombret H, Macintyre EA, Howe SJ, Gaspar HB, Thrasher AJ, Ifrah N, Payet-Bornet D, Duprez E, Andrau JC, **Asnafi V\***, Nadel B\*.

2- RUNX1 dependent RAG1 deposition instigates Human TCR $\delta$  locus rearrangement.

**Journal of Experimental Medicine J Exp Med. 2014 Aug 25;211(9):1821-32.**

Cieslak A, Le Noir S, Trinquand A, Lhermitte L, Franchini DM, Villarese P, Gon S, Bond J, Vanhile L, Reimann C, Verhoeyen E, Six E, Spicuglia S, André-Schmutz I, Langerak A, Nadel B, Macintyre E, Payet-Bornet D\*, **Asnafi V\***.

3-SET-NUP214 is a recurrent  $\gamma\delta$  lineage-specific fusion transcript associated with corticosteroid/chemotherapy resistance in adult T-ALL.

**Blood 2014 Mar 20;123(12):1860-3.**

Ben Abdelali R, Roggy A, Leguay T, Cieslak A, Renneville A, Touzart A, Banos A, Randriamalala E, Caillot D, Lioure B, Devidas A, Mossafa H, Preudhomme C, Ifrah N, Dombret H, Macintyre E, **Asnafi V\***.

4-Towards a NOTCH1/FBXW7/RAS/PTEN-based oncogenetic risk classification of adult T-ALL: a GRAALL Study.

**Journal of clinical oncology 2013 Dec 1;31(34):4333-42.**

Trinquand A, Tanguy-Schmidt A, Ben Abdelali R, Lambert J, Beldjord J, Lengliné E, De Gunzburg N, Payet-Bornet D, Lhermitte L, Mossafa H, Lhéritier V, Bond J, Huguet F, Buzyn A, Leguay T, Cahn JY, Thomas X, Chalandon Y, Delannoy A, Bonmati C, Maury S, Nadel B, Macintyre E, Ifrah N, Dombret H, **Asnafi V\***.

5-Receptor kinase profiles identify a rationale for multi-target kinase inhibition in immature T-ALL.

**Leukemia 2013 27:305-14.**

Lhermitte L, Abdelali RB, Villarese P, Bedajoui N, Guillemot V, Trinquand A, Libura M, Bedin AS, Petit A, Dombret H, Leverger G, Ifrah N, Hermine O, Macintyre E. **Asnafi V\***.

6-TLX homeodomain oncogenes mediate T-cell maturation arrest in T-ALL via interaction with ETS1 and suppression of TCR $\alpha$  gene expression.

**Cancer Cell. 2012 Apr 17;21(4):563-76.**

Dadi S, Le Noir S, Payet-Bornet D, Lhermitte L, Zacarias-Cabeza J, Bergeron J, Villarèse P, Vachez E, Dik WA, Millien C, Radford I, Verhoeyen E, Cosset FL, Petit A, Ifrah N, Dombret H, Hermine O, Spicuglia S, Langerak AW, Macintyre EA, Nadel B, Ferrier P\*, **Asnafi V\***.

7-Extensive molecular mapping of TCR $\alpha$  and TCR $\delta$  involved chromosomal translocations reveals distinct mechanisms of oncogenes activation in T-ALL.

**Blood 2012 120:3298-309.**

Le Noir S, Ben Abdelali R, Lelorch M, Bergeron J, Payer-Bornet D, Villarese P, Petit A, Callens C, Lhermitte L, Baranger L, Radford-Weiss I, Gregoire MJ, Dombret H, Ifrah N, Spicuglia S, Romana S, Soulier J, Nadel B, Macintyre E, **Asnafi V**\*.

8-Pediatric-inspired intensified therapy of adult T-ALL reveals the favorable outcome of NOTCH1/FBXW7 mutations, but not of low ERG/BAALC expression: a GRAALL study.

**Blood. 2011 Nov 10;118(19):5099-107**

**Asnafi V**, Ben Abdelali R, , Leguay T, Boissel N, Buzyn A, Chevallier P, Thomas X, Lepretre S, Huguet F, Vey N, Escoffre-Barbe M, Tavernier E, Reman O, Fegueux N, Turlure P, Rousselot P, Cahn JY, Lheritier V, Chalandon Y, Béné MC, Macintyre EA, Dombret H, Ifrah N; Group for Research on Adult Acute Lymphoblastic Leukemia.

9-Posttranscriptional deregulation of MYC via PTEN constitutes a major alternative pathway of MYC activation in T-cell acute lymphoblastic leukemia.

**Blood. 2011 Jun 16;117(24):6650-9.**

Bonnet M, Loosveld M, Montpellier B, Navarro JM, Quilichini B, Picard C, Di Cristofaro J, Bagnis C, Fossat C, Hernandez L, Mamessier E, Roulland S, Morgado E, Formisano-Tréziny C, Dik WA, Langerak AW, Prebet T, Vey N, Michel G, Gabert J, Soulier J, Macintyre EA, **Asnafi V**, Payet-Bornet D, Nadel B.

10-Regulatory T-cell depletion in angioimmunoblastic T-cell lymphoma.

**Am J Pathol. 2010 Aug; 177(2):570-4.**

Bruneau J, Canioni D, Renand A, Marafioti T, Paterson JC, Martin-Garcia N, Gaulard P, Delfau MH, Hermine O, Macintyre EA, Brousse N, **Asnafi V**\*.

11-JAK1 mutations are not frequent events in adult T-ALL: a GRAALL study.

**Br J Haematol. 2010 Jan;148(1):178-9.**

**Asnafi V**, Le Noir S, Lhermitte L, Gardin C, Legrand F, Vallantin X, Malfuson JV, Ifrah N, Dombret H, Macintyre EA.

12-TGF-beta induces degradation of TAL1/SCL by the ubiquitin-proteasome pathway through AKT-mediated phosphorylation.

**Blood. 2009 Jun 25;113(26):6695-8.**

Terme JM, Lhermitte L, **Asnafi V**, Jalinot P.

13-T-cell receptor genotyping and HOXA/TLX1 expression define three T lymphoblastic lymphoma subsets which might affect clinical outcome.

**Clin Cancer Res. 2008 Feb 1;14(3):692-700**

Baleyrier F, Decouvelaere AV, Bergeron J, Gaulard P, Canioni D, Bertrand Y, Lepretre S, Petit B, Dombret H, Beldjord K, Molina T, **Asnafi V**, Macintyre EA.

14-Prognostic and oncogenic relevance of TLX1/HOX11 expression level in T-ALLs.

**Blood 2007 Oct 1;110(7):2324-30.**

Bergeron J, Clappier E, Radford I, Buzyn A, Millien C, Soler G, Ballerini P, Thomas X, Soulier J, Dombret H, Macintyre EA, **Asnafi V**\*.

15-Prediction of relapse by day 100 BCR-ABL quantification after allogeneic stem cell transplantation for chronic myeloid leukemia.

**Leukemia. 2006 May;20(5):793-9.**

**Asnafi V**, Rubio MT, Delabesse E, Villar E, Davi F, Damaj G, Hirsch I, Dhédin N, Vernant JP, Varet B, Buzyn A, Macintyre E.

16-Impact of immunophenotype and genotype on outcome in adult T-Cell Acute Lymphoblastic Leukemia: a LALA-94 study.

**Blood 2005 Apr 15;105(8):3072-8.**

**Asnafi V**, Buzyn A, Thomas X, Huguet F, Vey N, Boiron JM, Reman O, Cayuela JM, Lheritier V, Vernant JP, Fiere D, Macintyre E, Dombret H.

17-Age-related differences in phenotype and oncogenic pathways in T-ALLs reflect thymic atrophy.

**Blood 2004 Dec 15;104(13):4173-80.**

**Asnafi V**, Beldjord K, Libura M, Villarese P, Millien C, Ballerini P, Kuhlein E, Lafage-Pochitaloff M, Delabesse E, Bernard O, Macintyre E.

18-CALM-AF10 is a common fusion transcript in T-ALL and is specific to the TCR  $\gamma\delta$  lineage.

**Blood 2003 Aug 1;102(3):1000-1006.**

**Asnafi V**, Radford-Weiss I, Dastugue N, Bayle C, Leboeuf D, Charrin C, Garand R, Lafage-Pochitaloff M, Delabesse E, Buzyn A, Troussard X, Macintyre E.

19-Analysis of TCR, pT $\alpha$  and RAG-1 in T Acute Lymphoblastic Leukemias improves understanding of early human T lymphoid lineage commitment.

**Blood 2003 Apr 1;101(7):2693-703.**

**Asnafi V**, Beldjord K, Boulanger E, Comba B, Le Tutour P, Estienne MH, Davi F, Landman-Parker J, Quartier P, Buzyn A, Delabesse E, Valensi F, Macintyre E.

20-Flt3 and MLL internal tandem duplications and topoisomerase II breakages reflect a common category of genotoxic stress.

**Blood. 2003 Sep 15;102(6):2198-204.**

Libura M, **Asnafi V**, Tu A, Delabesse E, Tigaud I, Cymbalista F, Bennaceur-Griscelli A, Villarese P, Solbu G, Hagemeijer A, Beldjord K, Hermine O, Macintyre E.

2 – 2 Bibliométrie globale (75 publications référencées pubmed) :

Journal	1 <sup>e</sup> ou dernier corresponding auteur	2 <sup>ème</sup> /3 <sup>ème</sup> auteur	Autres positions
Cancer Cell (IF: 26.9)	1		
Blood (IF: 9.1)	10	4	7
J Exp Med. (IF: 14.8)	1		1
Leukemia (IF: 10.2)	3		8
Nature communications (IF: 10.7)	1		
JCO (IF: 18.2)	1		1
Blood lettre	1		2
Leukemia lettre	2	1	1
Br J hematol (IF :4.9)			2
Br J hematol Lettre	1		
Haematologica (IF: 6.5)			2
Am J Pathol (IF:5.2)	1		
Gut (IF:10.6)		1	
Gastroenterology (IF:12)			2
Cancer letters (IF: 4.3)			2
J Clin Invest (IF:14.1)			1
J Allergy Clin Immunol (IF:9.3)			1
Cell Death Differ (IF: 9.1)			1
Stem Cells (IF:7.9)			1
Clin Cancer Res (IF:7.3)			1
Eur. J Haematol (IF:4.9)			1
Eur J Immunol (IF:4.9)			1
Plos one (IF: 3.7)			1

Pr. Vahid Asnafi, MD/PhD.

Responsable médical du laboratoire onco-hématologie et **co-responsable de l'équipe 10** (lymphopoïèse normale et pathologique) de l'institut Necker-Enfants Malades (INEM) UMR INSERM 1151 :

[http://www.institut-necker-enfants-malades.fr/index.php?menu=team\\_view&faculty\\_id=10](http://www.institut-necker-enfants-malades.fr/index.php?menu=team_view&faculty_id=10)

### **Leucémies aiguës lymphoblastiques T (LAL-T) : Modèle d'étude des mécanismes moléculaires de l'oncogenèse et de l'ontogénie T immature**

Les leucémies aiguës lymphoblastiques T (LAL-T) sont des proliférations malignes hétérogènes affectant les précurseurs lymphoïdes T, bloqués à un stade donné de leur développement. Cette maladie relativement rare mais grave atteint environ 200 nouveaux patients par an en France et malgré les progrès récents de leur prise en charge thérapeutique ces hémopathies conservent un pronostic médiocre notamment en cas de rechute. Il existe donc une réelle nécessité de développement de nouvelles approches de traitement et une optimisation de la stratification thérapeutique. Une des pistes les plus prometteuses consisterait à provoquer le déblocage de l'arrêt de maturation aboutissant à la mort des cellules tumorales.

L'oncogenèse des LAL-T est multigénique, avec coexistence de plusieurs dérégulations oncogéniques chez le même patient. Parmi les sous-groupes identifiés, figure l'important groupe « TLX » marqué par la surexpression des oncogènes TLX1 ou TLX3. Ces gènes se caractérisent par la présence d'une séquence d'ADN particulière, appelée « homeobox », qui code pour un domaine protéique conservé ou homéodomaine, de structure hélice-tour-hélice. Cette structure a la propriété de se lier à l'ADN et d'interagir avec des protéines partenaires. Les LAL-T TLX+ se caractérisent par un stade spécifique de blocage de la différenciation thymique dénommé « cortical précoce ». Nous avons récemment démontré (*Cancer Cell* 21:653, 2012) que le blocage de maturation au stade 'thymique cortical' observé dans les LAL-T TLX1/3+ est lié à une interaction de ces dernières avec un autre facteur de transcription, ETS-1. Notamment, ce partenariat permet le recrutement TLX au niveau de l'Enhancer transcriptionnel du gène TCR $\alpha$  induisant alors une configuration épigénétique suppressive de la région adjacente TCR-J $\alpha$ , un défaut de réarrangement V $\alpha$ -J $\alpha$  et ainsi l'arrêt de la progression développementale. La suppression de l'expression TLX1/3 dans des lignées de cellules leucémiques, mais également l'expression ectopique d'un récepteur TCR $\alpha\beta$  dans ces cellules, conduit à une reprise du développement cellulaire doublée d'une apoptose massive. Ces phénomènes, pour ouvrir des perspectives de thérapie 'différenciante' appliquée à ces hémopathies lymphoïdes, restent cependant à caractériser au plan de leur(s) mécanisme(s) moléculaire(s).

L'autre mécanisme oncogénique fréquent des LAL-T correspond à l'activation constitutive de la voie Notch1 notamment par des mutations gain de fonction affectant les gènes impliqués dans cette voie proliférative. Nous avons récemment montré que les mutations des gènes impliqués dans l'activation de la voie Notch1 sont associées à un impact pronostique favorable chez l'adulte. Ces travaux importants ont permis deux publications dans la revue *Blood* (2009 et 2011) et nous ont amené à réaliser un génotypage extensif et identifier ainsi les mutations des gènes N/K-RAS et PTEN comme des éléments complémentaires de celles de la voie Notch1 pour la stratification thérapeutique de ces leucémies (JCO 2013). De manière importante ces travaux ont trouvé une application directe dans la prise en charge concrète des LAL-T de l'adulte et le futur protocole GRAALL-2014 fera appel à une stratification de l'intensification thérapeutique issue de notre travail définissant un « classier » moléculaire incluant les 4 gènes NOTCH1, FBXW7, PTEN et RAS. Ainsi les patients définis comme de haut risque (ie NOTCH et FBXW7 non mutés ou RAS ou PTEN mutés) recevront dans le cadre du protocole un traitement spécifique par une nouvelle drogue de première intention, la Nelarabine.

Les leucémies aiguës lymphoblastiques T (LAL-T) sont des cancers de l'enfant et l'adulte jeune (la grande majorité des cas ont entre 5 et 30 ans au moment du diagnostic) avec un pronostic globalement défavorable. Ces tumeurs correspondent à une prolifération cancéreuse de cellules immatures, incapables de poursuivre leur maturation normale, du tissu sanguin. Malgré les progrès récents de leur prise en charge thérapeutique, leur évolution reste malheureusement sombre avec une survie à 5 ans estimée seulement à environ 70% et des taux de survie limités notamment en cas de rechute après chimiothérapie.

La compréhension des mécanismes moléculaires de cancérisation de ces leucémies a connu ces dernières années de grandes avancées. L'espoir est donc une meilleure identification des patients résistants à la chimiothérapie ou à fort risque de rechute sur la base des anomalies identifiées au diagnostic. Ceci permettra de meilleurs choix de schémas thérapeutiques susceptibles d'améliorer la survie chez ces patients.

Nos travaux récents ont permis d'une part d'identifier certaines anomalies génétiques impliquées directement le blocage de maturation des cellules leucémiques (Dadi *et al.* Cancer Cell, 2012) et d'autres part des mutations d'autres gènes (notamment associés à la famille « NOTCH1 ») avec un impact pronostique important (Trinquand *et al* Journal of Clinical Oncology, 2013). Enfin, très récemment, nous avons pu décrire un nouveau mécanisme de cancérisation impliquant une famille importante de régulateurs (dite « épigénétique ») dont le potentiel thérapeutique semble intéressant (Navarro *et al* Nature Communications, 2015).

Notre espoir est qu'une meilleure identification du rôle joué par la dérégulation des gènes impliqués dans le processus de cancérisation ouvrira des possibilités thérapeutiques nouvelles et ciblées. Dans cette logique, nos travaux ont trouvé une application directe dans la prise en charge concrète des LAL-T de l'adulte et le protocole national GRAALL-2014 fera appel à une stratification du traitement basée sur notre travail définissant un « classifieur » moléculaire incluant les 4 gènes NOTCH1, FBXW7, PTEN et RAS. Ainsi les patients, définis comme de haut risque, recevront dans le cadre du protocole un traitement spécifique par une nouvelle drogue (Nélarabine) en première intention avec l'espoir d'obtenir un meilleur taux de guérison.



## ARTICLE

Received 25 Nov 2014 | Accepted 11 Dec 2014 | Published 23 Jan 2015

DOI: 10.1038/ncomms7094

OPEN

# Site- and allele-specific polycomb dysregulation in T-cell leukaemia

Jean-Marc Navarro<sup>1,2,3,\*</sup>, Aurore Touzart<sup>4,\*</sup>, Lydie C. Pradel<sup>1,2,3,\*†</sup>, Marie Loosveld<sup>1,2,3,5,\*</sup>, Myriam Koubi<sup>6</sup>, Romain Fenouil<sup>1,2,3</sup>, Sandrine Le Noir<sup>4</sup>, Muhammad Ahmad Maqbool<sup>1,2,3,†</sup>, Ester Morgado<sup>1,2,3</sup>, Claude Gregoire<sup>1,2,3</sup>, Sebastien Jaeger<sup>1,2,3</sup>, Emilie Mamessier<sup>1,2,3</sup>, Charles Pignon<sup>1,2,3</sup>, Salima Hacein-Bey-Abina<sup>7</sup>, Bernard Malissen<sup>1,2,3</sup>, Marta Gut<sup>8</sup>, Ivo G. Gut<sup>8</sup>, Hervé Dombret<sup>9</sup>, Elizabeth A. Macintyre<sup>4</sup>, Steven J. Howe<sup>10</sup>, H. Bobby Gaspar<sup>10</sup>, Adrian J. Thrasher<sup>10</sup>, Norbert Ifrah<sup>11</sup>, Dominique Payet-Bornet<sup>1,2,3,§</sup>, Estelle Duprez<sup>5,§</sup>, Jean-Christophe Andrau<sup>1,2,3,§,†</sup>, Vahid Asnafi<sup>4,§</sup> & Bertrand Nadel<sup>1,2,3,§</sup>

T-cell acute lymphoblastic leukaemias (T-ALL) are aggressive malignant proliferations characterized by high relapse rates and great genetic heterogeneity. *TAL1* is amongst the most frequently deregulated oncogenes. Yet, over half of the *TAL1*<sup>+</sup> cases lack *TAL1* lesions, suggesting unrecognized (epi)genetic deregulation mechanisms. Here we show that *TAL1* is normally silenced in the T-cell lineage, and that the polycomb H3K27me3-repressive mark is focally diminished in *TAL1*<sup>+</sup> T-ALLs. Sequencing reveals that >20% of monoallelic *TAL1*<sup>+</sup> patients without previously known alterations display microinsertions or RAG1/2-mediated episomal reintegration in a single site 5' to *TAL1*. Using 'allelic-ChIP' and CrispR assays, we demonstrate that such insertions induce a selective switch from H3K27me3 to H3K27ac at the inserted but not the germline allele. We also show that, despite a considerable mechanistic diversity, the mode of oncogenic *TAL1* activation, rather than expression levels, impact on clinical outcome. Altogether, these studies establish site-specific epigenetic desilencing as a mechanism of oncogenic activation.

<sup>1</sup>Center of Immunology of Marseille Luminy, Aix-Marseille University, Parc Scientifique de Luminy case 906, 13288 Marseille, France. <sup>2</sup>INSERM U1104, 13288 Marseille, France. <sup>3</sup>CNRS UMR7280, 13288 Marseille, France. <sup>4</sup>Université Paris Descartes Sorbonne Cité, Institut Necker-Enfants Malades (INEM), Institut national de recherche médicale (INSERM) U1151, and Laboratory of Onco-Hematology, Assistance Publique-Hôpitaux de Paris (AP-HP), Hôpital Necker Enfants-Malades, 75015 Paris, France. <sup>5</sup>Laboratoire Hématologie, APHM, 13385 Marseille, France. <sup>6</sup>CRCM Inserm U1068, Institut Paoli Calmettes, Aix-Marseille Université, UM 105; CNRS UMR7258, 13009 Marseille, France. <sup>7</sup>Biotherapy Department, INSERM U429, Hôpital Necker-Enfants-Malades, 149 rue de Sèvres, 75015 Paris, France. <sup>8</sup>Centro Nacional de Análisis Genómico, 08028 Barcelona, Spain. <sup>9</sup>Department of Hematology, AP-HP Hôpital St-Louis, 75010 Paris, France. <sup>10</sup>Centre for Immunodeficiency, Molecular and Cellular Immunology, Institute of Child Health, University College London, London WC1N 1EH, UK. <sup>11</sup>Services des Maladies du sang CHU and UMR Inserm U 892/CNRS 6299, 49933 Angers, France. \* These authors contributed equally to this work. § Joint supervisors. † Present addresses: TAGC/INSERM U 1090, 13288 Marseille, France (L.C.P.); Institut de Génétique Moléculaire de Montpellier (IGMM), CNRS UMR5535, 1919 Route de Mende, 34293 Montpellier, France (M.A.M. and J.-C.A.). Correspondence and requests for materials should be addressed to V.A. (email: vahid.asnafi@nck.aphp.fr) or to B.N. (email: nadel@ciml.univ-mrs.fr).

**T**-cell acute lymphoblastic leukaemia's (T-ALL) are malignant proliferations of immature T-cell progenitors. Although the outcome of T-ALLs has greatly improved in the last 10 years, ~30% of cases relapse within the first 2 years following diagnosis; moreover, acute- and long-term toxicities remain important issues for long-term survivors, underlining the critical need of better risk stratification of T-ALL patients, and the implementation of more adapted and/or targeted therapies. A major obstacle in the molecular dissection of these processes is that T-ALLs constitute a particularly heterogeneous group of disease, characterized by complex combinations of multigenic aberrations and oncogenic cooperation. The deregulation of over 40 distinct oncogenes and tumour suppressors has been reported, occurring through a large diversity of genomic aberrations and epigenetic mechanisms<sup>1,2</sup>. Chromosomal alterations mostly consist of translocations, inversions and microdeletions occurring at the vicinity of proto-oncogenes and leading to their deregulated expression.

*TAL1* is one of the most frequently deregulated T-ALL oncogenes<sup>3</sup>. In physiological conditions, *TAL1* is a regulatory gene that promotes access to alternative fates in haematopoiesis. Expressed in early haematopoiesis, its expression is maintained in the erythroid lineage, but normally irreversibly epigenetically silenced in the T-cell lineage<sup>4–6</sup> (Supplementary Fig. 1). Events leading to the illegitimate maintenance or re-expression of *TAL1* in the T-cell lineage are thought to constitute strong drivers of T-ALL leukemogenesis. Known *TAL1* dysregulation mechanisms consist of t(1;14)(p34;q11) translocations (1–2%) and SIL-TAL deletions (15–20%). Yet, over half of the *TAL1*<sup>+</sup> cases lack *TAL1* lesions, suggesting unrecognized (epi)genetic deregulation pathways<sup>7</sup>. In such 'unresolved cases', *TAL1* expression can be monoallelic, compatible with a direct alteration in *cis* within or around the *TAL1* gene, or biallelic, likely reflecting indirect deregulation in *trans*<sup>7</sup>.

Here we sought to gain insights into the (epi)genetic deregulation pathways of *TAL1* 'unresolved' cases. Using ChIP-seq and an 'allelic-ChIP' assay allowing to discriminate histone marks separately on each allele, we describe a new process of oncogene activation, whereby the targeted eviction of polycomb H3K27me3 marks and concurrent recruitment of H3K27ac marks by micro- and macroinsertional events, trigger the monoallelic desilencing of *TAL1*. Incidentally, we also report the first example of oncogenic activation by recombination-activating gene (RAG)-mediated episomal reinsertion, a very elusive event predicted *in vitro* as a source of oncogenic activation over 10 years ago<sup>8,9</sup>, but never identified before in human cancer. We further show that this new epigenetic desilencing process is a recurrent event in T-ALL, accounting for >20% of unexplained cases of monoallelic *TAL1* oncogene activation. Finally, we demonstrate that the mode of activation (monoallelic in *cis* versus biallelic in *trans*) rather than the level of *TAL1* expression impacts on prognosis, with *cis*-mediated alterations significantly associated with adverse clinical outcome.

## Results

### Microinsertions induce epigenetic switch and *TAL1* expression.

To investigate the (epi)genetic deregulation pathways of *TAL1* 'unresolved' cases, we first took advantage of chromatin immunoprecipitation coupled to a high-throughput sequencing (ChIP-seq) data set describing active/inactive epigenetic marks in mouse developing thymocytes<sup>6,10</sup>. A large region starting upstream of the *TAL1* promoter and encompassing part of the gene body was enriched in H3K27me3, suggesting the involvement of polycomb complex (PcG) repressive activity in *TAL1* silencing (Fig. 1a). This profile was also observed in human

*TAL1*<sup>−</sup> peripheral CD4<sup>+</sup> T cells<sup>11</sup>, but absent in *TAL1*-expressing cells<sup>12</sup> (CD34<sup>+</sup> haematopoietic stem cells, HSC; erythroblasts; Fig. 1b), in line with the gradual deposition of H3K27me3-repressive marks during T-cell lineage specification<sup>6</sup> (Supplementary Fig. 1). To determine if deregulation of this silencing occurs in *TAL1*<sup>+</sup> T-ALLs, ChIP-seq was also performed in the Jurkat (*TAL1*<sup>+</sup>) T-ALL cell-line and a control *TAL1*<sup>−</sup> sample (DA). Sample DA displayed the expected H3K27me3 deposition, coherent with *TAL1* silencing in T cells (Fig. 1b). Surprisingly, however, low levels of H3K27me3 marks were also observed in Jurkat. Since, in contrast to normal *TAL1*-expressing cells, Jurkat displays monoallelic expression of *TAL1* (Supplementary Fig. 2), we reasoned that a monoallelic chromosomal alteration might have prevented H3K27me3 deposition on one of the two alleles, resulting in an averaged, intermediate ChIP-seq signal. To test this possibility, we sequenced ~10 kb upstream of *TAL1* (Supplementary Fig. 3), covering the regulatory region enriched in H3K27me3 marks. Amid single-nucleotide polymorphisms (SNPs), we found a monoallelic alteration consisting of a 12-bp microinsertion ~7 kb upstream of the *TAL1* p1a promoter, in a region prone to DNA looping with *TAL1* promoters<sup>13</sup>. Interestingly, this insertion mapped at the border of the repressive H3K27me3 pattern (Fig. 1a,b), in line with the possibility that it disrupted normal epigenetic silencing of the *TAL1* locus. To further investigate the association of the insertion with potential allelic distortion of the repressive H3K27me3 mark, we performed an 'allelic-ChIP' that discriminates H3K27me3 marks at the inserted versus germline allele (Fig. 2a). A significant decrease of H3K27me3 signal was observed at the inserted allele compared with the germline allele ( $P < 0.005$ ). Accordingly, knockdown (by shEZH2) or inhibition (using the EZH2 inhibitor GSK126) (ref. 14) of the Polycomb H3K27me3 methyl transferase EZH2, allowed partial reversion of H3K27me3 deposition at the germline (non-inserted) allele. Considering the cooperative role of histone modifications in expression regulation, we further analysed the relevance of acetylation in presence or absence of histone deacetylase inhibitor (sodium butyrate)<sup>15</sup>. ChIP-seq showed a slight enrichment of H3K27ac with significant overall increase on sodium butyrate treatment (Fig. 2b). Similar to H3K27me3, H3K27ac marks extended to the insertion site, suggesting dual epigenetic regulation and differential allelic recruitment. Indeed, allelic quantification through tag retrieval and allelic-ChIP revealed a difference of H3K27ac between inserted and GL alleles in a pattern symmetrical to and functionally coherent with H3K27me3. Acetylation levels were histone deacetylase inhibitor dependent. Overall, this suggested that Jurkat's microinsertion contributed to site- and allele-specific switch from H3K27me3 to H3K27ac deposition, leading to the maintenance of *TAL1* expression through T-cell differentiation.

**A recurrent epigenetic mechanism of *TAL1* deregulation.** To determine if similar structural abnormalities occurred recurrently in *TAL1* patients, 134 primary T-ALL samples were analysed by high-density Affymetrix SNP array-6 analysis; an ~700-bp region surrounding the Jurkat insertion site was also sequenced in a subset of 93 samples and six cell lines; in parallel, the literature was reviewed for cases with unexplained *TAL1* activation. While no macromolecular *TAL1* alteration was identified by SNP array (0/134), sequencing revealed seven new cases of similar microinsertions (1–9 bp), all precisely located at the Jurkat insertion breakpoint (Fig. 3a). Such insertions were not present in the germline from 2/2 available patients tested (Supplementary Fig. 4). No additional mutation/indel could be found in the

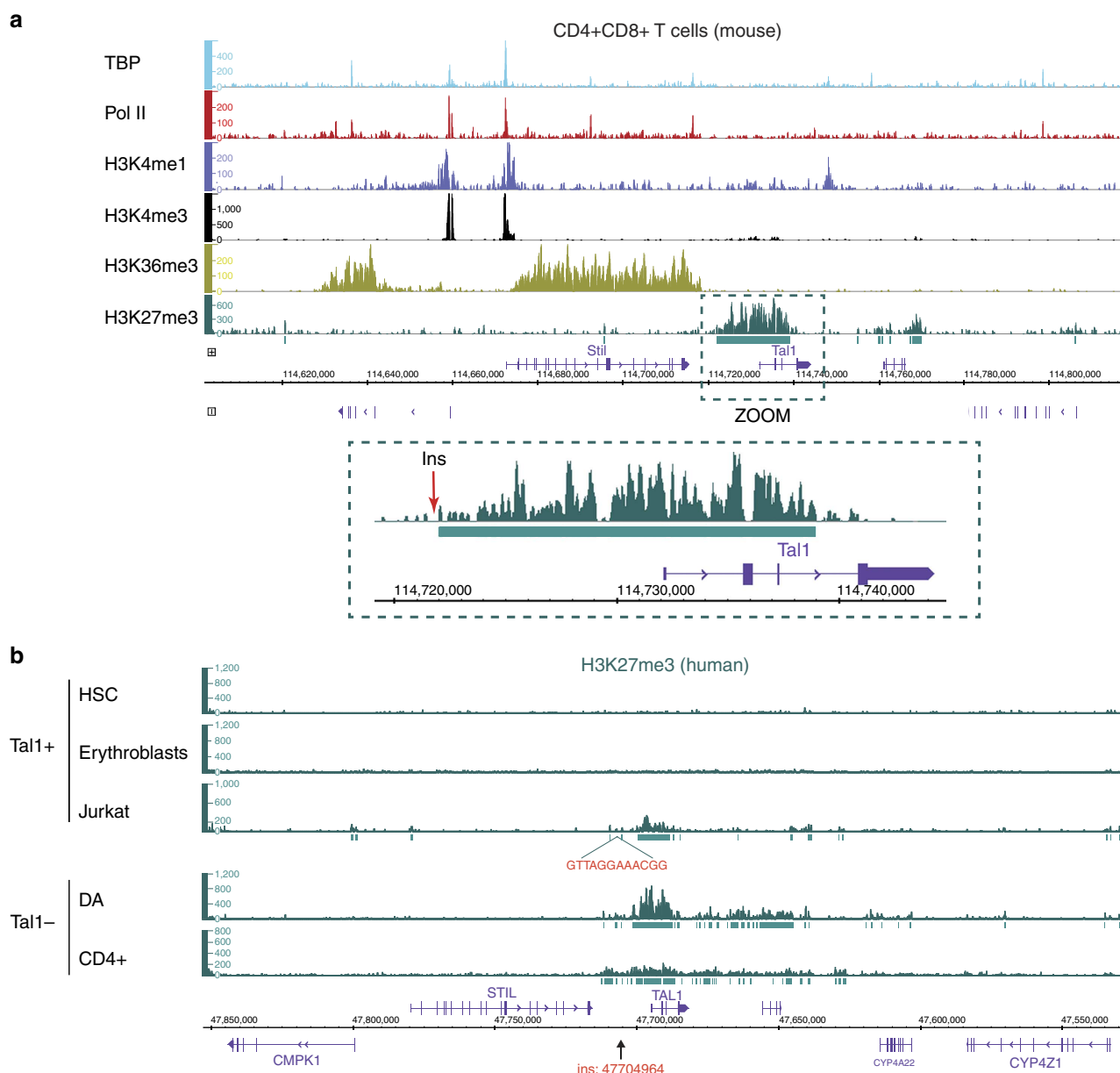


**Figure 1 | ChIP-seq analysis of the *TAL1* locus in *TAL1*-expressing and *TAL1*-repressed cells. (a)** ChIP-seq profiles of chromatin marks in normal mouse CD4<sup>+</sup>CD8<sup>+</sup> thymocytes. The *TAL1* genomic area on chromosome 4 (including the adjacent *STIL* gene, which is physiologically expressed at that developmental stage) is shown for TATA-binding protein-GTF recruited to promoters (TBP), Polymerase II (Pol II), H3K4me1 (active chromatin mark for enhancer/regulatory regions), H3K4me3 (active chromatin marks for promoters), H3K36me3 (active chromatin marks for gene bodies) and H3K27me3 (repressive chromatin mark dependent on the PcG). The *TAL1* region is zoomed, and the insertion breakpoint localization to the human orthologue region (114,722,607) is indicated by a red arrow. **(b)** ChIP-seq profiles of polycomb repressive chromatin mark H3K27me3 in normal human TAL1<sup>+</sup> (HSC; erythroblasts) and TAL1<sup>-</sup> (peripheral CD4<sup>+</sup> T cells) lineages, compared with TAL1<sup>+</sup> (Jurkat) and TAL1<sup>-</sup> (DA) T-ALL cells. The *TAL1* gene and surrounding area on chromosome 1 (including the *STIL* gene) is shown. The insertion breakpoint localization (47704964, HG19 coordinates) is indicated by an arrow. All profiles were input subtracted, except for HSC and erythroblasts for which input data were not available<sup>12</sup>. Significantly enriched areas are represented as green rectangles under the lanes (MACS2 peaks).

surrounding ~700 bp region in tumour samples. Significantly, insertions were exclusively found in TAL1<sup>+</sup> patients; moreover, among patients with informative SNPs in the *TAL1* 3' UTR allowing distinction of mono- from biallelic expression<sup>7</sup> ( $n = 60$ ), insertions were exclusively found in monoallelic cases (4/19, >20%), in agreement with a *cis*-mode of *TAL1* activation (Fig. 3b).

**Oncogenic RAG1/2-mediated episomal reintegration.** One additional candidate was recovered by data mining<sup>16</sup>. In this case

(patient #OC), TAL1<sup>high</sup> activation concurred with the insertion of a large piece of chromosome 7 disrupting the *TAL1* locus. Strikingly, breakpoint mapping by ligation-mediated PCR revealed that the insertion occurred at the very same insertion site, although this time with few nucleotide deletions on each side of the breakpoint (Fig. 3a). Detailed analysis of the junctions revealed the occurrence of RAG1/2-mediated reinsertion of an ~370-kb TCR $\beta$  episomal circle (TREC $\beta$ , excised during normal V(D)J recombination, Fig. 4 and Supplementary Fig. 5). This establishes the first example of oncogenic RAG1/2-mediated

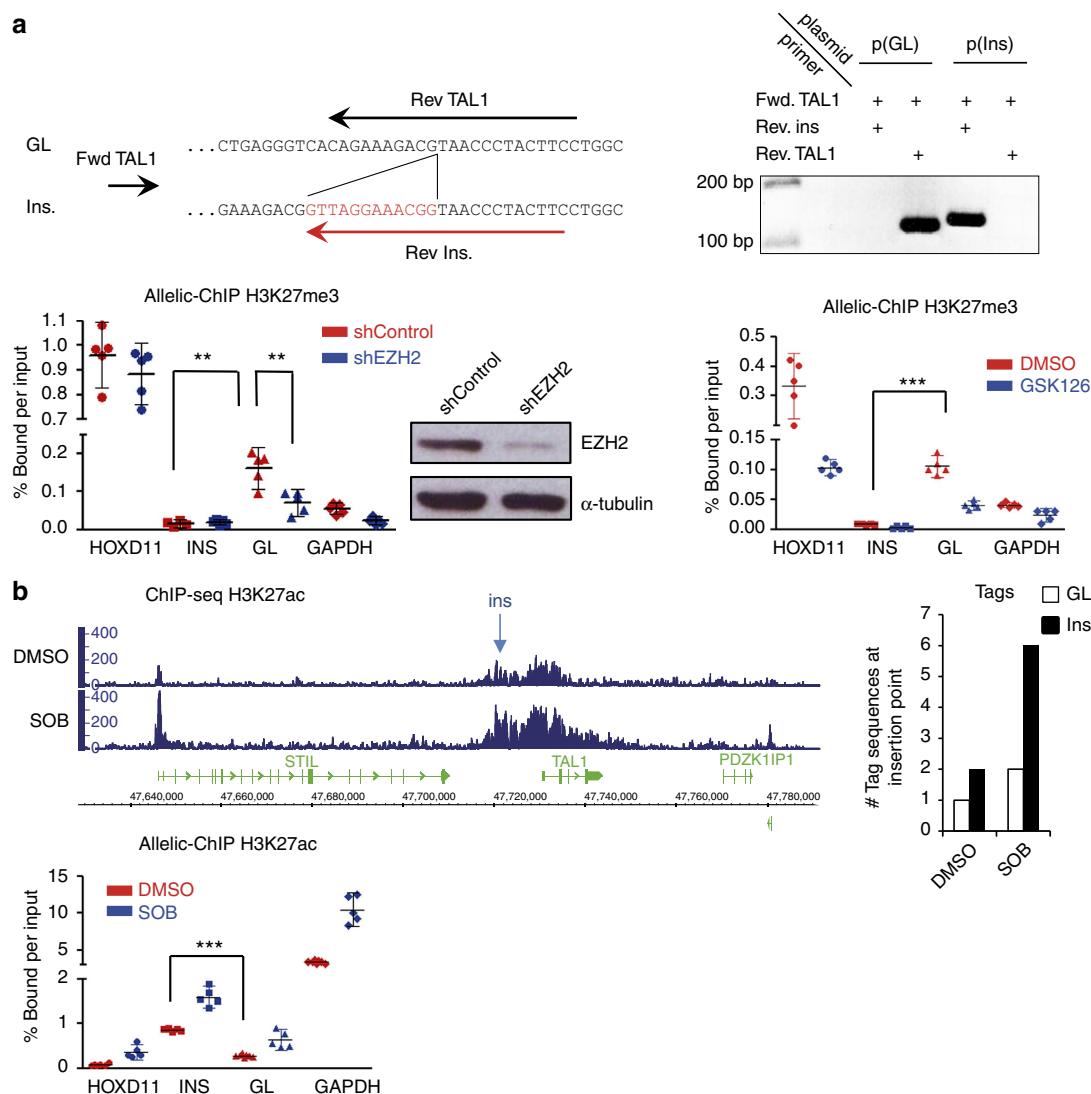


**Figure 2 | Site- and allele-specific analysis of histone methylation/acetylation marks at the insertion breakpoint in Jurkat.** (a) Allelic-ChIP assay of H3K27me3 marks. Top panel: the assay to discriminate the germline (GL) from the inserted allele (Ins.) by substituting one of the GL primers allowing detection of the GL configuration at the insertion site (Rev. TAL1), with an insertion-specific primer allowing detection of the inserted configuration (Rev. Ins, overlapping the 12-bp insertion). Primer pairs were tested on GL p(GL) or inserted p(Ins) cloned fragments (and on cell lines containing (Jurkat) or not (DND) the insertion) to exclusively amplify each configuration, and do not crossreact. Bottom middle panel: western blot of EZH2 protein content on shMock or EZH2 knockdown conditions. Allelic-ChIP assays were performed in presence of a non-silencing sh-RNA (shControl) or a sh-RNA-targeting EZH2 (shEZH2) (left panel) or after the incubation of Jurkat cells with GSK126 (0.5  $\mu$ M, 72H) or vehicle (dimethyl sulphoxide, DMSO; right panel). GAPDH and HoxD11 were used as controls for activated/repressed genes, modulated according to the polycomb-dependent H3K27me3 marks. Note that EZH2 knockdown/inhibition triggered only partial decrease of H3K27me3 marks at the PcG-repressed HoxD11 control gene, possibly due to incomplete knockdown/inhibition and/or redundancy of polycomb components in the adult lymphoid lineage<sup>42</sup>. (b) Enrichment of acetylation marks at the *TAL1* locus. H3K27Ac ChIP was performed with Jurkat cells incubated with vehicle (DMSO) or the histone deacetylase inhibitor sodium butyrate (SOB) (5 mM, 4H); DNA was then analysed by ChIP-seq (left panel) or by allelic-ChIP (bottom panel). For the ChIP-Seq, quantification of the number of tag sequences at the insertion point is shown (right panel). \*\*\* $P < 0.001$ ; \*\* $P < 0.001$ ; \* $P < 0.05$ , unpaired t-test. Errors bars represent 95% confidence interval.

reintegration, demonstrating that TRECs may indeed contribute to oncogenesis<sup>17</sup>. Owing to the large TREC $\beta$  size, we considered the possibility that, unlike other microinsertions, a promoter located in the episome could have initiated a >7-kb-long fusion transcript encompassing *TAL1* (Supplementary Fig. 6). However, reverse transcription-PCR (RT-PCR) exon walking and 5' RACE assays indicated that transcripts initiated from the *TAL1* p4 promoter, excluding this possibility.

**Epigenetic modulation and *TAL1* gene expression.** Allelic-ChIP was then performed on patients #TAMFA and #OC. Similar to

Jurkat, significant enrichment of the repressive H3K27me3 mark was consistently observed in germline compared with inserted alleles (Fig. 5a,b). The amplitude of the allelic distortion appeared higher in OC than in Jurkat and TAMFA, possibly due to the large difference in the insertion size. Of note, *TAL1* transcription levels were also higher in OC (Fig. 3b). Using CrispR DNA editing, we next mimicked site-specific insertion and disruption of the region 7 kb 5' of *TAL1* in the TAL-negative PEER cell line (Fig. 5b). In clone #2.4 recapitulating the 12-bp Jurkat insertion at its 3' end, an approximately fivefold increase of *TAL1* could be observed. While we cannot formally exclude the possibility that the selection cassette contributed to the fivefold

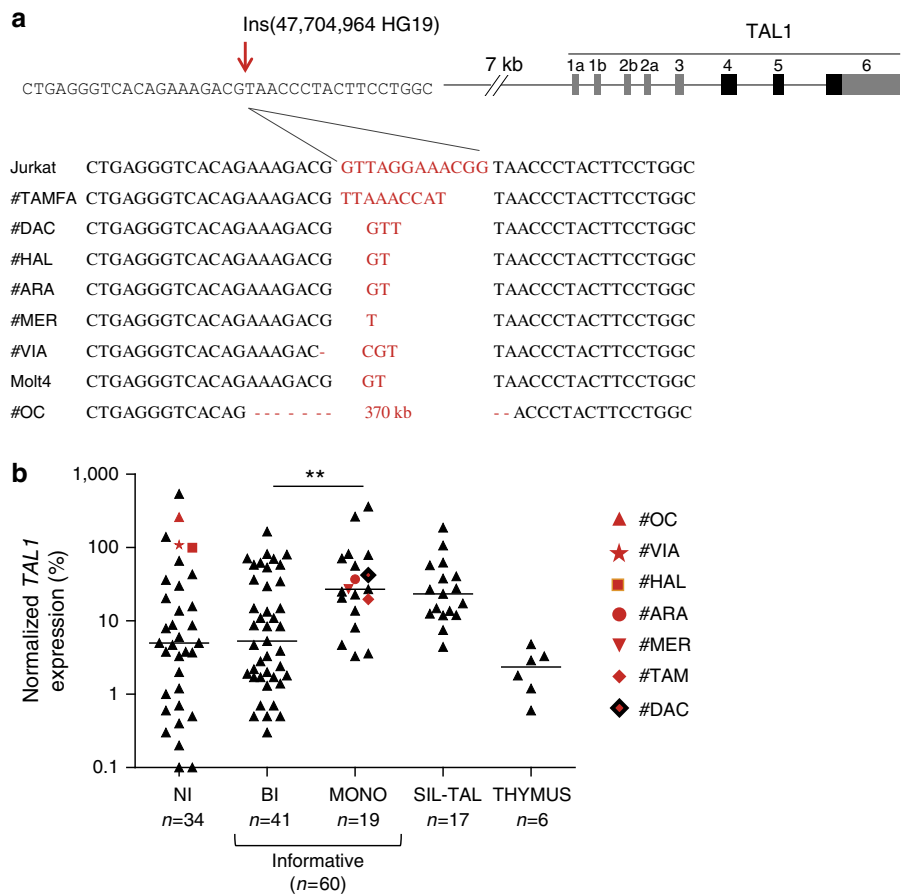


**Figure 3 | Micro- and episomal insertions are recurrently found in monoallelic *TAL1*<sup>+</sup> ‘unresolved cases’.** (a) Nucleotide sequences of episomal/microinsertions. All insertions were specifically and exclusively located at the indicated genomic position, and are pictured in red. Nucleotide deletions are indicated by a red dash. No SNPs are referenced at this position (Supplementary Fig. 8); (b) Relative *TAL1* expression in T-ALL patients ( $n = 111$ ) according to biallelic (BI), or monoallelic (MONO) expression; patients with micro/episomal insertions are indicated in red; SIL-TAL cases are shown separately; informative cases: the presence of SNPs in *TAL1* 3’UTR allows to determine if the expression is mono- or biallelic. NI: non-informative cases (absence of SNPs in *TAL1* 3’ UTR does not allow to determine if the expression is mono- or biallelic). The average physiological *TAL1* levels in thymus is shown as reference (Thymus); Horizontal bars indicate median expression levels; \*\*indicates significant difference between BI and MONO expression (Mann-Whitney *U*-test,  $P < 0.01$ ); note that a number of biallelic patients are reaching/below physiological thymus levels, and might result from the presence of residual *TAL1*-expressing erythroblasts among tumoral cells<sup>43</sup>; *TAL1* expression was analyzed by Taqman assay and is normalized to ABL (see Methods).

change in clone #2.4, a 55-fold increase was observed in clone #5.10, in which an  $\sim 1.3$  kb deletion 5’ of the insertion site mimicked locus disruption in patient #OC; furthermore, this was accompanied by an allelic switch from H3K27 methylation to acetylation. This provides direct evidence for a causal relationship between site mutagenesis, epigenetic modulation and *TAL1* gene expression.

**The mode of *TAL1* activation impacts on clinical outcome.** Patients with identified insertions were globally of adverse prognosis. We sought to determine if clinical outcome correlated with quantitative or qualitative aspects of *TAL1* deregulation. A cohort of 165 adult T-ALL treated prospectively in the GRAALL (Group for Research in Adult Acute Lymphoblastic Leukaemia) trial was split into *TAL1* expression quartiles, and compared for disease-free (DFS) and overall survival (OS). The seven patients with identified insertions (three of whom were GRAALL treated), all belonged to the high-expression quartiles (Q3–4). However, no significant difference in survival was observed between the quartiles (Fig. 6a,b), suggesting that quantitative *TAL1* expression does not correlate with clinical outcome. We next tested whether *cis*-mediated *TAL1* alterations leading to monoallelic expression (including or not the SIL-*TAL1*<sup>+</sup> cases) affected the clinical

outcome compared with *trans*-mediated events, associated with biallelic *TAL1* expression. Clinical outcome was indeed found to be significantly improved in the biallelic group (DFS,  $P = 0.04$ ; OS,  $P = 0.03$ ; Fig. 6c–f). Although numbers are low, monoallelic cases retained an inferior OS trend in multivariate analysis (including age, leukocytosis;  $P = 0.07$ , Cox analysis). Despite genetic heterogeneity, monoallelic cases also displayed higher blasts counts at diagnosis than biallelic cases and a significantly lower frequency of deregulation of recurrent oncogenes such as *TLX1*, *CALM-AF10* and *TLX3* (Supplementary Table 1). This supports the emerging notion that the mode of alteration may shape the oncogenic landscape in a more profound manner than (and potentially override the effect of) transcriptional levels, and that this may eventually impact on the tumour’s clinical behaviour<sup>18</sup>. Deciphering the mechanisms underlying the (epi)genetic deregulation of biallelic *TAL1*<sup>+</sup> cases will be instrumental to resolving this issue<sup>19–22</sup> (Supplementary Fig. 7 and Supplementary Table 2).

**Discussion**

Establishing the detailed maps of the complex oncogenic networks involved in T-ALL has contributed to major genetic discoveries, and has been of prime importance for further



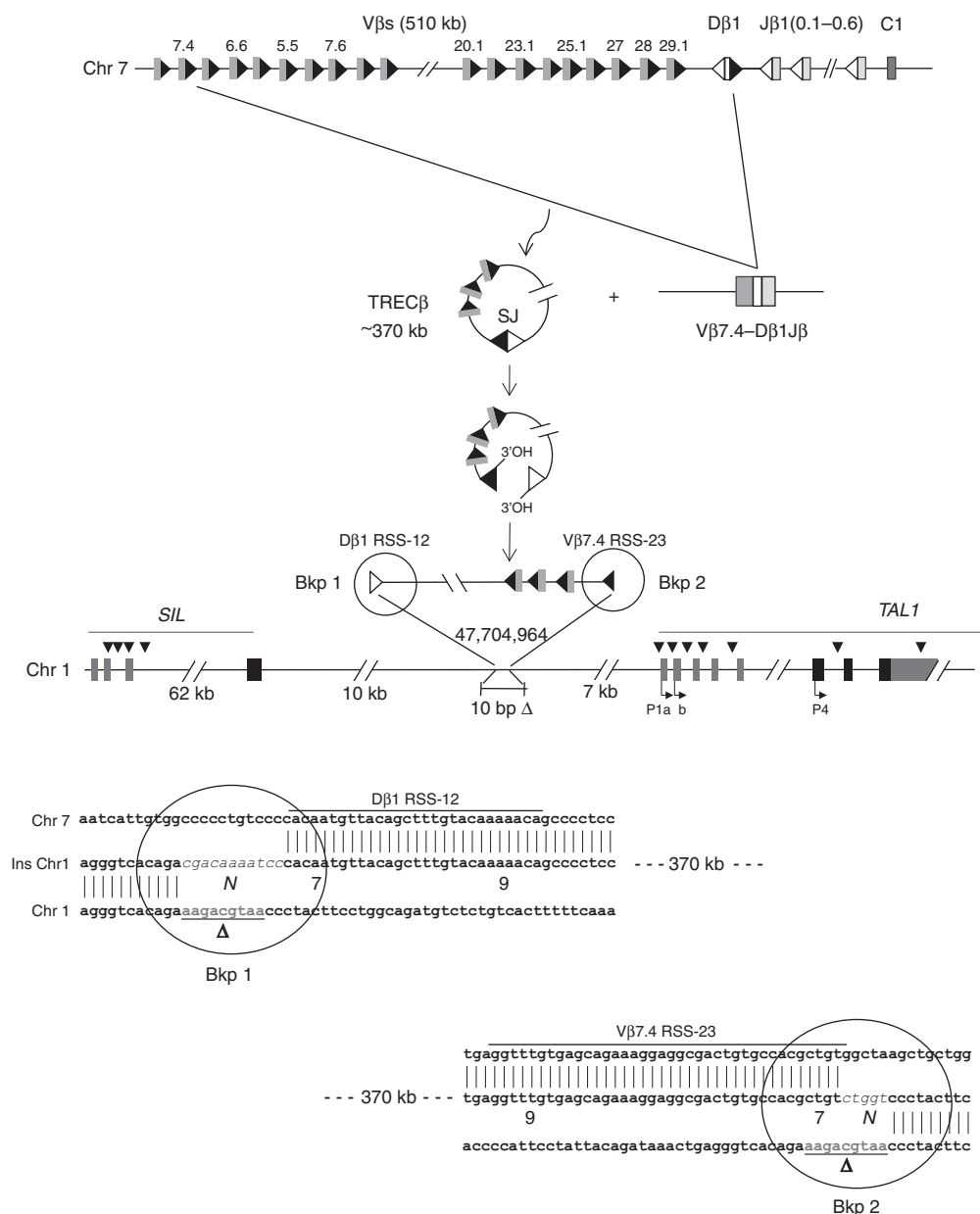


**Figure 4 | Schematic representation of the episomal reintegration in Patient OC.** The TCRβ locus is displayed (top lane, not to scale). A functional Vβ7.4-to-Dβ1 rearrangement generating an excised TRECβ, and containing a (Vβ7.4/Dβ1) signal joint (SJ) is represented. The episome might have been open at the SJ by a nick-nick process<sup>44</sup> generating 3' hydroxyl ends before integration in chromosome 1. The episome is integrated in reverse orientation 10 kb downstream of the *SIL* gene, and 7 kb upstream of the *TAL1* gene (middle lane). A 10-bp deletion (Δ, underlined) occurred at the insertion site. Localization of cryptic RSSs used by illegitimate V(D)J-mediated *SIL*-*TAL1* deletion, and by t(1;14) TCRδ/*TAL1* translocations are indicated by black arrow heads. *TAL1* promoters (P1a, P1b, P4) are indicated. The breakpoints sequences (Bkp1/2) are shown (bottom lane). N, N regions; Vβ7.4 and Dβ1 RSSs are indicated, with heptamers (7) and nonamers (9) depicted.

therapeutic improvement. Over three decades of intense efforts in genomic research have allowed unravelling the extraordinary diversity of the mechanisms by which oncogenes are deregulated in this disease<sup>1</sup>. Yet, a large number of major oncogene deregulations still remain unexplained to date. Among the diversity of mechanisms involved, V(D)J recombination-mediated alterations (translocations, microdeletions) constitute the hallmarks of T-ALLs<sup>23–26</sup>. Interestingly, despite arrays of biochemical and functional evidence that the reintegration of excised episomal circles (TRECs) by the V(D)J recombinase (RAG1/2) might constitute a potent source of genomic instability, such events remained so far unreported in human cancer patients<sup>8,9,27–30</sup>. Here we report the first case of such an

oncogenic RAG1/2-mediated episomal reintegration, demonstrating that TRECs can indeed contribute to human oncogenesis (Supplementary Fig. 1). Most intriguingly, this insertion occurred in a pediatric SCID-X1 patient who developed a leukaemia secondary to retroviral reinfection (in front of LMO2, a known TAL1-cooperating oncogene) following gene therapy<sup>16</sup>. The screening of two other SCID-X1 patients' leukaemic samples<sup>31,32</sup>, and of a large collection of T-ALLs did not reveal additional episomal insertions, and the reason for the extraordinary coincidence of two rare oncogenic integration events in this patient remains unanswered.

This and the other insertional mutagenesis T-ALL cases described here also revealed a novel oncogenic activation

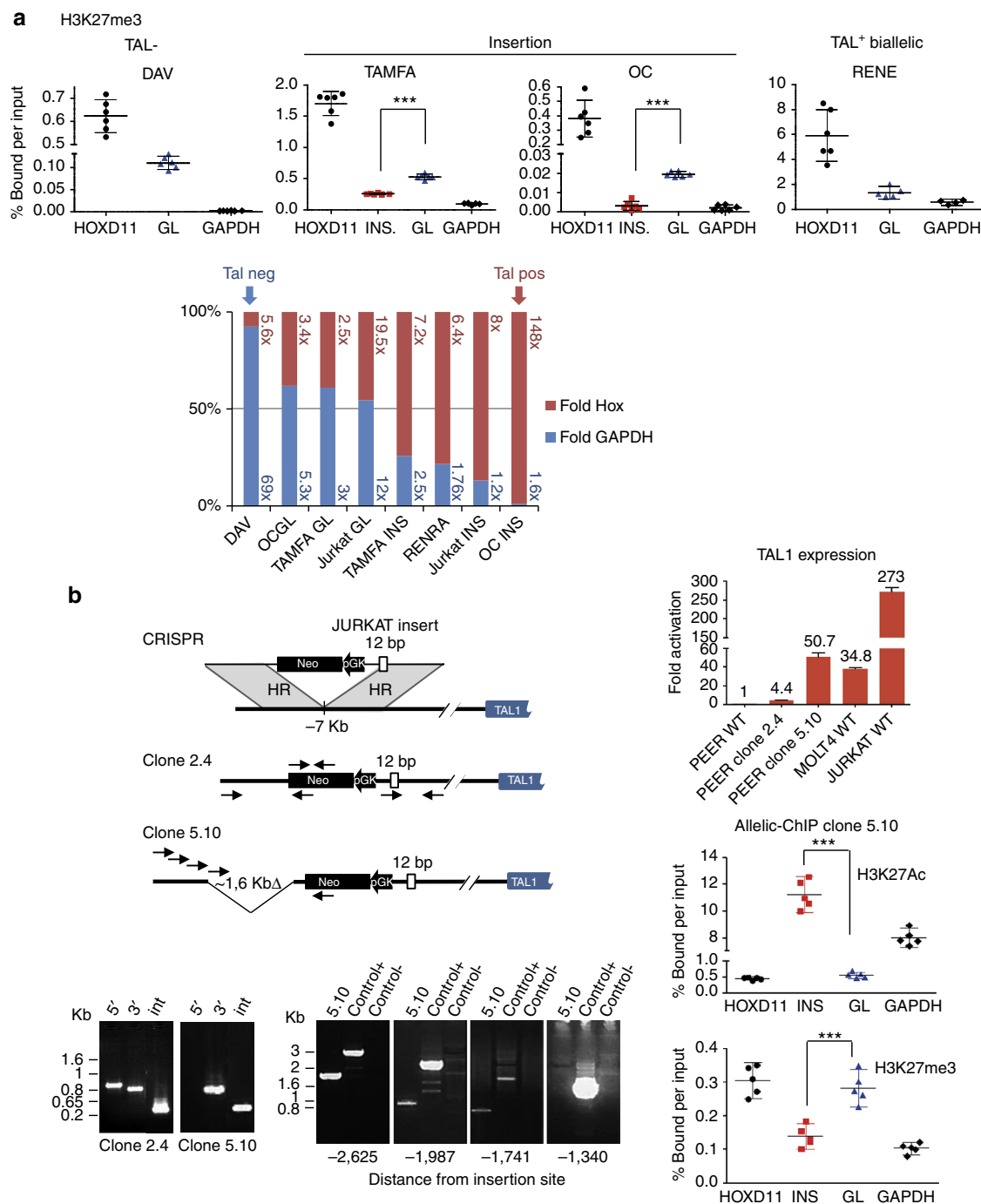


**Figure 5 | Insertional mutagenesis is associated with epigenetic modulation and *TAL1* gene expression.** (a) Allelic-ChIP analysis of H3K27me3 marks at the insertion breakpoint in primary patients. See legend to Fig. 2a. Marks at the GL alleles in one TAL1<sup>+</sup> biallelic (RENE) and in one TAL1<sup>-</sup> (DAV) patients were performed as controls. \*\*\**P* < 0.001, unpaired *t*-test; Relative-fold plots: Inserted and/or GL allele ChIP values were calculated as fold increases relative to GAPDH (numbers in blue) or HoxD11 (numbers in red), and folds plotted as relative percentages (GAPDH relative folds: blue histograms; HOXD11 relative folds: red histograms). Blue histograms over 50% indicate higher differences with the expressed than the repressed control genes and correspond to (partially) repressed *TAL1* expression; conversely, red histograms over 50% indicate higher differences with the repressed than the expressed control genes and correspond to (partially) derepressed *TAL1* expression; histograms are ordered according to decreasing *TAL1* repression. (b) Epigenetic modulation and *TAL1* gene expression by DNA editing mimicking insertional mutagenesis. Left panel: schematic representation of the CRISPR design for homologous recombination at the *TAL1* locus, and configuration of two edited clones in the PEER cell line. The locations of PCR primers (plain arrows) for detecting successful targeted events and for genome walking are indicated. Bottom left panel: successful homologous recombination was confirmed by PCR of the expected genome-donor and donor-insert boundaries. Top right panel: RQ-PCR analysis of *TAL1* expression after editing. Transcripts were normalized to ABL and reported as relative values to non-edited PEER cells. Four PCR replicates were performed on 1 (clone 2.4, due to impaired growth) or 2 (clone 5.10) independent RNA extractions. Bottom right panel: allelic-ChIP assays of H3K27me3 and H3K27ac marks in edited clone 5.10. See legend to Fig. 2a. \*\*\**P* < 0.001, unpaired *t*-test.

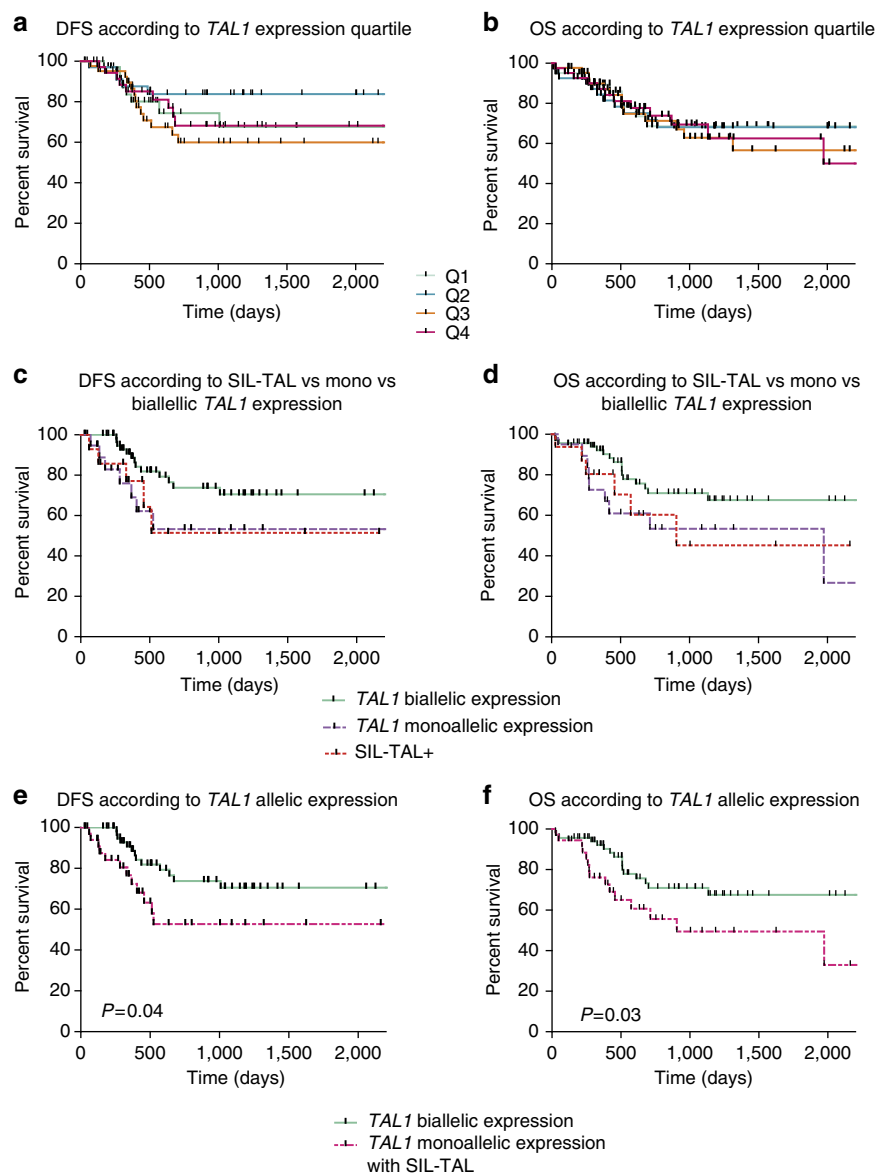


**Figure 6 | Survival analysis.** Kaplan-Meier analysis showing DFS and OS of 165 protocolar patients treated in the GRAALL trial according to: (a,b) *TAL1* expression quartiles; (c-f) the mode of *TAL1* expression. *P* values are indicated, log-rank (Mantle-Cox) test.

pathway, whereby a genetic alteration drives a site-specific and monoallelic epigenetic deregulation. We demonstrate that such insertions drove a switch from H3K27me3 to H3K27ac deposition, leading to the maintenance and/or re-expression of *TAL1* expression through T-cell differentiation. Interestingly, the difference in *TAL1* expression levels observed in mutants from the gene editing assay (Fig. 5) suggest that while small insertions might be sufficient to prevent the deposition of PcG repressive marks during T-cell lineage specification (thus permitting H3K27ac switch and maintenance of *TAL1* expression), further disruption of the region 5' of the insertion site (by deletion or insertional uncoupling) might be necessary to impose desilencing once *TAL1* extinction is established in the T-cell lineage<sup>6</sup> (Supplementary Fig. 1). These kinetics are coherent with thymocyte ontogeny in patient #OC, in which TREC $\beta$  rearrangement/reintegration (DN2-3) likely occurred after *TAL1* silencing (DN1-2). Altogether, our data are in line with current models of permanent gene extinction of transcription factors during T-lineage commitment<sup>6</sup> (Supplementary Fig. 1) and further identify locus control regions involved in deposition

and/or maintenance of *TAL1* silencing. Their genetic disruption constitute a recurrent epigenetic mechanism of *TAL1* deregulation in T-ALLs, contributing to a substantial fraction (>20%) of the *TAL1*<sup>+</sup> monoallelic 'unresolved cases', and associated with adverse prognostic. That a *cis*-deregulation regrouping as diverse mechanisms as SIL-TAL deletions, translocations or insertional desilencing impact more on prognosis than *TAL1* expression levels underlines the fundamental oncogenic difference between a deregulation targeting a single locus, and the wider effect of *trans*-acting factors. Transcription factors indeed often bind to a large number of target genes (hundreds to thousands) and their deregulation (whether gain or loss) will likely affect a complex set of cellular functions, some of which might antagonize tumour progression, or resistance to treatment. Recently, reports identifying loss-of-function mutations in polycomb-related components<sup>19–21,33</sup> have provided the framework by which global epigenetic modification might trigger the indirect (and biallelic) activation of numerous target genes, likely including a complex and conflicting set of oncogenes and tumour suppressors. In humans, PcG are recruited



to and repress specific regions in the genome through as yet undefined set(s) of DNA-binding transcription factors and long non-coding RNAs<sup>34</sup>. The insertional mutagenesis described here identifies a site- and allele-specific switch from H3K27me3 recruitment/maintenance to H3K27ac, providing new avenues to decipher the mechanisms and DNA-binding intermediates involved<sup>3</sup>. A complex interplay between transcription factors and PcG would be in line with recent findings that Notch1 activation antagonizes PRC2 silencing of Notch1 target genes in T-ALL oncogenesis<sup>19</sup>. In intricate T-ALL networks where both NOTCH and TAL1 deregulation can coexist, we find that while NOTCH patients are associated with a favourable prognosis, monoallelic, but not biallelic TAL1, expression tends to convert the clinical outcome towards more adverse prognosis in the Notch subgroup, and to further aggravate the bad prognosis of Notch1<sup>WT</sup> patients. This suggests that distinct modes of deregulation of the same epigenetic complex might coexist in a tumour cell, leading to complex and potentially conflicting clinical outcomes which ought to be clarified when considering epigenetic inhibitors for new lines of treatment<sup>15,33,35</sup>.

## Methods

**ChIP.** ChIP was performed as previously described<sup>10</sup>. In brief, the cells were chemically crosslinked by the addition of one-tenth volume of fresh 11% formaldehyde solution for 10 min at room temperature. Following the quenching of the reaction with glycine (250 mM final concentration, 5 min, room temperature), cells were rinsed twice with  $1 \times$  PBS and flash frozen in liquid nitrogen and stored at  $-80^\circ\text{C}$  before use. Cells were resuspended, lysed and sonicated to solubilize and shear crosslinked DNA. Sonication was conducted using a Bioruptor (Next Gen, Diagenode) for 15 min (30 s on, 30 s off), resulting in sheared DNA between 100 and 400 bp with the bulk at  $\sim 250$  bp. The resulting whole-cell extract was incubated overnight at  $4^\circ\text{C}$  with 100  $\mu\text{l}$  of Dynal Protein G magnetic beads that had been preincubated with the appropriate antibody. The anti-H3K27me3 antibodies used were: # 07-449, Millipore (2  $\mu\text{g}$ ), and # ab6002, Abcam (1  $\mu\text{g}$ ); the anti-H3K27ac antibodies used were: #ab4729, Abcam (2  $\mu\text{g}$ ) and # 39133, active motif (5  $\mu\text{g}$ ). Beads were washed eight times with RIPA buffer and one time with TE containing 50 mM NaCl. Bound complexes were eluted from the beads by heating at  $65^\circ\text{C}$  with occasional vortexing, and crosslinking was reversed by overnight incubation at  $65^\circ\text{C}$ . Whole-cell extract DNA (reserved from the sonication step) was also treated for crosslink reversal. Immunoprecipitated DNA and whole-cell extract DNA were then purified by treatment with RNaseA, proteinase K and multiple phenol:chloroform: isoamyl alcohol extractions.

**ChIP-seq.** Before sequencing, ChIP DNA was quantified using the picogreen method (Invitrogen, USA) and quality controlled on a 2100 Bioanalyzer (Agilent). At least 1 ng of ChIP or input DNA was used for library preparation according to the Illumina ChIP-seq protocol. After end repair and adapter ligation, fragments were size selected on a gel before preamplification and clustering. The resulting fragments were again verified on a 2100 Bioanalyzer before clustering and 25 or 36 cycle sequencing on a Genome Analyzer II (Illumina, USA) according to the manufacturer's instructions. Raw data were bowtie aligned and the tags elongated and further processed to wiggle files as described<sup>36</sup>. ChIP-seq experiments were performed on two independent biological replicates (samples for primary cells or culture for cell lines). Data presented in Fig. 1 are available under accession number GSE29362 for TBP, Pol II, H3K4me1, H3K4me3 and H3K36me3 or GSE38577 for H3K27me3(1A), and for H3K27me3 in human cells (1B) GSE12646 for HSC and erythroblast, GSE12889 for CD4+ and GSE59257 for the data newly generated (Jurkat and DA) in this article. Technical replicates were merged before alignment with Bowtie and the resulting BAM files were used as treatment in MACS2. Input data sets were used as control when available (Jurkat, DA). Enriched regions for genomic tracks of Fig. 1a,b were extracted as BED files using MACS2 peak detection algorithm with the following parameters: genome sizes =  $2.70 \times 10^9$  for human and  $1.87 \times 10^9$  for mouse, bandwidth = 300, model fold = (5, 50),  $q$  value cutoff =  $5.00 \times 10^{-2}$ , larger scaled towards smaller,  $\lambda$  range = 1,000–10,000 bps, Broad on.

**Assessment of wt versus inserted ChIP-seq signal.** To identify a difference in H3K27ac enrichment in ChIP-seq between alleles with and without insertion (12 bp) in Fig. 2b, we aligned all 25 bp reads of each experiment to this specific region of insertion using the R package 'Biostrings'. This alignment was performed against a region of 52 bp around the insertion site allowing for up to two mismatches, and the number of hits on forward and reverse strands was cumulated. For the mutant allele, the Jurkat insert sequence (5'-CCGTTTCCTAAG-3') was inserted in the reference sequence before alignment, extending the initial alignment region to a size of 64 bp.

**Allelic-ChIP.** Input and IP genomic DNAs were analysed by RT-PCR using power SybrGreen on a 7,500 Fast Real-time PCR system (Applied Biosystems). IgG control 'cycle over the threshold' Ct values were subtracted to Input or IP Ct values and converted into bound value by  $2^{-(\text{IP Ct or input Ct} - \text{IgG IP Ct})}$ . Allelic-ChIP was carried out using allele-specific primers (by substituting one of the germline primers with a primer located in or overlapping the insertion). EZH2 knockdown was achieved using a doxycycline-induced short hairpin RNA (sh-RNA)-targeting EZH2 (pTRIPZ-EZH2, openbiosystem # V21HS-63066). A non-silencing sh-RNA (pTRIPZ-NS) was used as control. Jurkat cells were electroporated and cells containing the pTRIPZ were selected on puromycin. Knockdown of EZH2 was obtained by the addition of doxycycline ( $2 \mu\text{g ml}^{-1}$ ) to the cells during 10 days. Western blot was performed using the anti-EZH2 BD Biosciences # 612666.

**Sequencing and SNP array.** For Jurkat mapping, a region of 10 kb 5' of TAL1 exon 1 was mapped on both alleles by LRP/PCR/cloning and standard Sanger sequencing as previously described<sup>37</sup> (see Supplementary Fig. 2 for details on mapping strategy). Identification of allelic variants (SNPs versus somatic indels/mutations) was performed with vector NTI using alignment against reference TAL1 sequence and variants (<http://www.ncbi.nlm.nih.gov/SNP>; <http://projects.tcag.ca/variation>, Supplementary Fig. 8). For the sequencing screen on T-ALL patients and cell lines, a region of  $\sim 700$  bp surrounding the Jurkat insertion site was directly PCR/sequenced on both strands in a subset of 93 samples and six cell lines. Heterogeneous sequences (ambiguous reading due to allelic differences) were systematically cloned, sequenced and analysed as above. For SNP array, hybridization on Affymetrix Cytogenetics SNP Array-6 was performed according to the manufacturer's recommendations. Data analysis was performed with Chromosome Analysis Suite software using the following settings: the CGH log2 copy number ratio for heterozygous deletion was defined as 0.5 to 1.5, whereas log2 copy number ratios  $< 1.5$  were defined as homozygous deletions. Gene copy number (GCN) aberrations were compared with the Database of Genomic variants (<http://projects.tcag.ca/variation>) to study only non-variant GCV aberrations.

**Patients.** Diagnostic samples from a consecutive series T-ALLs from 165 adults (older than 16 years) included in GRAALL-03/05 trial (registration #NCT00327678 and #NCT00222027) were analysed for TAL1 expression. Sample collection and analyses were approved by the local ethical committee. Informed consent was obtained from the patients or relatives in accordance with the Declaration of Helsinki, with the institutional review board approval of all involved hospitals. Diagnosis of T-ALL was based on the World Health Organization 2008 criteria, defined by expression of cytoplasmic and/or surface CD3, and negativity of CD19 and MPO, as reported<sup>38</sup>. To be included, samples had to contain at least 80% of lymphoblasts. Immuno-geno/phenotyping and oncogene quantification were performed as previously described<sup>38,39</sup>.

**Cell lines.** Cell lines used in this study were purchased from the ATCC collection and were mycoplasma free.

**RQ-PCR.** RNA was reverse transcribed using MMLV (Invitrogen). We used a TaqMan assay to quantify TAL1 transcript with the following primers: TAL1 F: 5'-ACA-ATC-GAG-TGA-AGA-GGA-GAC-CTT-C-3', TAL1 Probe: fam-5'-CTA-TGA-GAT-GGA-GAT-GGA-GAT-TAC-TGA-TG-3'-tamra, TAL1 R: 5'-ACG-CCG-CAC-AAC-TTT-GGT-G-3', 40 cycles were run on ABI 7500HT (Applied Biosystem) as described<sup>40</sup>. TAL1 transcript quantification was performed after normalization with the housekeeping gene ABL using the  $\Delta\text{Ct}$  method and results calculated according to the following formula  $2^{\Delta(\text{Ct}_{\text{ABL}} - \text{Ct}_{\text{TAL1}})}$ .

**TAL1 allelic expression analysis.** Allelic expression was performed as previously described<sup>7</sup>. In brief, polymorphic markers in the 3' UTR of the TAL1 gene were identified by PCR amplification and direct sequencing of 100 ng of genomic DNA. Allelic expression analysis was performed by PCR amplification and by direct sequencing of RT-PCR products from heterozygous patient samples. Three different PCRs were made to cover nine most frequent SNP among the 11 SNP previously described<sup>7</sup>.

**Statistical analysis.** ChIP. The power of  $t$ -test was estimated a priori using pwrR-package, and the expected variations between conditions evaluated. Differences in ChIP data between inserted and GL TAL1 alleles were analysed by unpaired  $t$ -test. Samples collections constituted of five or six technical replicates were first checked for normal distribution using Kolmogorov-Smirnov test and the equality of variances was tested using F test. Results of  $t$ -test are shown as two-tailed  $P$  values. The statistical power of executed  $t$ -tests was at least 80%. Errors bars on histograms represent s.e.m.

OS/DFS. Patients' characteristics were compared using the Fisher's exact test. Median comparisons were performed using the Mann-Whitney  $U$ -test. OS and DFS were calculated from the date of prephase initiation. Events accounting for DFS were induction failure and first relapse from any cause in first CR. OS and DFS were estimated by the Kaplan-Meier method and then compared by

the log-rank test. All calculations were performed using the SPSS software, version 15.0 and the GraphPad Prism, La Jolla, CA, USA.

**Ligation-mediated PCR.** Genomic DNA was extracted using QIAamp deoxyribonucleic acid Blood mini kit according to the manufacturer's instructions (Qiagen). DNA (500 ng) was used for LM-PCR; DNA was digested by *DraI*, *EcoRV*, *PvuII*, *SmaI*, *SspI* or *StuI* restriction endonucleases. Purified digested DNAs were ligated with an adapter (composed of two complementary primers GWA<sup>+</sup> and GWAB<sup>-</sup>). A primary PCR amplification was performed using an adapter-specific primer (AP1) and primer specific for the different TCR $\beta$  gene segments (ext). A secondary PCR was performed using nested AP2 and TCR $\beta$  primers (int), and analysed on 1% agarose gel. Non-germline PCR products were purified and sequenced. The functional and non-functional V(D)J rearrangements from patient OC were obtained using  $\beta$ 2.7-extB/intB and AP1/2 primers. The breakpoints corresponding to the episomal insertion were then obtained using V $\beta$ 7.4-extB/intB, D $\beta$ 1-extA/intA and AP1/2 primers, and validated by direct PCR using TAL1.OC.1B and V $\beta$ 7.4-intB primers.

**RT-PCR exon walking and 5' RACE.** Total RNA was extracted using a column-based system RNeasy mini kit (Qiagen) according to the manufacturer's instructions. Reverse transcription was performed with SuperScript III Reverse transcriptase (Invitrogen) and random primers (Applied Biosystems). cDNAs were analysed by real-time quantitative PCR (RT-PCR) using power SybrGreen on an ABI PRISM 7500 (Applied Biosystems). All PCRs were performed in duplicate. 5'-RACE was performed using 2  $\mu$ g of total RNA and the 5'/3' RACE kit, 2nd generation (Roche). Modifications from the instruction manufacturer were the generation a poly(G) tailing of first strand cDNA and the use of an oligo d(C) anchor primer. PCR was performed using the Pfu Ultra II fusion HS DNA polymerase (Agilent technologies).

**Genome editing in T-ALL cell line by type II CRISPR system.** PEER T-ALL cells line were cultured in RPMI medium (Life Technologies) containing 20% fetal calf serum, 1% L-glutamine, 1% sodium pyruvate and 100 U ml<sup>-1</sup> penicillin/streptomycin (Life Technologies) at 37°C in the presence of 5% CO<sub>2</sub>. The day of transfection, 1 million cells were nucleofected according to the manufacturer's instruction (Lonza), with 500 ng DNA donor sequence containing Neomycin-resistant gene and 2  $\mu$ g of the Cas9/gRNA expression vector (Addgene #42230). The chimeric guide RNA targeted *TAL1* insertion site, and was cloned according to Cong *et al.*<sup>41</sup>. One day after nucleofection, cells were plated in 96-wells plate at 10<sup>4</sup> cells per well and incubated in presence of 1,200  $\mu$ g ml<sup>-1</sup> geneticin G418 (Life Technologies) for 2 weeks. After selection and growing, a PCR was conducted to amplify the targeted region with genomic DNA derived from the surviving clones, and amplicons were separated on a 1% agarose gel then extracted with GEL/PCR clean up wizard (Promega) and sequenced (MWG-Biotech). CRISPR guide RNA: 5'-GAAAGACGTAACCTACTTCC-3'.

Primers list is available on request.

## References

- Teitell, M. A. & Pandolfi, P. P. Molecular genetics of acute lymphoblastic leukemia. *Annu. Rev. Pathol.* **4**, 175–198 (2009).
- Van Vlierberghe, P., Pieters, R., Beverloo, H. B. & Meijerink, J. P. Molecular-genetic insights in paediatric T-cell acute lymphoblastic leukaemia. *Br. J. Haematol.* **143**, 153–168 (2008).
- Sanda, T. *et al.* Core transcriptional regulatory circuit controlled by the TAL1 complex in human T cell acute lymphoblastic leukemia. *Cancer Cell* **22**, 209–221 (2012).
- Mouthon, M. A. *et al.* Expression of tal-1 and GATA-binding proteins during human hematopoiesis. *Blood* **81**, 647–655 (1993).
- Herblot, S., Steff, A. M., Hugo, P., Aplan, P. D. & Hoang, T. SCL and LMO1 alter thymocyte differentiation: inhibition of E2A-HEB function and pre-T alpha chain expression. *Nat. Immunol.* **1**, 138–144 (2000).
- Zhang, J. A., Mortazavi, A., Williams, B. A., Wold, B. J. & Rothenberg, E. V. Dynamic transformations of genome-wide epigenetic marking and transcriptional control establish T cell identity. *Cell* **149**, 467–482 (2012).
- Ferrando, A. A. *et al.* Biallelic transcriptional activation of oncogenic transcription factors in T-cell acute lymphoblastic leukemia. *Blood* **103**, 1909–1911 (2004).
- Hiom, K., Melek, M. & Gellert, M. DNA transposition by the RAG1 and RAG2 proteins: a possible source of oncogenic translocations. *Cell* **94**, 463–470 (1998).
- Agrawal, A., Eastman, Q. M. & Schatz, D. G. Transposition mediated by RAG1 and RAG2 and its implications for the evolution of the immune system. *Nature* **394**, 744–751 (1998).
- Koch, F. *et al.* Transcription initiation platforms and GTF recruitment at tissue-specific enhancers and promoters. *Nat. Struct. Mol. Biol.* **18**, 956–963 (2011).
- Cuddapah, S. *et al.* Global analysis of the insulator binding protein CTCF in chromatin barrier regions reveals demarcation of active and repressive domains. *Genome Res.* **19**, 24–32 (2009).
- Cui, K. *et al.* Chromatin signatures in multipotent human hematopoietic stem cells indicate the fate of bivalent genes during differentiation. *Cell Stem Cell* **4**, 80–93 (2009).
- Zhou, Y. *et al.* Chromatin looping defines expression of TAL1, its flanking genes and regulation in T-ALL. *Blood* **122**, 4199–4209 (2013).
- McCabe, M. T. *et al.* EZH2 inhibition as a therapeutic strategy for lymphoma with EZH2-activating mutations. *Nature* **492**, 108–112 (2012).
- Cardoso, B. A. *et al.* TAL1/SCL is downregulated upon histone deacetylase inhibition in T-cell acute lymphoblastic leukemia cells. *Leukemia* **25**, 1578–1586 (2011).
- Howe, S. J. *et al.* Insertional mutagenesis combined with acquired somatic mutations causes leukemogenesis following gene therapy of SCID-X1 patients. *J. Clin. Invest.* **118**, 3143–3150 (2008).
- Brandt, V. L. & Roth, D. B. V(D)J recombination: how to tame a transposase. *Immunol. Rev.* **200**, 249–260 (2004).
- Clappier, E. *et al.* The C-MYB locus is involved in chromosomal translocation and genomic duplications in human T-cell acute leukemia (T-ALL), the translocation defining a new T-ALL subtype in very young children. *Blood* **110**, 1251–1261 (2007).
- Ntziachristos, P. *et al.* Genetic inactivation of the polycomb repressive complex 2 in T cell acute lymphoblastic leukemia. *Nat. Med.* **18**, 298–301 (2012).
- Simon, C. *et al.* A key role for EZH2 and associated genes in mouse and human adult T-cell acute leukemia. *Genes Dev.* (2012).
- Zhang, J. *et al.* The genetic basis of early T-cell precursor acute lymphoblastic leukaemia. *Nature* **481**, 157–163 (2012).
- Grossmann, V. *et al.* EZH2 mutations and their association with PICALM-MLLT10 positive acute leukaemia. *Br. J. Haematol.* **157**, 387–390 (2012).
- Van Vlierberghe, P. & Ferrando, A. The molecular basis of T cell acute lymphoblastic leukemia. *J. Clin. Invest.* **122**, 3398–3406 (2012).
- Marculescu, R., Le, T., Simon, P., Jaeger, U. & Nadel, B. V(D)J-mediated translocations in lymphoid neoplasms: a functional assessment of genomic instability by cryptic sites. *J. Exp. Med.* **195**, 85–98 (2002).
- Mendes, R. D. *et al.* PTEN microdeletions in T-cell acute lymphoblastic leukemia are caused by illegitimate RAG-mediated recombination events. *Blood* **124**, 567–578 (2014).
- Marculescu, R. *et al.* Distinct t(7;9)(q34;q32) breakpoints in healthy individuals and individuals with T-ALL. *Nat. Genet.* **33**, 342–344 (2003).
- Vanura, K. *et al.* In vivo reinsertion of excised episodes by the V(D)J recombinase: a potential threat to genomic stability. *PLoS Biol.* **5**, e43 (2007).
- Reddy, Y. V. R., Perkins, E. J. & Ramsden, D. A. Genomic instability due to V(D)J recombination-associated transposition. *Genes Dev.* **20**, 1575–1582 (2006).
- Curry, J. D. *et al.* Chromosomal reinsertion of broken RSS ends during T cell development. *J. Exp. Med.* **204**, 2293–2303 (2007).
- Messier, T. L., O'Neill, J. P., Hou, S. M., Nicklas, J. A. & Finette, B. A. *In vivo* transposition mediated by V(D)J recombinase in human T lymphocytes. *EMBO J.* **22**, 1381–1388 (2003).
- Hacein-Bey-Abina, S. *et al.* Sustained correction of X-linked severe combined immunodeficiency by *ex vivo* gene therapy. *New Engl. J. Med.* **346**, 1185–1193 (2002).
- Hacein-Bey-Abina, S. *et al.* LMO2-associated clonal T cell proliferation in two patients after gene therapy for SCID-X1. *Science* **302**, 415–419 (2003).
- Ntziachristos, P. *et al.* Contrasting roles of histone 3 lysine 27 demethylases in acute lymphoblastic leukaemia. *Nature* **514**, 513–517 (2014).
- Bracken, A. P. & Helin, K. Polycomb group proteins: navigators of lineage pathways led astray in cancer. *Nat. Rev. Cancer* **9**, 773–784 (2009).
- Van der Meulen, J., Van Roy, N., Van Vlierberghe, P. & Speleman, F. The epigenetic landscape of T-cell acute lymphoblastic leukemia. *Int. J. Biochem. Cell Biol.* (2014).
- Fenouil, R. *et al.* CpG islands and GC content dictate nucleosome depletion in a transcription-independent manner at mammalian promoters. *Genome Res.* **22**, 2399–2408 (2012).
- Roulland, S. *et al.* Follicular lymphoma-like B cells in healthy individuals: a novel intermediate step in early lymphomagenesis. *J. Exp. Med.* **203**, 2425–2431 (2006).
- Asnafi, V. *et al.* Analysis of TCR, pT alpha, and RAG-1 in T-acute lymphoblastic leukemias improves understanding of early human T-lymphoid lineage commitment. *Blood* **101**, 2693–2703 (2003).
- Asnafi, V. *et al.* Age-related phenotypic and oncogenic differences in T-acute lymphoblastic leukemias may reflect thymic atrophy. *Blood* (2004).
- Bergeron, J. *et al.* Prognostic and oncogenic relevance of TLX1/HOX11 expression level in T-ALLs. *Blood* **110**, 2324–2330 (2007).
- Cong, L. *et al.* Multiplex genome engineering using CRISPR/Cas systems. *Science* **339**, 819–823 (2013).
- Mochizuki-Kashio, M. *et al.* Dependency on the polycomb gene *Ezh2* distinguishes fetal from adult hematopoietic stem cells. *Blood* **118**, 6553–6561 (2011).

43. Delabesse, E. *et al.* TAL1 expression does not occur in the majority of T-ALL blasts. *Br. J. Haematol.* **102**, 449–457 (1998).
44. Neiditch, M. B., Lee, G. S., Huy, L. E., Brandt, V. L. & Roth, D. B. The V(D)J recombinase efficiently cleaves and transposes signal joints. *Mol. Cell* **9**, 871–878 (2002).

## Acknowledgements

This work was supported by grants to BN laboratory from la Fondation pour la Recherche Médicale (#INE2003114116), Le Conseil Général des Bouches du Rhône, le Canceropôle PACA, CALYM consortium, l'Institut National du Cancer (INCa PLBIO09), la Fondation de France (#2008001490) and institutional grants from INSERM, CNRS and AMU. M.L. is a recipient of a fellowship from INCa (#ASC12035ASA). B.N. is the recipient of a CHRT INSERM/Assistance Publique-Hôpitaux de Marseille (HP-HM). Work in the Necker laboratory was supported by grants from the 'Association Laurette Fugain', the Institut National du Cancer and the 'Comité départemental de la Ligue Contre le Cancer'. S.L.N. was supported by the 'Institut National du Cancer (INCa-DHOS) and a grant from the 'Association pour la Recherche sur le Cancer (ARC)'. R.F. is supported by a Centre National de la Recherche Scientifique grant. M.A.M. was supported by an ANR chromaTin and by the Fondation pour la Recherche Médicale (FRM AJE20130728183). The sequencing costs for ChIP-seq experiments were partially granted by an ESGI consortium grant from the Seventh Framework Programme (FP7/2007–2013) under grant agreement no. 262055. E.D. gratefully acknowledges support from the Association pour la Recherche sur le Cancer and the Fondation pour la Recherche Médicale. We thank participants in the GRAALL-2003 and -2005 study groups for collecting and providing biological samples and data sets. The GRAALL was supported by grants P0200701 and P030425/AOM03081 from the Programme Hospitalier de Recherche Clinique, Ministère de l'Emploi et de la Solidarité, France and the Swiss Federal Government in Switzerland. Samples were collected and processed by the AP-HP 'Direction de Recherche Clinique' Tumour Bank at Necker-Enfants Malades. We are grateful to V. Lheritier for her help in collecting clinical samples, L. Spinelli for statistical advice, T. Guignard for Macs2

analyses and C Pignon for technical help. We are grateful to Dr T Cathomen for expert advices in DNA editing.

## Author contributions

ChIP-seq experiments were performed and analysed by L.C.P., R.F., M.A.M., M.G., I.G.G. and J.-C.A.; allelic-ChIP experiments were performed and analysed by J.-M.N., L.C.P., M.L., M.K., C.P., D.P.-B. and E.D.; T-ALL sample characterizations were performed and analysed by A.T., J.-M.N., L.C.P., S.L.N., S.J., L.S., E.A.M. and V.A.; TALEN/CRISPR assays were performed and analysed by J.-M.N., M.L. and D.P.-B. with the advice of C.G. and B.M.; episomal reintegration characterization was performed by J.-M.N., E.A.M., S.H.-B.-A., S.J.H., H.B.G. and A.J.T.; survival analysis was carried out by A.T., H.D., E.A.M., N.I. and V.A.; V.A. and B.N. conceived and directed the project, and B.N. wrote the paper.

## Additional information

**Supplementary Information** accompanies this paper at <http://www.nature.com/naturecommunications>

**Competing financial interests:** The authors declare no competing financial interests.

**Reprints and permission** information is available online at <http://npg.nature.com/reprintsandpermissions/>

**How to cite this article:** Navarro, J.-M. *et al.* Site- and allele-specific polycomb dysregulation in T-cell leukaemia. *Nat. Commun.* **6**:6094 doi: 10.1038/ncomms7094 (2015).



This work is licensed under a Creative Commons Attribution 4.0 International License. The images or other third party material in this article are included in the article's Creative Commons license, unless indicated otherwise in the credit line; if the material is not included under the Creative Commons license, users will need to obtain permission from the license holder to reproduce the material. To view a copy of this license, visit <http://creativecommons.org/licenses/by/4.0/>

# Toward a *NOTCH1*/*FBXW7*/*RAS*/*PTEN*-Based Oncogenetic Risk Classification of Adult T-Cell Acute Lymphoblastic Leukemia: A Group for Research in Adult Acute Lymphoblastic Leukemia Study

Amélie Trinquand, Aline Tanguy-Schmidt, Raouf Ben Abdelali, Jérôme Lambert, Kheira Beldjoud, Etienne Lengliné, Noémie De Gunzburg, Dominique Payet-Bornet, Ludovic Lhermitte, Hossein Mossafa, Véronique Lhéritier, Jonathan Bond, Françoise Huguet, Agnès Buzyn, Thibaud Leguay, Jean-Yves Cahn, Xavier Thomas, Yves Chalandon, André Delannoy, Caroline Bonmati, Sébastien Maury, Bertrand Nadel, Elizabeth Macintyre, Norbert Ifrah, Hervé Dombret, and Vahid Asnafi

Author affiliations appear at the end of this article.

Published online ahead of print at [www.jco.org](http://www.jco.org) on October 28, 2013.

Support information appears at the end of this article.

Written on behalf of the Group for Research in Adult Acute Lymphoblastic Leukemia (GRAALL).

A.T. and A.T.-S. are co-first authors.

H.D. and V.A. are co-director authors.

Presented in part at the 54th Annual Meeting of the American Society of Hematology, Atlanta, GA, December 8-11, 2012; at the 2013 Congress of the Société Française d'Hématologie, Paris, France, March 27-29, 2013; and at the Second European School of Haematology-European Hematology Association Scientific Workshop on T-Cell Acute Lymphoblastic Leukemia, Lisbon, Portugal, March 22-24, 2013.

Authors' disclosures of potential conflicts of interest and author contributions are found at the end of this article.

Clinical trial information: NCT00327678, NCT00222027.

Corresponding author: Vahid Asnafi, MD, Hôpital Necker-Enfants Malades, Laboratoire d'Hématologie, 149 rue de Sévres, 75015 Paris, France; e-mail: [vahid.asnafi@nck.aphp.fr](mailto:vahid.asnafi@nck.aphp.fr).

© 2013 by American Society of Clinical Oncology

0732-183X/13/3134w-4333w/\$20.00

DOI: 10.1200/JCO.2012.48.5292

## ABSTRACT

### Purpose

The Group for Research in Adult Acute Lymphoblastic Leukemia (GRAALL) recently reported a significantly better outcome in T-cell acute lymphoblastic leukemia (T-ALL) harboring *NOTCH1* and/or *FBXW7* (*N/F*) mutations compared with unmutated T-ALL. Despite this, one third of patients with *N/F*-mutated T-ALL experienced relapse.

### Patients and Methods

In a series of 212 adult T-ALLs included in the multicenter randomized GRAALL-2003 and -2005 trials, we searched for additional *N/K-RAS* mutations and *PTEN* defects (mutations and gene deletion).

### Results

*N/F* mutations were identified in 143 (67%) of 212 patients, and lack of *N/F* mutation was confirmed to be associated with a poor prognosis. *K-RAS*, *N-RAS*, and *PTEN* mutations/deletions were identified in three (1.6%) of 191, 17 (8.9%) of 191, and 21 (12%) of 175 patients, respectively. The favorable prognostic significance of *N/F* mutations was restricted to patients without *RAS/PTEN* abnormalities. These observations led us to propose a new T-ALL oncogenetic classifier defining low-risk patients as those with *N/F* mutation but no *RAS/PTEN* mutation (97 of 189 patients; 51%) and all other patients (49%; including 13% with *N/F* and *RAS/PTEN* mutations) as high-risk patients. In multivariable analysis, this oncogenetic classifier remained the only significant prognostic covariate (event-free survival: hazard ratio [HR], 3.2; 95% CI, 1.9 to 5.15; *P* < .001; and overall survival: HR, 3.2; 95% CI, 1.9 to 5.6; *P* < .001).

### Conclusion

These data demonstrate that the presence of *N/F* mutations in the absence of *RAS* or *PTEN* abnormalities predicts good outcome in almost 50% of adult T-ALL. Conversely, the absence of *N/F* or presence of *RAS/PTEN* alterations identifies the remaining cohort of patients with poor prognosis.

*J Clin Oncol* 31:4333-4342. © 2013 by American Society of Clinical Oncology

## INTRODUCTION

T-cell acute lymphoblastic leukemia (T-ALL) corresponds to a heterogeneous group that accounts for 30% of adult *BCR-ABL*-negative acute lymphoblastic leukemias (ALLs).<sup>1</sup> Recognized T-ALL oncogenic pathways include proto-oncogene activation, tumor suppressor gene deletion, and activation of the Notch1 pathway by *NOTCH1*/*FBXW7* (*N/F*) mutations,<sup>2,3</sup> leading to various combinations of gene alterations and complex oncogenic

networks.<sup>4-8</sup> *N/F* mutations involve either the heterodimerization domain, probably facilitating cleavage of the NOTCH receptor, and/or the negative regulatory PEST domain,<sup>9</sup> increasing the half-life of intracellular NOTCH. An alternative mechanism of constitutive Notch1 pathway activation involves loss-of-function mutations of *FBXW7*, leading to the inhibition of ubiquitin-mediated degradation of activated NOTCH1.<sup>10</sup>

Even if the complete remission (CR) rate in adults with *BCR-ABL*-negative ALLs reaches 90%,



long-term outcome remains unsatisfactory, with a 5-year overall survival (OS) rate of approximately 45%.<sup>1</sup> Historical prognostic factors used for therapeutic stratification are predominantly initial clinical features, including age, WBC count, immunophenotype, and CNS involvement.<sup>11</sup> Minimal residual disease (MRD) quantification is a strong prognostic factor<sup>12</sup> but requires stringent standardization and is obviously not available at baseline. The Group for Research in Adult Acute Lymphoblastic Leukemia (GRAALL) reported a significant improvement in the outcome of adults with *BCR-ABL*-negative ALL using a pediatric-inspired intensified treatment protocol,<sup>13</sup> which in T-ALL was particularly beneficial for patients harboring *N/F* mutations, compared with unmutated patients.<sup>3</sup> Despite this, approximately one third of patients with *N/F*-mutated T-ALL experience relapse, suggesting that other factors may dampen the positive effect of *N/F* and making the identification of a subgroup with a favorable outcome a desirable goal.

The two pro-proliferative Ras/Raf/MEK/ERK and PI3K/PTEN/Akt/mTOR pathways have also been reported to be deregulated in limited series of pediatric T-ALL,<sup>14,15</sup> but corresponding data for adult T-ALL are scanty. More specifically, *RAS*, a regulator of the Ras/Raf/MEK/ERK pathways, and *PTEN*, the main negative regulator of the PI3K/PTEN/Akt/mTOR pathways, both play roles in cell proliferation and resistance to chemotherapy.

Here, we identified *PTEN* loss-of-function deletions/mutations or *K-RAS/N-RAS* activating mutations as two virtually mutually exclusive genetic abnormalities found in 23% of adult T-ALLs treated on

GRAALL trials. Importantly, the absence of *N/F* or presence of *RAS/PTEN* alterations identifies the 50% of patients who are most likely to benefit from alternative therapies that target either the PI3K/PTEN/Akt/mTOR or the Ras/Raf/MEK/ERK pathways.

## PATIENTS AND METHODS

The GRAALL-2003 protocol was a multicenter phase II trial that enrolled 76 adults with T-ALL between November 2003 and November 2005,<sup>13</sup> of whom 57 had material available for the present study and have been previously reported.<sup>3</sup> The multicenter randomized GRAALL-2005 trial was the following phase III trial and was similar to the GRAALL-2003 trial, with the addition of the randomized evaluation of an intensified sequence of hyperfractionated cyclophosphamide during induction and late intensification. Between May 2006 and May 2010, 189 adults with T-ALL were randomly assigned in the GRAALL-2005 study. The present study concerns 155 of these patients, for whom diagnostic DNA and/or cDNA was available. As for the GRAALL-2003 trial, these 155 patients were representative of the total GRAALL-2005 T-ALL population, with a 3-year OS of 67% (95% CI, 60% to 74%). The GRAALL-2003 and GRAALL-2005 protocols are briefly described in the Data Supplement. Informed consent was obtained from all patients at trial entry. Both trials were conducted in accordance with the Declaration of Helsinki and approved by local and multicenter research ethical committees. In these trials, allogeneic (allo) stem-cell transplantation (SCT) was offered in first CR in patients who had a matched sibling or 10/10 fully matched unrelated donor and at least one of the following criteria: CNS involvement at diagnosis; early resistance to

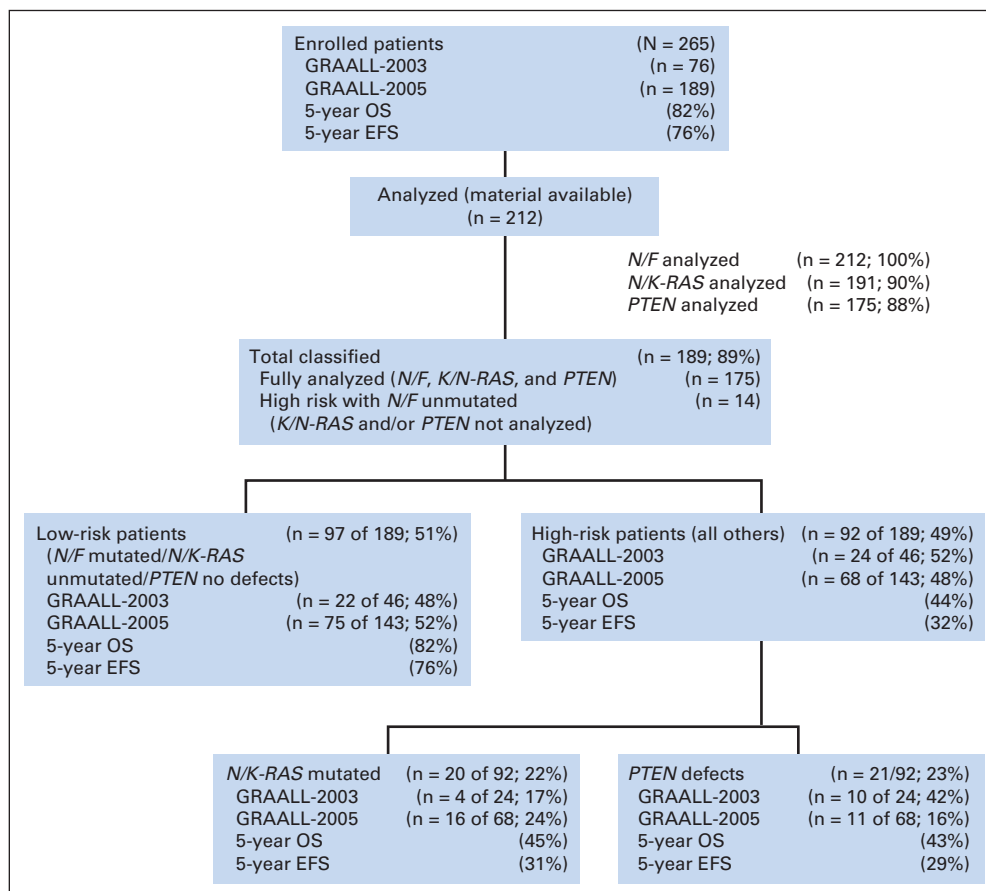


**Fig 1.** Patient flow diagram. EFS, event-free survival; GRAALL, Group for Research in Adult Acute Lymphoblastic Leukemia; *N/F*, *NOTCH1/FBXW7*; OS, overall survival.

corticosteroid after the first 1-week prephase; early resistance to chemotherapy after 1 additional week of treatment; and CR not achieved after first induction.

Among the 212 consecutive adults with T-ALL included in the present study (57 GRAALL-2003 and 155 GRAALL-2005 patients), 133 were eligible for allo-SCT and 67 actually received transplantation in first CR (16 GRAALL-2003 and 51 GRAALL-2005 patients). With a point date on December 31, 2011, the median follow-up time was 4.2 years (6.0 and 3.3 years for GRAALL-2003 and GRAALL-2005 patients, respectively). Complete methods are available in the Data Supplement.

Patient characteristics and CR rates were compared using either the Fisher's exact test or the Mann-Whitney *U* test. Median comparisons were performed using the Mann-Whitney *U* test. OS and event-free survival (EFS)

were calculated from the date of prephase initiation. Events accounting for EFS were induction failure, first hematologic relapse, and death from any cause in first CR. Cumulative incidence of relapse (CIR) and relapse-free survival (RFS) were calculated from the date of CR achievement. For the analysis of survival outcomes, SCT was not considered to be a censoring event in patients who received allo-SCT in first CR. OS and EFS were estimated using the Kaplan-Meier method and then compared using the log-rank test.<sup>16</sup> Multivariable regressions were performed with the Cox model.<sup>17</sup> CIR was estimated taking into account death in first CR for competing risk and then compared using cause-specific hazard Cox models. Specific hazards of relapse (SHRs) and hazard ratios (HRs) were given with 95% CIs. Interactions were assessed by introducing an interaction term in the Cox model. Prognostic discriminatory powers were evaluated by concordance probability estimates<sup>18</sup> and then

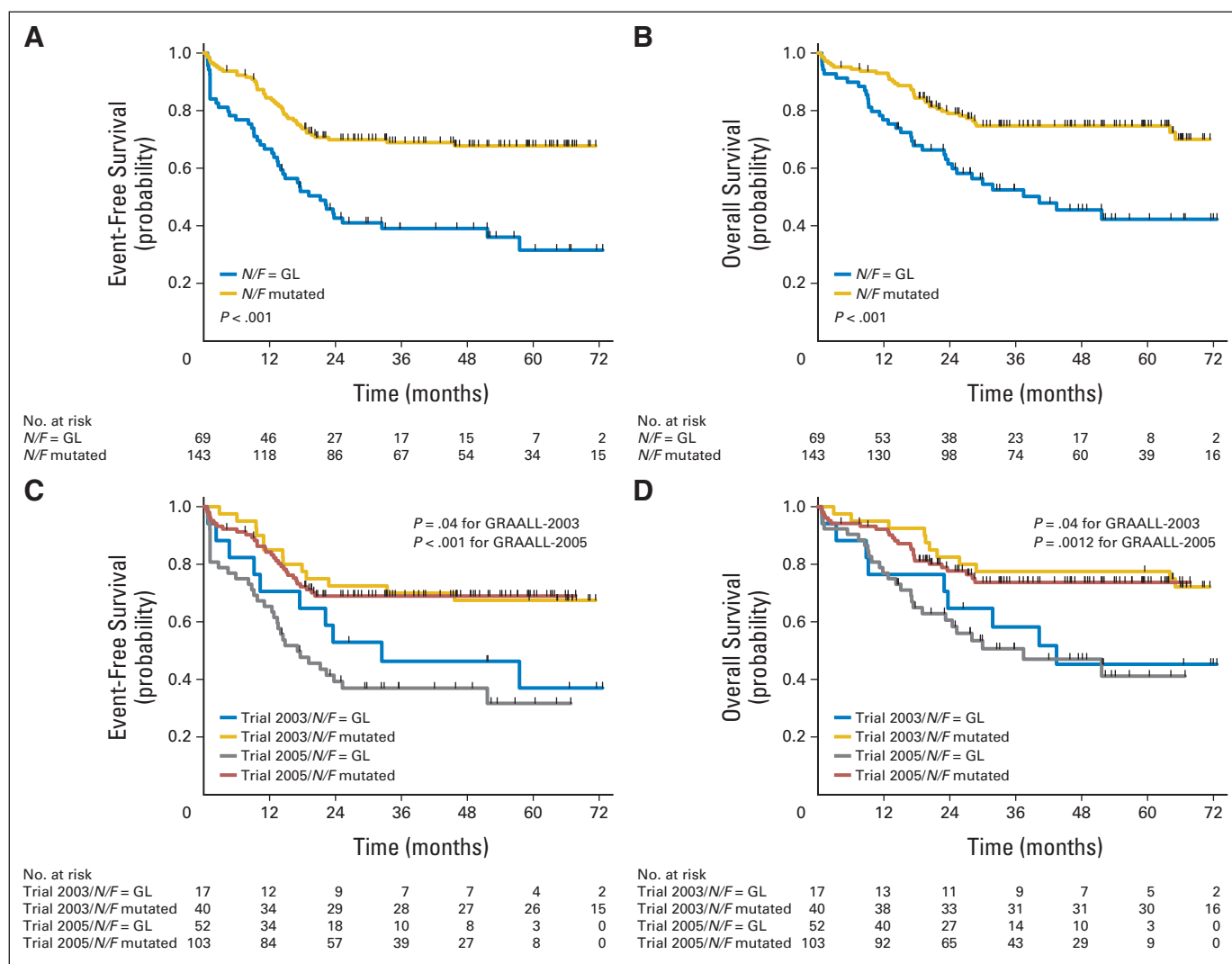


**Fig 2.** Event-free survival (EFS) and overall survival (OS) by *NOTCH1/FBXW7* (N/F) status and trial. (A) EFS by N/F status. At 5 years, EFS was estimated at 32% (95% CI, 19% to 45%) in patients with unmutated N/F, compared with 69% (95% CI, 60% to 76%) in those with N/F mutation. The hazard ratio (HR) for shorter EFS in the former group was 2.6 (95% CI, 1.7 to 3.9;  $P < .001$ ). (B) OS by N/F status. At 5 years, OS was estimated at 42% (95% CI, 29% to 55%) in patients with unmutated N/F, compared with 75% (95% CI, 66% to 81%) in those with N/F mutation. The HR for shorter OS in the former group was 2.45 (95% CI, 1.5 to 3.9;  $P < .001$ ). (C) EFS by N/F status in the Group for Research in Adult Acute Lymphoblastic Leukemia (GRAALL)-2003 and GRAALL-2005 trials. For GRAALL-2003 patients, 5-year EFS was estimated at 37% (95% CI, 14% to 61%) in patients with unmutated N/F, compared with 67.5% (95% CI, 51% to 80%) in those with N/F mutation. The HR for shorter EFS in the former group was 2.3 (95% CI, 1.01 to 5.2;  $P = .04$ ). For GRAALL-2005 patients, 5-year EFS was estimated at 32% (95% CI, 18% to 47%) in patients with unmutated N/F, compared with 69% (95% CI, 59% to 77%) in those with N/F mutation. The HR for shorter EFS in the former group was 2.65 (95% CI, 1.6 to 4.3;  $P < .001$ ). (D) OS by N/F status in the GRAALL-2003 and GRAALL-2005 trials. For GRAALL-2003 patients, 5-year OS was estimated at 45% (95% CI, 21% to 67%) in patients with unmutated N/F, compared with 77.5% (95% CI, 61% to 88%) in those with N/F mutation. The HR for shorter OS in the former group was 2.45 (95% CI, 1.01 to 5.9;  $P = .04$ ). For GRAALL-2005 patients, 5-year OS was estimated at 41% (95% CI, 24% to 57%) in patients with unmutated N/F, compared with 74% (95% CI, 63% to 81%) in those with N/F mutation. The HR for shorter OS in the former group was 2.4 (95% CI, 1.4 to 4.2;  $P = .0012$ ). GL, germline.

compared using the bootstrap method. STATA/SE 10.1 software (STATA, College Station, TX) was used. All tests were two-sided, with a type I error at 5%.

## RESULTS

### Lack of N/F Mutation Identifies a Poor Prognostic Subset of Adult T-ALL

N/F mutations were identified in 143 (67%; 95% CI, 61% to 74%) of the 212 analyzed patients with T-ALL (Fig 1). The mutation rate of N/F was similar in the GRAALL-2003 (70%; 95% CI, 57% to 82%) and GRAALL-2005 (67%; 95% CI, 58% to 74%) cohorts. In keeping with our previous report,<sup>3,19</sup> EFS and OS were significantly ( $P < .001$  and  $P < .001$ , respectively) better in T-ALLs harboring N/F mutations, compared with unmutated T-ALL (Figs 2A and 2B, respectively). Furthermore, as shown in Figures 2C and 2D, the favorable impact of N/F mutation was also observed when GRAALL-2003 and GRAALL-2005 patients were analyzed separately.

Despite this, one third of patients with N/F mutations experienced an EFS event, mostly within the first 2 years of follow-up (Fig 2A). To identify a genetic surrogate for relapsing T-ALLs, we studied Ras/Raf/MEK/ERK and PI3K/PTEN/Akt/mTOR pathway activation by N/K-RAS and PTEN alteration, respectively.

### N/K-RAS Mutations Are Frequent Events in Adult T-ALL

Among the 212 patients with T-ALL tested for N/F mutations, 191 were explored for activating RAS mutations. K-RAS and N-RAS mutations were identified in three (2%; 95% CI, 0.3% to 5%) of 191 and 17 (9%; 95% CI, 5% to 14%) of 191 patients, respectively. Overall, 20 (11%; 95% CI, 7% to 16%) of 191 GRAALL T-ALLs harbored activating RAS mutations. Clinical, immunophenotypic and oncogenic features of the patients were analyzed according to the absence or presence of RAS abnormalities (Table 1), and full details of individual patients with RAS abnormalities are reported in the Data Supplement.

Patients with RAS mutations did not differ significantly from patients without mutations with respect to age, sex, or WBC counts greater than  $100 \times 10^9/L$  at diagnosis (Table 1). CNS involvement was found in 25% of patients with RAS mutations versus 6% of patients without mutations ( $P = .02$ ). RAS mutations were also more frequently observed in T-ALL with no classical oncogenic markers compared with T-ALLs harboring *TLX1/3*, *SIL-TAL1*, or *CALM-AF10* abnormalities (78% v 50%, respectively;  $P = .03$ ). No significant correlation was found with European Group for the Immunological Classification of Leukemias class or N/F status or early sensitivity to corticosteroids and chemotherapy, but RAS mutations were notably absent in T-cell receptor (TCR)-positive T-ALLs.

### PTEN Genomic Deletions and Mutations Lead to PTEN Loss in 12% of Adult T-ALLs

PTEN mutations were identified in 17 (10%; 95% CI, 6% to 15%) of 175 patients with available material (all of whom had been tested for RAS mutations). All mutations were nonsense or, more frequently, frameshift insertions or insertions/deletions as reported in

**Table 1.** Characteristics of Patients With T-ALL According to Their RAS Status

Characteristic	All Patients		N/K-RAS Exon 1				P*
	No.	%	Mutation No.	%	Wild Type No.	%	
Total patients	191		20	10	171	90	
TCR subsets analyzed	172						
Immature	44	26	7	41	37	24	.14
Pre- $\alpha\beta$	92	53	10	59	82	53	.8
TCR positive	36	21	0	0	36	23	.025†
EGIL	180						
I-II	70	39	9	50	61	38	.32
III	89	49	9	50	80	49	1.0
IV	21	12	0	0	21	13	.14
Genotype subsets analyzed	183						
<i>CALM-AF10</i>	9	5	0	0	9	5	.6
<i>SIL-TAL1</i>	16	9	0	0	16	10	.37
<i>TLX1</i>	37	20	2	11	35	21	.54
<i>TLX3</i>	25	14	2	11	23	14	1.0
None of above	96	52	14	78	82	50	.03†
N/F mutation	132	69	16	80	116	68	.32
Clinical subsets analyzed							
Male	143	75	14	70	129	76	.59
Age, years							
Median	31		34		31		.23
> 35	77	41	9	45	68	40	.64
WBC count, $\times 10^9/L$							
Median	36.4		47.1		36.4		.99
> 100	53	28	5	25	48	28	1.0
CNS involvement	16	8	5	25	11	6	.02†
CR	176	92	19	95	157	92	.56
Cs	105	55	11	55	94	55	1.0
CHs	108	57	12	60	96	56	.82

Abbreviations: CHs, chemosensitivity; CR, complete remission; Cs, corticosteroid sensitivity; EGIL, European Group for the Immunological Classification of Leukemias; N/F, *NOTCH1* and/or *FBXW7*; T-ALL, T-cell acute lymphoblastic leukemia; TCR, T-cell receptor.

\*Determined using *t* test or Fisher's exact test when appropriate.

†Significant value.

the Data Supplement. We then analyzed the whole *PTEN* locus by high-resolution comparative genomic hybridization (CGH) array for 100 patients already screened for *PTEN* exon7 mutations. Overall, *PTEN* deletions were detected in five (5%; 95% CI, 2% to 11%) of 100 patients. The deletions were mainly large, ranging from 60 to 7,464 kb, but were focal and intragenic in two patients (Fig 3A) and biallelic in one patient. Because the breakpoints were relatively heterogeneous, a common deleted region, including exon 2, was identified (Fig 3A, right panel).

To validate the CGH array findings, *PTEN* (introns 2 and 8) genomic allele quantification by quantitative polymerase chain reaction was performed. As shown in Figure 3A, all patients with *PTEN* deletions identified by CGH array demonstrated a low *PTEN*/*ALBUMIN* gene dosage ratio (range, 0.05 to 0.59) compared with 39 patients without deletions (range, 0.72 to 1.4). This genomic quantitative polymerase chain reaction system was then used to identify

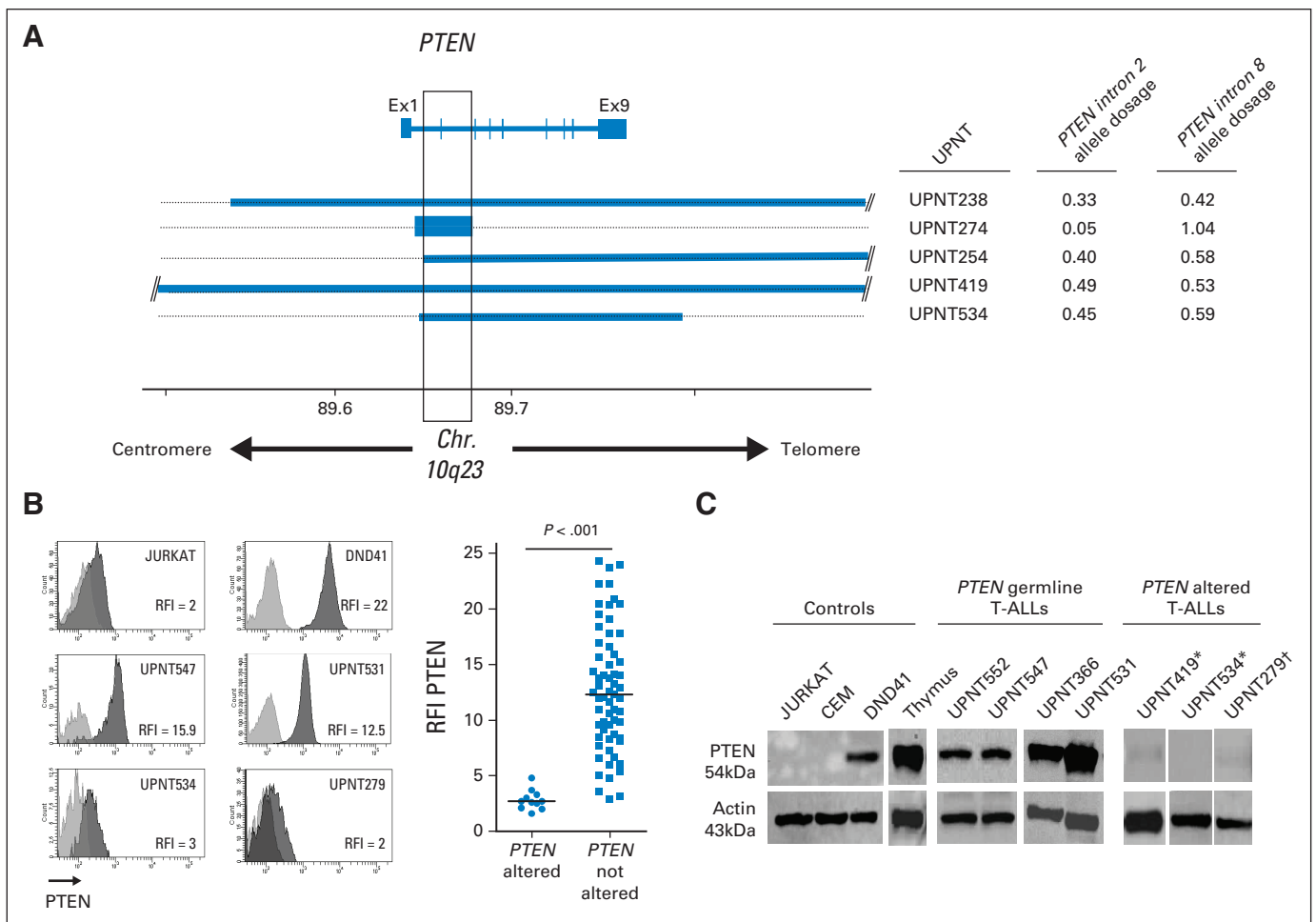


**Fig 3. PTEN analysis.** (A) Schematic representation of *PTEN* deletions (left) and *PTEN* exon 2/*ALB* and *PTEN* intron 8/*ALB* genomic quantitative polymerase chain reaction (qPCR) ratios (right) in five T-cell acute lymphoblastic leukemias (T-ALLs). Patient UPNT238 harbors a monoallelic deletion of *PTEN* concordant with gene dosage results (*PTEN* exon 2/*ALB* and *PTEN* intron 8/*ALB* qPCR ratios, 0.33 and 0.42, respectively). Patient UPNT274 harbors a biallelic deletion of the exon 2 and intron 2 of *PTEN* concordant with gene dosage results (*PTEN* exon 2/*ALB* qPCR ratio of 0.05 and *PTEN* intron 8/*ALB* qPCR ratio of 1.04). (B) Flow cytometry analysis of *PTEN* expression in T-ALL cell lines and primary T-ALL samples (left) and representation of *PTEN* ratio of fluorescence intensity (RFI) according to *PTEN* status (right). Lighter gray histograms represent the isotypic control, and the darker gray histograms represent *PTEN* levels. JURKAT is a *PTEN*-null cell line. DND41 harbors *PTEN* levels similar to germline *PTEN* primary T-ALLs. The two *PTEN*-altered primary T-ALLs show low *PTEN* protein. RFI was less than 5 in all *PTEN*-altered T-ALLs, whereas RFI ranged from 2.9 and 44.2 (median, 12.6) in *PTEN*-nonaltered T-ALLs. (C) *PTEN* Western blot analysis in T-ALL cell lines, normal human thymus, and primary T-ALL samples. Tested T-ALLs with germline *PTEN* status harbored higher level of *PTEN* protein compared with T-ALLs with genomic *PTEN* alterations. Actin was used as a loading control. Western blot data are in concordance with flow cytometric results. (\*) Deletion. (†) Mutation.

*PTEN* deletion in the remaining 75 patients tested for *PTEN* mutations but not by CGH array. This allowed identification of one additional patient with *PTEN* deletion (*PTEN*/*ALBUMIN* ratio, 0.53). Overall, *PTEN* genomic deletions occurred in six (3%; 95% CI, 0.9% to 6%) of 175 patients. Two patients with heterozygous *PTEN* deletions also harbored *PTEN* mutations (Data Supplement). Altogether, *PTEN* genomic abnormalities by deletion and/or mutation were identified in 21 (12%; 95% CI, 78% to 18%) of 175 patients.

To determine whether the observed *PTEN* genomic abnormalities led to inactivation of *PTEN* expression and function, we then analyzed protein expression by immunophenotyping and Western blot in 82 and 57 T-ALLs, respectively, with available material. All tested patients harboring *PTEN* genomic alteration (four deletions and seven mutations) demonstrated loss of or low-level *PTEN* protein expression as measured by Western blot or flow analysis (Figs 3B and 3C).

### ***PTEN* Genomic Abnormalities Occur Frequently in Unmutated N/F- and SIL-TAL1-Positive Adult T-ALLs but Are Mutually Exclusive With N/K-RAS Mutations**

Clinical, immunophenotypic, and oncogenic features of patients were analyzed as a function of *PTEN* status (Table 2). Full clinical, immunophenotypic, oncogenic, and karyotypic data of individual patients with *PTEN* abnormalities are reported in the Data Supplement. *PTEN* abnormalities were more frequent in unmutated N/F-T-ALLs; only eight (38%; 95% CI, 18% to 62%) of 21 T-ALLs with *PTEN* mutations/deletions harbored N/F mutations compared with 112 (73%; 95% CI, 65% to 80%) of 154 germline *PTEN* T-ALLs ( $P = .002$ ). With respect to recurrent oncogenic subtypes, *SIL-TAL1*-positive patients demonstrated the highest rate of *PTEN* abnormalities; seven (33%; 95% CI, 15% to 57%) of 21 T-ALLs with *PTEN* mutations/deletions harbored *SIL-TAL1* fusion compared with only nine (6%; 95% CI, 2.8% to 11.2%) of 149 *PTEN* wild-type T-ALLs ( $P = .001$ ).



**Table 2.** Characteristics of Patients With T-ALL According to Their *PTEN* Status (*PTEN* CGH array, *PTEN*/*ALB* allelic ratios, and *PTEN* exon 7 mutation)

Characteristic	All Patients		PTEN				P <sup>a</sup>
			Altered		Not Altered		
	No.	%	No.	%	No.	%	
Total patients	175		21	12	154	88	
TCR subsets analyzed	160						
Immature	41	26	1	5	40	28	.046†
Pre- $\alpha\beta$	85	53	9	47	76	54	.6
TCR positive	34	21	9	47	25	18	.006†
EGIL	167						
I-II	65		5	25	60	41	.22
III	82		10	50	72	49	1.0
IV	20		5	25	15	10	.07
Genotype subsets analyzed	170						
<i>CALM-AF10</i>	8	5	1	5	7	5	1.0
<i>SIL-TAL1</i>	16	9	7	33	9	6	< .001†
<i>TLX1</i>	31	18	1	5	30	20	.13
<i>TLX3</i>	24	14	2	10	22	15	.74
None of above	91	54	10	48	81	54	.64
<i>N/F</i> mutated	120	69	8	38	112	73	.002†
Clinical subsets analyzed							
Male	131	75	18	86	113	73	.29
Age, years							
Median	30.8		24.9		31.4		.001†
> 35	69	39	3	14	66	43	.02†
WBC, $\times 10^9/L$							
Median	36.8		110		29.9		.001†
> 100	49	28	13	62	36	23	< .001†
CNS involvement	16	9	4	19	12	8	.11
CR	160	96	20	95	140	96	1.0
Cs	94	54	8	38	86	56	.16
CHs	98	56	15	71	83	54	.16

Abbreviations: CGH, comparative genomic hybridization; CHs, chemosensitivity; CR, complete remission; Cs, corticosteroid sensitivity; EGIL, European Group for the Immunological Classification of Leukemias; *N/F*, *NOTCH1* and/or *FBXW7*; T-ALL, T-cell acute lymphoblastic leukemia; TCR, T-cell receptor.

\*Determined using *t* test or Fisher's exact test when appropriate.

†Significant value.

*PTEN*-altered patients did not significantly differ from wild-type patients with respect to sex, CNS involvement, or early sensitivity to corticosteroids or chemotherapy (Table 2), but WBC counts greater than  $100 \times 10^9/L$  at diagnosis were found in 62% of *PTEN*-altered patients compared with 23% of unmutated patients ( $P < .001$ ). *PTEN*-altered status was also more frequently observed in patients younger than 35 years of age ( $P = .02$ ) and in mature T-ALLs expressing surface TCR (47% v 18% not expressing surface TCR;  $P = .006$ ). Overall, *PTEN* alteration was more frequent in younger, mature, TCR-positive, *SIL-TAL1*-positive, *N/F* unmutated patients with high leukemic bulk tumors. Interestingly, only one patients with *RAS* mutation was also mutated for *PTEN* but only within a subpopulation of leukemic cells (Data Supplement), suggesting that these two oncogenic alterations affecting two different interlinked pro-proliferative pathways may be virtually mutually exclusive in adult T-ALL.

## ***N/K-RAS* Mutations and *PTEN* Genomic Abnormalities Predict Similar Poor Outcome**

Figures 4A, 4B, and 4C show that both *N/K-RAS* mutations and *PTEN* genomic abnormalities were associated with marked trends to shorter CIR, RFS, and OS (see the Data Supplement for *PTEN* abnormalities alone and within *N/F* subgroups). Because of their biologic pro-proliferative function, mutual exclusion, and similar poor prognostic significance, we regrouped all patients with *N/K-RAS* mutations or *PTEN* genomic abnormalities in one unique *RAS/PTEN* alteration subgroup. Figures 4D, 4E, and 4F illustrate the significant prognostic impact of these oncogenetic alterations on CIR, RFS, and OS, respectively.

## ***RAS*, *PTEN*, and *N/F* Mutational Status Identifies a Strong Classifier in Adult T-ALL**

We then analyzed how the presence of these virtually exclusive *N/K-RAS* mutations and *PTEN* genomic abnormalities may modulate the good prognosis associated with *N/F* mutations and whether prognostic interactions may exist between these two genomic pathways. For this purpose, we performed a multivariable Cox model for CIR, RFS, and OS, entering the two *N/F* and *RAS/PTEN* covariates, as well as their interaction term. As illustrated in Figures 5A, 5B, and 5C, this analysis indicated that the prognostic significance of *N/F* mutations was still observed but with significant interactions between *N/F* and *RAS/PTEN* mutations, indicating that the favorable impact of *N/F* mutation was only observed in patients without *RAS/PTEN* mutation (Figs 5A to 5C). Importantly, sensitivity analyses of patients treated as part of the GRAALL-2003 trial or during the GRAALL-2005 trial demonstrated that statistical significance of the classifier was consistent in both groups (Data Supplement).

These observations led us to propose a new T-ALL oncogenetic classifier defining low-risk patients as those with *N/F* mutation but no *RAS/PTEN* mutation (here, 97 of 189 studied patients; 51%) and all other patients (49%) as high-risk patients. Figures 5D, 5E, and 5F show CIR, RFS, and OS according to this new strong oncogenetic classifier. As a whole, 23 patients who would have been classified as low risk based on their *N/F* status joined the high-risk subgroup based on their *RAS/PTEN* status. Importantly, these patients did not differ from their *N/F*-mutated, *RAS/PTEN*-unaltered counterparts (Data Supplement). Comparing the oncogenetic risk classification based only on the *N/F* mutational status to this refined oncogenetic classifier, HRs for high-risk patients increased from 2.6 (95% CI, 1.7 to 4.0) to 3.25 (95% CI, 2.0 to 5.3) for EFS and from 2.5 (95% CI, 1.5 to 4.0) to 3.3 (95% CI, 1.9 to 5.8) for OS. Concordance probability estimates of the old *N/F* versus the new *N/F-RAS-PTEN* classifier were 0.603 (95% CI, 0.561 to 0.645) versus 0.633 (95% CI, 0.589 to 0.677) for EFS and 0.600 (95% CI, 0.552 to 0.647) versus 0.636 (95% CI, 0.587 to 0.684) for OS, respectively.

When adjusting the effect of the *N/F-RAS-PTEN* classifier to age (using the 35-year cutoff) and WBC count (using the  $100 \times 10^9/L$  cutoff), the oncogenetic classifier remained the only significant prognostic covariate (EFS: HR, 3.2; 95% CI, 1.9 to 5.15;  $P < .001$ ; and OS: HR, 3.2; 95% CI, 1.9 to 5.6;  $P < .001$ ).

A limited subset of 89 patients (46 new low-risk and 43 new high-risk patients, according to this *N/F-RAS-PTEN* classifier) were evaluated for genomic immunoglobulin/TCR MRD level at time of CR achievement after the first induction course. Using the  $10^{-4}$  MRD cutoff, there was only a nonstatistically significant trend toward a

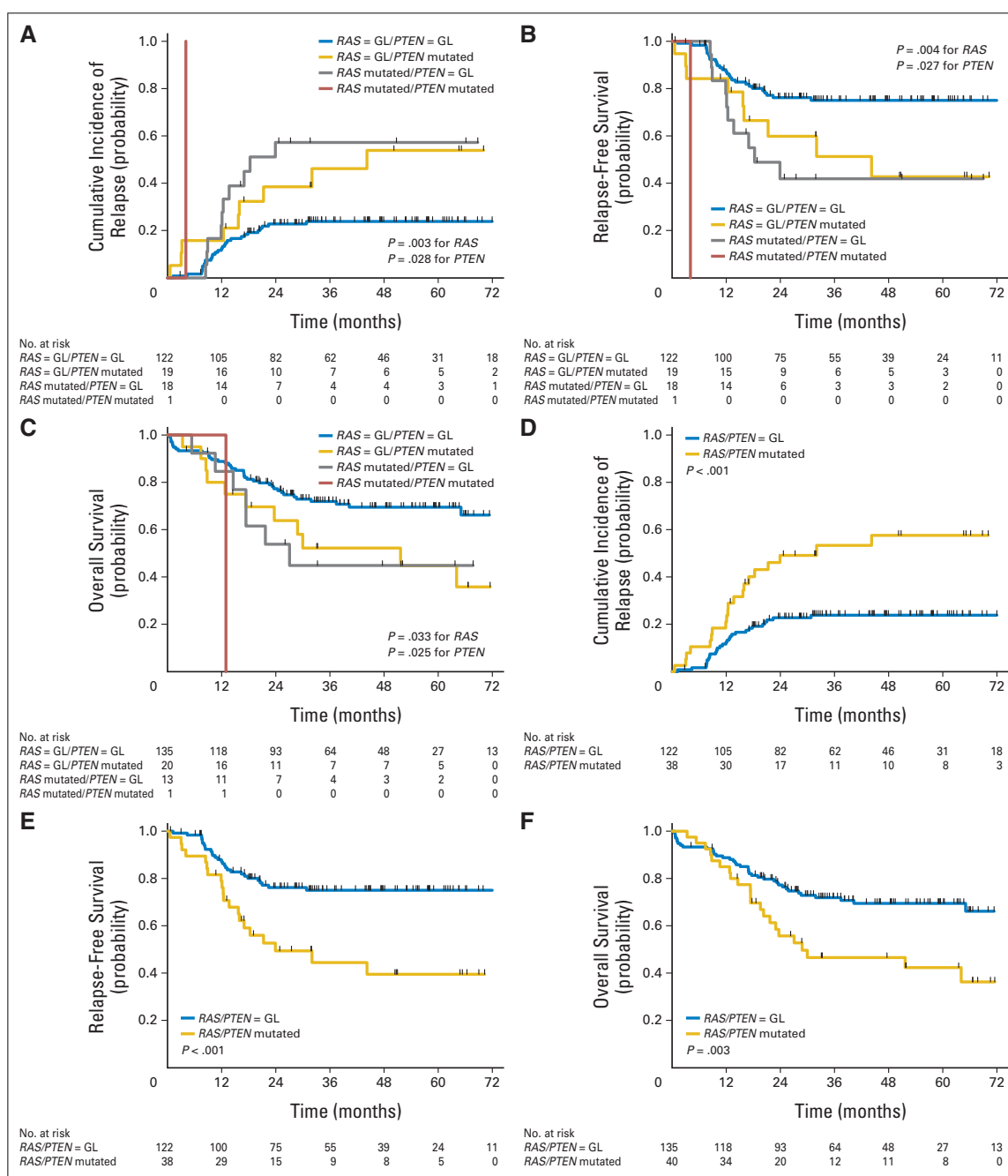


**Fig 4.** Cumulative incidence of relapse (CIR), relapse-free survival (RFS), and overall survival (OS) by *N/K-RAS* mutation or *PTEN* genomic abnormality. (A) CIR according to the presence of *N/K-RAS* mutation alone, *PTEN* genomic abnormality alone, or both (one single patient). At 5 years, CIR was estimated at 24% (95% CI, 17% to 33%) in patients with no *N/K-RAS* mutation or *PTEN* genomic abnormality, compared with 57% (95% CI, 36% to 80%) in those with *N/K-RAS* mutation and 54% (95% CI, 32% to 79%) in those with *PTEN* genomic abnormality. In the latter subgroups, the specific hazards of relapse (SHRs) were 2.6 (95% CI, 1.4 to 5.1;  $P = .003$ ) and 2.1 (95% CI, 1.1 to 4.3;  $P = .028$ ), respectively. (B) RFS according to the presence of *N/K-RAS* mutation alone, *PTEN* genomic abnormality alone, or both (one single patient). At 5 years, RFS was estimated at 75% (95% CI, 66% to 82%) in patients with no *N/K-RAS* mutation or *PTEN* genomic abnormality, compared with 42% (95% CI, 19% to 64%) in those with *N/K-RAS* mutation and 43% (95% CI, 18% to 66%) in those with *PTEN* genomic abnormality. In the latter groups, hazard ratios (HRs) for shorter RFS were 2.6 (95% CI, 1.3 to 5.0;  $P = .004$ ) and 2.2 (95% CI, 1.1 to 4.3;  $P = .027$ ), respectively. (C) OS according to the presence of *N/K-RAS* mutation alone, *PTEN* genomic abnormality alone, or both (one single patient). At 5 years, OS was estimated at 69% (95% CI, 60% to 77%) in patients with no *N/K-RAS* mutation or *PTEN* genomic abnormality, compared with 45% (95% CI, 18% to 69%) in those with *N/K-RAS* mutation and 43% (95% CI, 20% to 64%) in those with *PTEN* genomic abnormality. In the latter groups, HRs for shorter OS were 2.0 (95% CI, 1.04 to 3.8;  $P = .033$ ) and 2.0 (95% CI, 1.06 to 3.8;  $P = .029$ ), respectively. (D) CIR according to the presence of *N/K-RAS* mutation and/or *PTEN* genomic abnormality. At 5 years, CIR was estimated at 24% (95% CI, 17% to 33%) in patients with no *N/K-RAS* mutation or *PTEN* genomic abnormality, compared with 58% (95% CI, 41% to 75%) in those with *N/K-RAS* mutation and/or *PTEN* genomic abnormality. The SHR was 2.8 (95% CI, 1.5 to 4.9) in the latter group ( $P < .001$ ). (E) RFS according to the presence of *N/K-RAS* mutation and/or *PTEN* genomic abnormality. At 5 years, RFS was estimated at 75% (95% CI, 66% to 82%) in patients with no *N/K-RAS* mutation or *PTEN* genomic abnormality, compared with 40% (95% CI, 22% to 57%) in those with *N/K-RAS* mutation and/or *PTEN* genomic abnormality. The HR for shorter RFS in the latter group was 2.7 (95% CI, 1.5 to 4.8;  $P < .001$ ). (F) OS according to the presence of *N/K-RAS* mutation and/or *PTEN* genomic abnormality. At 5 years, OS was estimated at 69.5% (95% CI, 60% to 77%) in patients with no *N/K-RAS* mutation or *PTEN* genomic abnormality, compared with 42% (95% CI, 26% to 58%) in those with *N/K-RAS* mutation and/or *PTEN* genomic abnormality. The HR for shorter OS in the latter group was 2.1 (95% CI, 1.3 to 3.6;  $P = .003$ ). GL, germline.

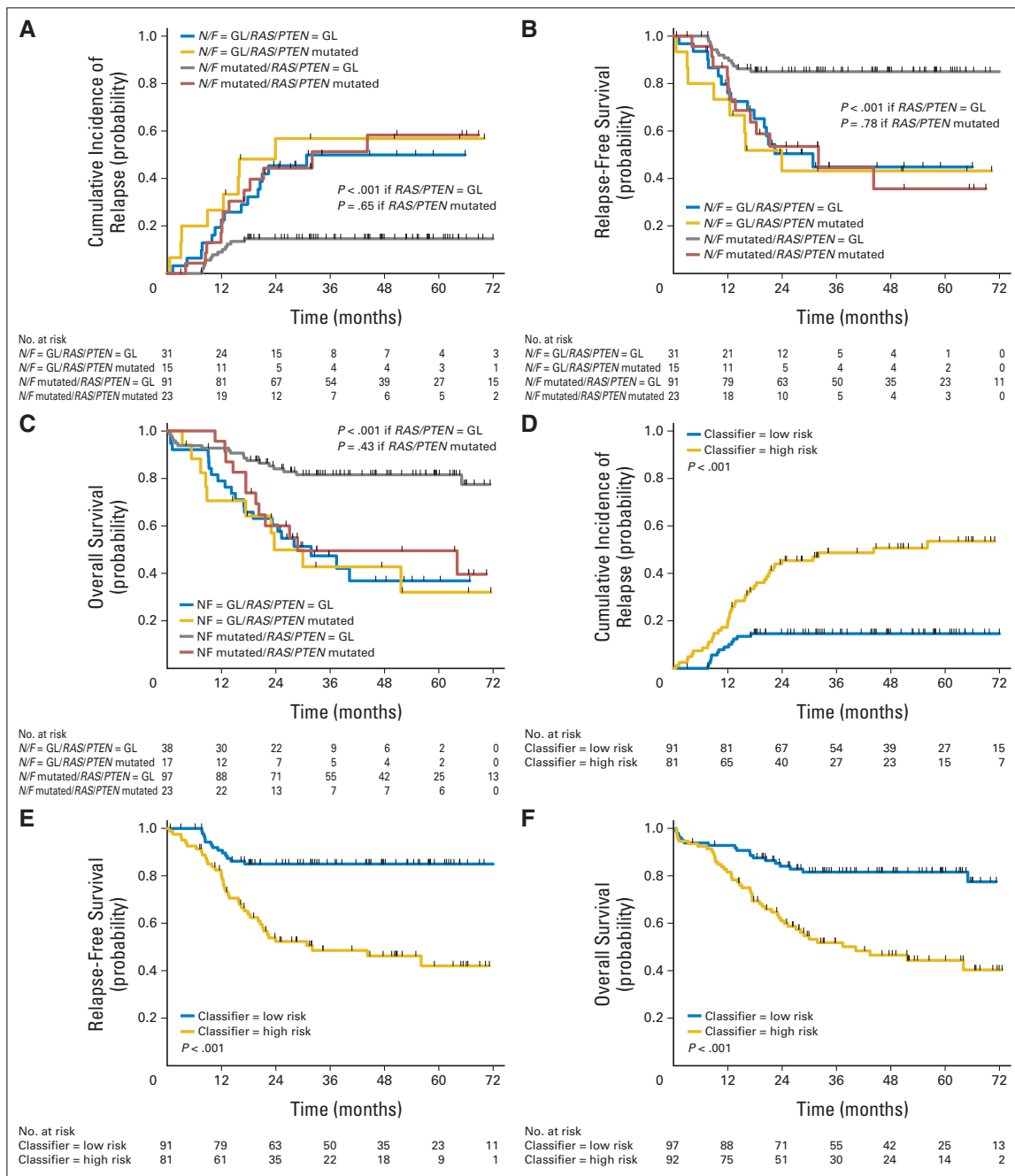


**Fig 5.** Cumulative incidence of relapse (CIR), relapse-free survival (RFS), and overall survival (OS) by *NOTCH1/FBXW7* (N/F) and *RAS/PTEN* mutational status. (A) CIR according to the presence of N/F and/or *RAS/PTEN* mutations. In patients with no N/K-RAS mutation or *PTEN* genomic abnormality, 5-year CIR was estimated at 15% (95% CI, 9% to 24%) in patients with N/F mutation, compared with 50% (95% CI, 34% to 64%) in those without N/F mutation. The specific hazard of relapse (SHR) was 3.3 (95% CI, 2.0 to 10.0) in the latter group ( $P < .001$ ). Conversely, in those with N/K-RAS mutation and/or *PTEN* genomic abnormality, 5-year CIR was similarly poor in patients with N/F mutation and in those without N/F mutation (58%; 95% CI, 37% to 80% v 57%; 95% CI, 33% to 83%, respectively). The SHR was 1.25 (95% CI, 0.5 to 3.3) in the latter group ( $P = .65$ ). (B) RFS according to the presence of N/F and/or *RAS/PTEN* mutations. In patients with no N/K-RAS mutation or *PTEN* genomic abnormality, 5-year RFS was estimated at 85% (95% CI, 76% to 91%) in patients with N/F mutation, compared with 45% (95% CI, 25% to 63%) in those without N/F mutation. The hazard ratio (HR) for shorter RFS in the latter group was 4.0 (95% CI, 2.0 to 10.0;  $P < .001$ ). Conversely, in those with N/K-RAS mutation and/or *PTEN* genomic abnormality, 5-year RFS was similarly poor in patients with N/F mutation and in those without N/F mutation (36%; 95% CI, 13% to 59% v 43%; 95% CI, 17% to 67%, respectively). The HR for shorter RFS in the latter group was 1.1 (95% CI, 0.45 to 2.5;  $P = .78$ ). (C) OS according to the presence of N/F and/or *RAS/PTEN* mutations. In patients with no N/K-RAS mutation or *PTEN* genomic abnormality, 5-year OS was estimated at 82% (95% CI, 72% to 88%) in patients with N/F mutation, compared with 37% (95% CI, 19% to 55%) in those without N/F mutation. The HR for shorter OS in the latter group was 3.3 (95% CI, 2.0 to 7.1;  $P < .001$ ). Conversely, in those with N/K-RAS mutation and/or *PTEN* genomic abnormality, 5-year OS was similarly poor in patients with N/F mutation and in those without N/F mutation (49%; 95% CI, 27% to 68% v 32%; 95% CI, 10% to 57%, respectively). The HR for longer OS in the former group was 0.7 (95% CI, 0.3 to 1.7;  $P = .43$ ). (D) CIR according to the new N/F, N/K-RAS, and *PTEN* oncogenetic classifier. At 5 years, CIR was estimated at 15% (95% CI, 9% to 24%) in low-risk patients, compared with 54% (95% CI, 42% to 66%) in high-risk patients. The SHR was 4.1 (95% CI, 2.2 to 7.7) in the latter group ( $P < .001$ ). (E) RFS according to the new N/F, N/K-RAS, and *PTEN* oncogenetic classifier. At 5 years, RFS was estimated at 85% (95% CI, 76% to 91%) in low-risk patients, compared with 42% (95% CI, 29% to 55%) in high-risk patients. The HR for shorter RFS in the latter group was 4.2 (95% CI, 2.3 to 8.0;  $P < .001$ ). (F) OS according to the new N/F, N/K-RAS, and *PTEN* oncogenetic classifier. At 5 years, OS was estimated at 82% (95% CI, 72% to 88%) in low-risk patients, compared with 44% (95% CI, 33% to 55%) in high-risk patients. The HR for shorter OS in the latter group was 3.3 (95% CI, 1.9 to 5.8;  $P < .001$ ). GL, germline.

higher MRD response rate in low-risk compared with high-risk patients (74% v 60%, respectively;  $P = .18$ ). When adjusting the effect of the *N/F-RAS-PTEN* classifier to age (using the 35-year cutoff), WBC count (using the  $100 \times 10^9/L$  cutoff), and MRD response (using the  $10^{-4}$  cutoff) in these 89 patients, the oncogenetic classifier remained the only significant prognostic factor for OS (HR, 4.8; 95% CI, 1.6 to 14.8;  $P = .006$ ).

Taken together, these data demonstrate that the detection of *RAS* and *PTEN* mutations adds significant prognostic value to assessment of the *N/F* status in isolation and allows identification of a significant proportion (48%) of good prognosis adult T-ALLs with *N/F* mutations but no *RAS/PTEN* abnormalities that cannot be identified by classical parameters.

## DISCUSSION

Much progress has been made recently toward the identification of molecular-genetic abnormalities in T-ALL.<sup>7</sup> A number of these genetic events, sometimes defined as type A mutations,<sup>20</sup> act mainly to block T-cell differentiation at a specific developmental stage and delineate T-ALL subgroups displaying specific gene expression profiles.<sup>5,6</sup> In contrast, type B mutations act by gain-of-function alterations affecting cell cycle, self-renewal, pre-TCR signaling, or constitutive tyrosine kinase activation. *RAS* and *PTEN* defects belong to this category and are involved in pre-TCR complex signaling (reviewed in Van Vlierberghe et al<sup>20</sup>), which leads to the downstream activation of both the *RAS/MAPK* and *PI3K/AKT* pathways.<sup>21</sup> There is also increasing recognition of the role played by tumor suppressor gene inactivation in T-ALL.<sup>7</sup> *PTEN* is a lipid and protein phosphatase that negatively regulates the *PI3K/AKT/mTOR* pathway through dephosphorylation of the *PIP3* lipid second messenger.<sup>22</sup> *PTEN* plays critical roles in cell growth, survival, and migration.<sup>23</sup> The *PTEN* expression level can be regulated by multiple mechanisms.<sup>23</sup> In leukemia, *PTEN* loss promotes self-renewable leukemia stem-cell formation and leukemogenesis.<sup>24</sup> Whether *PTEN* abnormalities are of prognostic value remains debated in childhood T-ALLs.<sup>15,25,26</sup> In general, *PTEN* genomic deletions are of poor prognosis, but *PTEN* mutations were reported to be without significant prognostic impact,<sup>15</sup> albeit in a small series of pediatric T-ALL. We now show that *PTEN* modification is disproportionately associated with TCR-positive, high WBC, younger adult T-ALLs that demonstrate a relatively low incidence of *N/F* mutation and poor prognosis.

Several studies have also highlighted the oncogenic role of *RAS* in leukemogenesis.<sup>27,28</sup> Oncogenic *K-RAS* and *N-RAS* mutations are described in only 2% of pediatric T-ALLs without clinical impact.<sup>29</sup> *RAS*-mutated adult T-ALLs represent 10% and tend to have more frequently an immature immunophenotype. This association has been recently suggested<sup>30</sup> and, because immature phenotypes are more frequent in adult compared with pediatric T-ALLs,<sup>31</sup> might explain the higher incidence of *RAS* mutation in our series. As such,

*RAS*- and *PTEN*-mutated patients have distinct features, in keeping with their virtually mutually exclusive occurrence.

Taken together, we have identified a significant subgroup (40 of 175 patients; 23%) of adult patients with poor prognosis T-ALL with genetic anomalies of either the *PI3K/PTEN/Akt/mTOR* or the *Ras/Raf/MEK/ERK* pathway. The intricate links in cell signaling between these pathways and the rationale for targeting both to prevent chemotherapeutic drug resistance and re-emergence of cancer-initiating cells have led to the development of specific inhibitors of these two pathways. Therefore, it was logical to regroup *RAS/PTEN*-modified T-ALLs and to develop an oncogenetic classifier of T-ALL as an extension of our previous *N/F*-based classification. Adults with *N/F*-mutated, *RAS/PTEN* germline T-ALL compose approximately 50% of patients and have an excellent prognosis. It is important to note that these new risk factors are independent from the two most important classical prognostic factors (ie, WBC count  $> 100 \times 10^9/L$  and European Group for the Immunological Classification of Leukemias class).<sup>32,33</sup> The added value of MRD assessment in these oncogenetically defined subgroups remains to be determined.

At a practical level, increasing availability of high-throughput sequencing strategies will facilitate rapid genotyping (including allelic mutation or deletion of *PTEN*) of diagnostic samples, thus allowing therapeutic stratification at an earlier stage that is possible with MRD-based stratification. These considerations are currently impacting the design of the next GRAALL T-ALL study.

## AUTHORS' DISCLOSURES OF POTENTIAL CONFLICTS OF INTEREST

*Although all authors completed the disclosure declaration, the following author(s) and/or an author's immediate family member(s) indicated a financial or other interest that is relevant to the subject matter under consideration in this article. Certain relationships marked with a "U" are those for which no compensation was received; those relationships marked with a "C" were compensated. For a detailed description of the disclosure categories, or for more information about ASCO's conflict of interest policy, please refer to the Author Disclosure Declaration and the Disclosures of Potential Conflicts of Interest section in Information for Contributors.*

**Employment or Leadership Position:** None **Consultant or Advisory Role:** Françoise Huguet, Amgen (C), ARIAD Pharmaceuticals (C), Bristol-Myers Squibb (C), Novartis (C), Pfizer (C) **Stock Ownership:** None **Honoraria:** Françoise Huguet, ARIAD Pharmaceuticals, Bristol-Myers Squibb, Novartis **Research Funding:** None **Expert Testimony:** None **Patents:** None **Other Remuneration:** None

## AUTHOR CONTRIBUTIONS

**Conception and design:** Hervé Dombret, Vahid Asnafi  
**Provision of study materials or patients:** All authors  
**Collection and assembly of data:** All authors  
**Data analysis and interpretation:** Amélie Trinquand, Vahid Asnafi  
**Manuscript writing:** All authors  
**Final approval of manuscript:** All authors

## REFERENCES

1. Pui CH, Evans WE: Treatment of acute lymphoblastic leukemia. *N Engl J Med* 354:166-178, 2006
2. Aifantis I, Raetz E, Buonamici S: Molecular pathogenesis of T-cell leukaemia and lymphoma.

*Nat Rev Immunol* 8:380-390, 2008

3. Ben Abdelali R, Asnafi V, Leguay T, et al: Pediatric-inspired intensified therapy of adult T-ALL reveals the favorable outcome of NOTCH1/FBXW7 mutations, but not of low ERG/BAALC expression: A GRAALL study. *Blood* 118:5099-5107, 2011

4. De Keersmaecker K, Atak ZK, Li N, et al: Exome sequencing identifies mutation in CNOT3 and ribosomal genes RPL5 and RPL10 in T-cell acute lymphoblastic leukemia. *Nat Genet* 45:186-190, 2013

5. Ferrando AA, Neuberg DS, Staunton J, et al: Gene expression signatures define novel oncogenic pathways in T cell acute lymphoblastic leukemia.



Cancer Cell 1:75-87, 2002

6. Soulier J, Clappier E, Cayuela JM, et al: HOXA genes are included in genetic and biologic networks defining human acute T-cell leukemia (T-ALL). *Blood* 106:274-286, 2005

7. Van Vlierberghe P, Ferrando A: The molecular basis of T cell acute lymphoblastic leukemia. *J Clin Invest* 122:3398-3406, 2012

8. Zhang J, Ding L, Holmfeldt L, et al: The genetic basis of early T-cell precursor acute lymphoblastic leukaemia. *Nature* 481:157-163, 2012

9. Weng AP, Ferrando AA, Lee W, et al: Activating mutations of NOTCH1 in human T cell acute lymphoblastic leukemia. *Science* 306:269-271, 2004

10. O'Neil J, Grim J, Strack P, et al: FBW7 mutations in leukemic cells mediate NOTCH pathway activation and resistance to gamma-secretase inhibitors. *J Exp Med* 204:1813-1824, 2007

11. Rowe JM, Buck G, Burnett AK, et al: Induction therapy for adults with acute lymphoblastic leukemia: Results of more than 1500 patients from the international ALL trial: MRC UKALL XII/ECOG E2993. *Blood* 106:3760-3767, 2005

12. Campana D: Minimal residual disease in acute lymphoblastic leukemia. *Hematology Am Soc Hematol Educ Program* 2010:7-12, 2010

13. Huguet F, Leguay T, Raffoux E, et al: Pediatric-inspired therapy in adults with Philadelphia chromosome-negative acute lymphoblastic leukemia: The GRAALL-2003 study. *J Clin Oncol* 27:911-918, 2009

14. Bonnet M, Loosveld M, Montpellier B, et al: Posttranscriptional deregulation of MYC via PTEN constitutes a major alternative pathway of MYC activation in T-cell acute lymphoblastic leukemia. *Blood* 117:6650-6659, 2011

15. Gutierrez A, Sanda T, Grebliunaite R, et al: High frequency of PTEN, PI3K, and AKT abnormali-

ties in T-cell acute lymphoblastic leukemia. *Blood* 114:647-650, 2009

16. Kaplan EL, Meier P: Nonparametric estimation from incomplete observations. *J Am Stat Assoc* 53:457-481, 1958

17. Cox D: Regression models and life tables. *J R Stat Soc B* 34:187-220, 1972

18. Gönen M, Heller G: Concordance probability and discriminative power of proportional hazards regression. *Biometrika* 92:965-970, 2005

19. Asnafi V, Buzyn A, Le Noir S, et al: NOTCH1/FBXW7 mutation identifies a large subgroup with favorable outcome in adult T-cell acute lymphoblastic leukemia (T-ALL): A Group for Research on Adult Acute Lymphoblastic Leukemia (GRAALL) study. *Blood* 113:3918-3924, 2009

20. Van Vlierberghe P, Pieters R, Beverloo HB, et al: Molecular-genetic insights in paediatric T-cell acute lymphoblastic leukaemia. *Br J Haematol* 143:153-168, 2008

21. Germain RN, Stefanová I: The dynamics of T cell receptor signaling: Complex orchestration and the key roles of tempo and cooperation. *Annu Rev Immunol* 17:467-522, 1999

22. Leslie NR, Downes CP: PTEN: The down side of PI 3-kinase signalling. *Cell Signal* 14:285-295, 2002

23. Song MS, Salmena L, Pandolfi PP: The functions and regulation of the PTEN tumour suppressor. *Nat Rev Mol Cell Biol* 13:283-296, 2012

24. Guo W, Lasky JL, Chang CJ, et al: Multi-genetic events collaboratively contribute to Pten-null leukaemia stem-cell formation. *Nature* 453:529-533, 2008

25. Bandapalli OR, Zimmermann M, Kox C, et al: NOTCH1 activation clinically antagonizes the unfavorable effect of PTEN inactivation in BFM-treated

children with precursor T-cell acute lymphoblastic leukemia. *Haematologica* 98:928-936, 2013

26. Zuurbier L, Petricoin EF 3rd, Vuerhard MJ, et al: The significance of PTEN and AKT aberrations in pediatric T-cell acute lymphoblastic leukemia. *Haematologica* 97:1405-1413, 2012

27. Parikh C, Subrahmanyam R, Ren R: Oncogenic NRAS rapidly and efficiently induces CMML- and AML-like diseases in mice. *Blood* 108:2349-2357, 2006

28. Zhang J, Wang J, Liu Y, et al: Oncogenic Kras-induced leukemogenesis: Hematopoietic stem cells as the initial target and lineage-specific progenitors as the potential targets for final leukemic transformation. *Blood* 113:1304-1314, 2009

29. Perentesis JP, Bhatia S, Boyle E, et al: RAS oncogene mutations and outcome of therapy for childhood acute lymphoblastic leukemia. *Leukemia* 18:685-692, 2004

30. Van Vlierberghe P, Ambesi-Impombato A, Perez-Garcia A, et al: ETV6 mutations in early immature human T cell leukemias. *J Exp Med* 208:2571-2579, 2011

31. Asnafi V, Beldjord K, Libura M, et al: Age-related phenotypic and oncogenic differences in T-cell acute lymphoblastic leukemias may reflect thymic atrophy. *Blood* 104:4173-4180, 2004

32. Digel W, Schultze J, Kunzmann R, et al: Poor prognosis of prethymic phenotype acute lymphoblastic leukemia (pre-T-ALL). *Leukemia* 8:1406-1408, 1994

33. Thiel E, Kranz BR, Raghavachar A, et al: Prethymic phenotype and genotype of pre-T (CD7+/ER-) cell leukemia and its clinical significance within adult acute lymphoblastic leukemia. *Blood* 73:1247-1258, 1989

## Affiliations

Amélie Trinquand, Raouf Ben Abdelali, Etienne Lengliné, Noémie De Gunzburg, Ludovic Lhermitte, Jonathan Bond, Agnès Buzyn, Elizabeth Macintyre, and Vahid Asnafi, University Paris Descartes, Centre National de la Recherche Scientifique (CNRS) Unité Mixte de Recherche (UMR)-8147, and Assistance Publique-Hôpitaux de Paris (AP-HP), Hôpital Necker-Enfants Malades; Jérôme Lambert, UMR-S-717, Hôpital Saint-Louis, AP-HP; Kheira Beldjord, Etienne Lengliné, and Hervé Dombret, University Paris 7, Hôpital Saint-Louis, AP-HP, and Institut Universitaire d'Hématologie, EA3518, Paris; Aline Tanguy-Schmidt and Norbert Ifrah, Pôle de Recherche et d'Enseignement Supérieur L'Université Nantes Angers Le Mans, Centre Hospitalier Universitaire Angers Service des Maladies du Sang et L'Institut National de la Santé et de la Recherche Médicale (INSERM) U892, Angers; Dominique Payet-Bornet and Bertrand Nadel, Center of Immunology of Marseille Luminy, Aix-Marseille University, INSERM U1104 and Centre National de la Recherche Scientifique (CNRS) UMR-7280, Marseille; Hossein Mossafa, Laboratoire Cerba, Cergy-Pontoise; Véronique Lhéritier and Xavier Thomas, Centre Hospitalier Lyon Sud, Lyon; Françoise Huguet, Hôpital Purpan, Toulouse; Thibaud Leguay, Centre Hospitalier du Haut Lévéque, Pessac; Jean-Yves Cahn, UMR-5525 CNRS-Université Joseph Fourier, Grenoble; Caroline Bonmati, Centre Hospitalier Régional Hôpital de Brabois, Vandoeuvre Les Nancy; Sébastien Maury, Hôpital Henry Mondor, Creteil, France; Yves Chalandon, University Hospital of Geneva, Geneva, Switzerland; and André Delannoy, Hôpital de Jolimont, La Louvière, Belgium.

## Support

Supported by grants to Necker Laboratory from the Association Laurette Fugain, the Comité Départemental de la Ligue Contre le Cancer, and the Institut National du Cancer. The Group for Research in Adult Acute Lymphoblastic Leukemia (GRAALL) was supported by Grants No. P0200701 and P030425/AOM03081 from Le Programme Hospitalier de Recherche Clinique, Ministère de l'Emploi et de la Solidarité, France, and the Swiss Federal Government in Switzerland. Samples were collected and processed by the Assistance Publique-Hôpitaux de Paris Direction de Recherche Clinique Tumor Bank at Necker-Enfants Malades. AT was supported by Soutien pour la formation à la recherche translationnelle en cancérologie dans le cadre du Plan cancer 2009-2013 and Fondation pour la Recherche Médicale. J.B. was supported by a Kay Kendall Leukaemia Fund Intermediate Research Fellowship.



# TLX Homeodomain Oncogenes Mediate T Cell Maturation Arrest in T-ALL via Interaction with ETS1 and Suppression of TCR $\alpha$ Gene Expression

Saïda Dadi,<sup>1,3,9</sup> Sandrine Le Noir,<sup>1,9</sup> Dominique Payet-Bornet,<sup>3,9</sup> Ludovic Lhermitte,<sup>1</sup> Joaquin Zacarias-Cabeza,<sup>3</sup> Julie Bergeron,<sup>1</sup> Patrick Villarèse,<sup>1</sup> Elodie Vachez,<sup>3</sup> Willem A. Dik,<sup>4</sup> Corinne Millien,<sup>1</sup> Isabelle Radford,<sup>2</sup> Els Verhoeven,<sup>5</sup> François-Loïc Cosset,<sup>5</sup> Arnaud Petit,<sup>6</sup> Norbert Ifrah,<sup>7</sup> Hervé Dombret,<sup>8</sup> Olivier Hermine,<sup>1</sup> Salvatore Spicuglia,<sup>3</sup> Anton W. Langerak,<sup>4</sup> Elizabeth A. Macintyre,<sup>1,10</sup> Bertrand Nadel,<sup>3,10</sup> Pierre Ferrier,<sup>3,10,\*</sup> and Vahid Asnafi<sup>1,10,\*</sup>

<sup>1</sup>Department of Hematology, Université de Médecine Paris Descartes Sorbonne Cité, Centre National de la Recherche Scientifique (CNRS) UMR8147

<sup>2</sup>Department of Cytogenetics, Université Paris 5-Descartes

Assistance Publique-Hôpitaux de Paris, Hôpital Necker-Enfants-Malades, Paris, 75015, France

<sup>3</sup>Centre d'Immunologie de Marseille-Luminy (CIML), Institut National de la Santé et de la Recherche Médicale (Inserm U1104), CNRS UMR7280, Université de la Méditerranée, 13009 Marseille, France

<sup>4</sup>Department of Immunology, Erasmus MC, University Medical Center, 3016 Rotterdam, Netherlands

<sup>5</sup>Université de Lyon, F69000; Inserm, EVIR, U758, Human Virology Department, F-69007; Ecole Normale Supérieure de Lyon, F-69007; Université Lyon 1, F-69007, Lyon, France

<sup>6</sup>Department of Hematology, AP-HP Hôpital Armand Trousseau, Paris 75012, France

<sup>7</sup>Department of Hematology, Centre Hospitalier, Angers 49933, France

<sup>8</sup>Department of Hematology, AP-HP Hôpital St-Louis, Paris 75010, France

<sup>9</sup>These authors contributed equally to this work

<sup>10</sup>These authors contributed equally to this work

\*Correspondence: vahid.asnafi@nck.aphp.fr (V.A.), ferrier@ciml.univ-mrs.fr (P.F.)

DOI 10.1016/j.ccr.2012.02.013

## SUMMARY

Acute lymphoblastic leukemias (ALLs) are characterized by multistep oncogenic processes leading to cell-differentiation arrest and proliferation. Specific abrogation of maturation blockage constitutes a promising therapeutic option in cancer, which requires precise understanding of the underlying molecular mechanisms. We show that the cortical thymic maturation arrest in T-lineage ALLs that overexpress TLX1 or TLX3 is due to binding of TLX1/TLX3 to ETS1, leading to repression of T cell receptor (TCR)  $\alpha$  enhanceosome activity and blocked TCR-J $\alpha$  rearrangement. TLX1/TLX3 abrogation or enforced TCR $\alpha\beta$  expression leads to TCR $\alpha$  rearrangement and apoptosis. Importantly, the autoextinction of clones carrying TCR $\alpha$ -driven TLX1 expression supports TLX “addiction” in TLX-positive leukemias and provides further rationale for targeted therapy based on disruption of TLX1/TLX3.

## INTRODUCTION

Acute leukemias are characterized by a multistep oncogenic process leading to the maturation arrest and malignant transformation of a hematopoietic precursor (Pui et al., 2004). Under-

standing of the molecular mechanisms leading to this block in maturation is a prerequisite for the development of therapeutic approaches aiming to unblock differentiation of leukemic blasts (Look, 1997). Transcription factors (TFs) that are involved in the control of cell differentiation or proliferation of normal

### Significance

Targeted therapy, including abrogation of a block to cell maturation, is a promising therapeutic approach in leukemias but has so far proved difficult to implement, partly due to their multistep oncogenic nature, especially in T-ALL where few oncogenes/tumor suppressors have emerged as tangible candidates. Among T-ALL patients, aberrant expression of TLX1/TLX3 defines a large subgroup of leukemias with a cortical thymic developmental arrest. Our data show that this differentiation block is due to failure to rearrange TCR $\alpha$  and that sustained TLX expression is required for leukemic maintenance despite the acquisition of a variety of additional genetic abnormalities. Taken together, our results provide further rationale for targeted therapy based on disruption of TLX1/TLX3 in this T-ALL subset.

hematopoietic progenitors and are deregulated in acute leukemias could represent promising therapeutic targets, as described for the treatment of PML-RARA<sup>+</sup> acute promyelocytic leukemia (Degos, 1992).

Human T-lymphocyte ontogeny is a hierarchical process occurring in the thymus in which the ordered somatic recombination of V, D, and J gene segments at the TCR $\delta$ , TCR $\gamma$ , TCR $\beta$ , or TCR $\alpha$  loci determine the development into either  $\gamma\delta$  or  $\alpha\beta$  T cell lineages (Dik et al., 2005; Spits, 2002) (Figure S1 available online). Progressive lineage restriction and acquisition of T cell potential following migration from the bone marrow to the thymus involve successive differentiation steps defined by the acquisition of a number of surface molecules, including CD5, CD1a, CD34, CD3, CD4, and CD8. TCR $\delta$  rearrangement is the first to occur, at the CD5<sup>+</sup>, CD1a<sup>-</sup> CD4/8 double-negative (DN) stage, followed by concurrent TCR $\gamma$  and TCR $\beta$  rearrangements coinciding with CD1a expression (Dik et al., 2005). While the occurrence of productive TCR $\gamma$  and TCR $\delta$  rearrangements will determine the assembly of a  $\gamma\delta$  receptor, a complete productive TCR $\beta$  gene rearrangement will first allow surface expression of a pre-TCR complex formed by the assembly of the TCR $\beta$  chain with a pre-T $\alpha$  (pT $\alpha$ ) invariant chain. Pre-TCR surface expression, referred to as the  $\beta$ -selection process, is marked by arrest of TCR $\beta$  gene rearrangements and extensive cellular expansion. It is mandatory to the progression of  $\alpha\beta$  T cell precursors to the CD4/CD8 double-positive (DP) cortical thymic cell stage, and to the initiation of V $\alpha$ -J $\alpha$  rearrangements (von Boehmer et al., 1998). The TCR $\delta$  locus being interspersed between the V $\alpha$  and J $\alpha$  segments, it is deleted out during V $\alpha$ -J $\alpha$  recombination, marking definitive engagement to the TCR $\alpha\beta$  lineage. The “frontiers” of the TCR $\delta$  locus may be regarded as being defined by the 5' $\delta$ Rec and 3' $\psi$ J $\alpha$  elements, as all 5'V and 3'J $\alpha$  gene segments located outside these segments contribute to the functional repertoire of  $\alpha\beta$  T cells, including a few V $\alpha$ /V $\delta$  gene segments that occasionally recombine with J $\delta$  gene segments (Krangel et al., 1998). The TCR $\alpha$  rearrangement is a highly regulated process, in which the TCR $\alpha$  enhancer (E $\alpha$ ) plays a primary role (Bassing et al., 2003; Sleckman et al., 1997). The molecular regulation of E $\alpha$  has been intensively studied (Hawwari and Krangel, 2005; Ho et al., 1989, 1990; McMurry and Krangel, 2000). The minimal E $\alpha$  core contains binding sites for three TFs, LEF-1, RUNX1/AML1, and ETS1, which have been demonstrated to be crucial for the transcriptional and *cis*-chromatin opening activities of the so-called E $\alpha$  enhanceosome (Giese et al., 1995; Ho et al., 1989, 1990; Roberts et al., 1997).

T-ALL is a heterogeneous group of acute leukemias that are arrested at various stages of normal thymic-cell differentiation (Asnafi et al., 2003; Ferrando et al., 2002). Recognized T-ALL oncogenic events include transcriptional activation of proto-oncogenes, submicroscopic deletion of tumor suppressor genes, and activation of the Notch1 pathway by *NOTCH1* or *FBXW7* mutations (Aifantis et al., 2008). Among the various T-ALL oncogenic alterations reported to date, TCR chromosomal translocations represent a recurrent oncogenic hallmark of T-ALL (Cauwelier et al., 2006). Such translocations are generally believed to result from illegitimate V(D)J recombination events that lead to the ectopic activation of oncogenes owing to their relocation to the vicinity of potent *cis*-activating elements within the involved TCR locus.

Overexpression of the orphan homeobox (HOX) proteins TLX1 and TLX3 represents the most frequent oncogenic event due to chromosomal translocation in human T-ALL. TLX1 and TLX3 belong to the NKL subtype of HOX proteins. They contain a highly conserved homeodomain (HD) that is known to be involved in DNA and protein-protein interactions (Holland et al., 2007). In T-ALL, both proteins are associated with specific gene expression profiles, a variety of additional genetic mutations, and differentiation arrest at an early cortical stage of thymocyte maturation (Asnafi et al., 2004; Ferrando et al., 2002; Soulier et al., 2005). Physiological expression of *TLX1* and *TLX3* is restricted to embryonic development (Roberts et al., 1994; Shirasawa et al., 2000), and no specific function of these genes in the T cell lineage has been reported. Transgenic expression of human *TLX1* in mice induces an initial DN2 thymic block followed by development of aneuploid T-ALL, mitotic checkpoint defects, clonal TCR $\beta$  rearrangements, a mostly cortical phenotype, and a transcriptional profile similar to that observed in human TLX1<sup>+</sup> T-ALLs (De Keersmaecker et al., 2010). Corresponding data are not yet available for TLX3, and the molecular mechanisms underlying the observed developmental arrest in TLX1<sup>+</sup> and TLX3<sup>+</sup> T-ALLs remain elusive. We therefore undertook to determine if and how TLX oncoproteins were linked to the cortical thymic maturation arrest and what the impact of this specific oncogenic function was on the initiation, development, and maintenance of TLX<sup>+</sup> T-ALLs.

## RESULTS

### TLX-Expressing T-ALLs Undergo V $\beta$ DJ $\beta$ Rearrangements but Display a Strong Bias against V $\alpha$ -J $\alpha$ Joins

A series of 230 T-ALLs were analyzed by real-time quantitative PCR (RT-qPCR) for *TLX1* and *TLX3* expression. Applying a TCR-based classification (Asnafi et al., 2003), 52 cases were immature/uncommitted (surface (s) and cytoplasmic (c) TCR $\beta$  negative) and comprised IM0, IM $\delta$ , and IM $\gamma$  subtypes (i.e., harboring, respectively, a germline configuration of all three TCR $\beta$ ,  $\delta$ , and  $\gamma$  loci, or a TCR $\delta$ - or TCR $\gamma$ -rearranged locus, and in some cases with an incompletely rearranged DJ $\beta$  locus); 103 cases were early cortical IM $\beta$ /pre- $\alpha\beta$  and included IM $\beta$  and pre- $\alpha\beta$  subtypes (displaying V $\beta$ DJ $\beta$  rearrangement and, respectively, either a cTCR $\beta$ <sup>-</sup> or sTCR $\beta$ <sup>-</sup>/cTCR $\beta$ <sup>+</sup> phenotype); 39 cases were sTCR $\alpha\beta$ <sup>+</sup>; and 36 were sTCR $\gamma\delta$ <sup>+</sup> (of which 20 also harbored a V $\beta$ DJ $\beta$ -rearranged locus) (Table S1). Sixty-five cases (28%) demonstrated *TLX1* or *TLX3* overexpression in a mutually exclusive manner, and were henceforth referred to as TLX<sup>+</sup>. Among TLX<sup>+</sup> T-ALLs, all but one demonstrated at least one V $\beta$ DJ $\beta$  rearrangement; this included all TCR $\gamma\delta$ -expressing cases ( $p < 0.001$ ). Strikingly, none of the TLX<sup>+</sup> samples displayed a sTCR $\alpha\beta$ <sup>+</sup> phenotype, implying a uniform arrest in maturation at an early cortical cell stage, prior to TCR $\alpha$  chain expression.

To determine whether the lack of TCR $\alpha\beta$  expression in TLX<sup>+</sup> T-ALLs was due to a defect in TCR $\alpha$  gene rearrangement or TCR $\alpha$  chain expression, we analyzed, by Southern blotting and DNA PCR, the status of the TCR $\delta$  locus (which is deleted during V $\alpha$ -to-J $\alpha$  rearrangement) in 52 phenotypically matched IM $\beta$ /pre- $\alpha\beta$  T-ALLs (Asnafi et al., 2003), including 26 TLX<sup>+</sup> (13 each of TLX1 and TLX3) and 26 TLX<sup>-</sup> T-ALLs (Table 1). Remarkably,

**Table 1. TCR $\delta$  Allele Rearrangement Status in IM $\beta$ /Pre- $\alpha\beta$  TLX $^+$  (n = 26) and TLX $^-$  (n = 26) T-ALL**

Allelic Status	TLX $^+$ (n = 52)	TLX $^-$ (n = 52)	p Value
IM $\beta$ /Pre- $\alpha\beta$ T-ALL TCR $\delta$			
GL, D-D, D-J or V-D	6 (11%)	5 (10%)	ns
VDJ	37 <sup>a</sup> (71%)	10 <sup>b</sup> (19%)	< 0.001
Deletion	3 (6%)	31 (60%)	< 0.001
Translocated alleles	6 (11%)	6 (11%)	ns

See also Table S1 and Figures S1 and S2.

<sup>a</sup>Includes 15 atypical rearrangements (seven V $\alpha$ -J $\delta$ , three V $\delta$ 8-J $\delta$ 1, one V $\delta$ 6-J $\delta$ 2, and one V $\delta$ 7-J $\delta$ 1) and 20 typical rearrangements using conventional V $\delta$ 1–3 segments.

<sup>b</sup>Only one atypical rearrangement (V $\delta$ 5-J $\delta$ 1).

49 of 52 (94%) TCR $\delta$  alleles were readily detected (i.e., were not deleted) in TLX $^+$  T-ALLs compared with 21 of 52 (40%) TCR $\delta$  alleles in TLX $^-$  controls (p < 0.001). The TCR $\delta$  locus may be regarded as defined by the 5' $\delta$ Rec and 3' $\psi$ J $\alpha$  elements (Figure S1), as all functional 5'V and 3'J $\alpha$  gene segments located outside these limits were found to potentially undergo rearrangement in  $\alpha\beta$ T cells, including a few V $\alpha$ /V $\delta$  gene segments that occasionally recombine with J $\delta$  gene segments (Kranzel et al., 1998). Thorough analysis of TCR $\delta$  rearrangements in TLX $^+$  versus TLX $^-$  samples by PCR cloning and sequencing demonstrated that the majority of the former samples harbored complete V $\delta$ DJ $\delta$  joints with, intriguingly, a high proportion involving TCR $\delta$ -specific, distal 5' V $\delta$  gene segments (V $\delta$ 4–6), dual TCR $\delta$ / $\alpha$  (V $\delta$ 7, V $\delta$ 8), or even TCR $\alpha$ -specific (V $\alpha$ ) gene segments, accounting for a total of 41% of the VDJ rearranged alleles compared to only 10% in TLX $^-$  cases (Table 1). Overall, TLX1 $^+$  and TLX3 $^+$  T-ALL samples displayed no significant difference in their profiles of TCR $\delta$  locus rearrangement (data not shown). These results, coupled with the lower level of TCR $\delta$  locus deletion and absence of TCR $\alpha\beta$  expression, strongly argue for a block in V-to-J $\alpha$  rearrangement in TLX $^+$  versus TLX $^-$  T-ALL samples. As E $\alpha$  is required for optimal V $\alpha$ -to-J $\alpha$  recombination (Bassing et al., 2003; Sleckman et al., 1997), we hypothesized that E $\alpha$  activity could be compromised during the course of TLX $^+$  T-ALL leukemic transformation in humans.

### TLX $^+$ T-ALL Show Reduced Accessibility of the TCR $\alpha$ Locus

In the mouse, E $\alpha$  is occupied by dedicated TFs from the CD44<sup>lo</sup>CD25<sup>+</sup> (DN3) stage of thymocyte development onward, well before transcriptional and recombinational activation of—and, indeed, establishment of chromosomal accessibility at—the TCR-J $\alpha$ /C $\alpha$  locus, arguing that E $\alpha$  binding by TFs is dissociated from its functional activity (Hernández-Munain et al., 1999; Mauvieux et al., 2003; Spicuglia et al., 2000). In order to assess the chromosomal status of the 3' part of the TCR $\alpha$  locus, including E $\alpha$ , in human TLX $^+$  T-ALL, we used the formaldehyde-assisted isolation of regulatory elements (FAIRE) assay, which allows the isolation of nucleosome-depleted (hence, mainly accessible) genomic DNA regions (Giresi et al., 2007). Using two primary TLX $^+$  T-ALLs, we recovered large amounts of E $\alpha$ -overlapping chromosomal DNA, but the recovery of upstream DNA sequences containing the TEA promoter or the J $\alpha$ 58 or J $\alpha$ 28 segments was within the range observed for the

unrelated T-ALL repressed genes PCDHGA12 and RPIB9 (Figure 1A and data not shown). In addition, quantification of the expression by RT-qPCR demonstrated a drastic decrease (~100-fold on average) of C $\alpha$  transcripts in TLX $^+$  T-ALL compared with TLX $^-$  T-ALL (Figure 1B), corroborating microarray data on gene-expression analysis of similar leukemia samples (Ferrando et al., 2002). Finally, using chromatin-immunoprecipitation (ChIP)-on-chip assays we found that the H3K27me3 mark, a hallmark of silent chromatin, is significantly enriched in the TCR-J $\alpha$ /C $\alpha$  genomic region in TLX $^+$  T-ALL compared to TLX $^-$  T-ALL (Figures 1C and S2). In contrast, similar H3K27me3 profiles were observed in all T-ALL samples in the repressed (GATA1; H3K27me3-enriched) or activated (GAPDH; H3K27me3-depleted) control loci. Consistent with the FAIRE data of nucleosomal depletion along E $\alpha$ -containing sequences, H3K27me3 enrichment in TLX $^+$  T-ALL closely surrounded but spared this discrete region. Overall, these findings imply that the unrearranged TCR-J $\alpha$ /C $\alpha$  alleles typically found in TLX $^+$  T-ALL blasts are poorly transcribed and most likely embedded within repressive chromatin, despite localized accessibility of E $\alpha$  DNA. They further suggest that in the presence of TLX, E $\alpha$  is unable to confer chromosomal accessibility to the adjacent genomic regions, notably the TCR TEA/J $\alpha$ -containing region.

### TLX1 and TLX3 Repress E $\alpha$ Activity via Their Homeodomain

To further test the possibility that the TLX1 and TLX3 proteins interfere with E $\alpha$  transcriptional activity, we used an E $\alpha$ -dependent reporter that expressed chloramphenicol acetyl transferase (E $\alpha$ -CAT). We found that ectopic expression of either GFP-TLX1 or GFP-TLX3 repressed E $\alpha$ -CAT expression by approximately 6-fold, and that this expression was partly rescued by the co-expression of TLX1 or TLX3 siRNA, respectively (Figure 2A). We therefore evaluated the level of E $\alpha$ -CAT repression exerted by TLX1 and TLX3 mutants with or without their HD (HD $^+$  and HD $^{\text{del}}$ , respectively), in reference to that of the corresponding full-length (FL) proteins. As shown in Figure 2B, both TLX1 HD $^{\text{del}}$  and TLX3 HD $^{\text{del}}$  exerted a reduced repressive activity compared with their respective full-length (FL) proteins. Conversely, TLX1 HD $^+$  exerted an activity roughly equivalent to FL TLX1, whereas TLX3 HD $^+$  retained about half the repressive effect of FL TLX3. We exclude the possibility that the reduced repression activity by TLX1 HD $^{\text{del}}$  and TLX3 HD $^{\text{del}}$  was due to their lack of nuclear localization by demonstrating that both predominantly localized to the nucleus (Figures 2C and 2D). We conclude that TLX1 and TLX3 repress E $\alpha$  transcriptional activity primarily in an HD-dependent manner.

### TLX1 and TLX3 Exert Their E $\alpha$ Repressive Activity by Interacting with ETS1

The E $\alpha$ -mediated transcriptional activity depends on the cooperative binding of the ETS1 and RUNX1 TFs to E $\alpha$ , together with the lymphoid-specific HMG domain protein LEF1. To test whether TLX1/TLX3-mediated E $\alpha$  repression is ETS1, RUNX1, or LEF1 dependent, we repeated the reporter assays and removed each TF individually. The fact that E $\alpha$ -CAT expression was not totally abolished in the absence of any one of these TFs (Giese et al., 1995) makes it possible to quantify repression of the residual activity after individual TF removal. In these conditions,



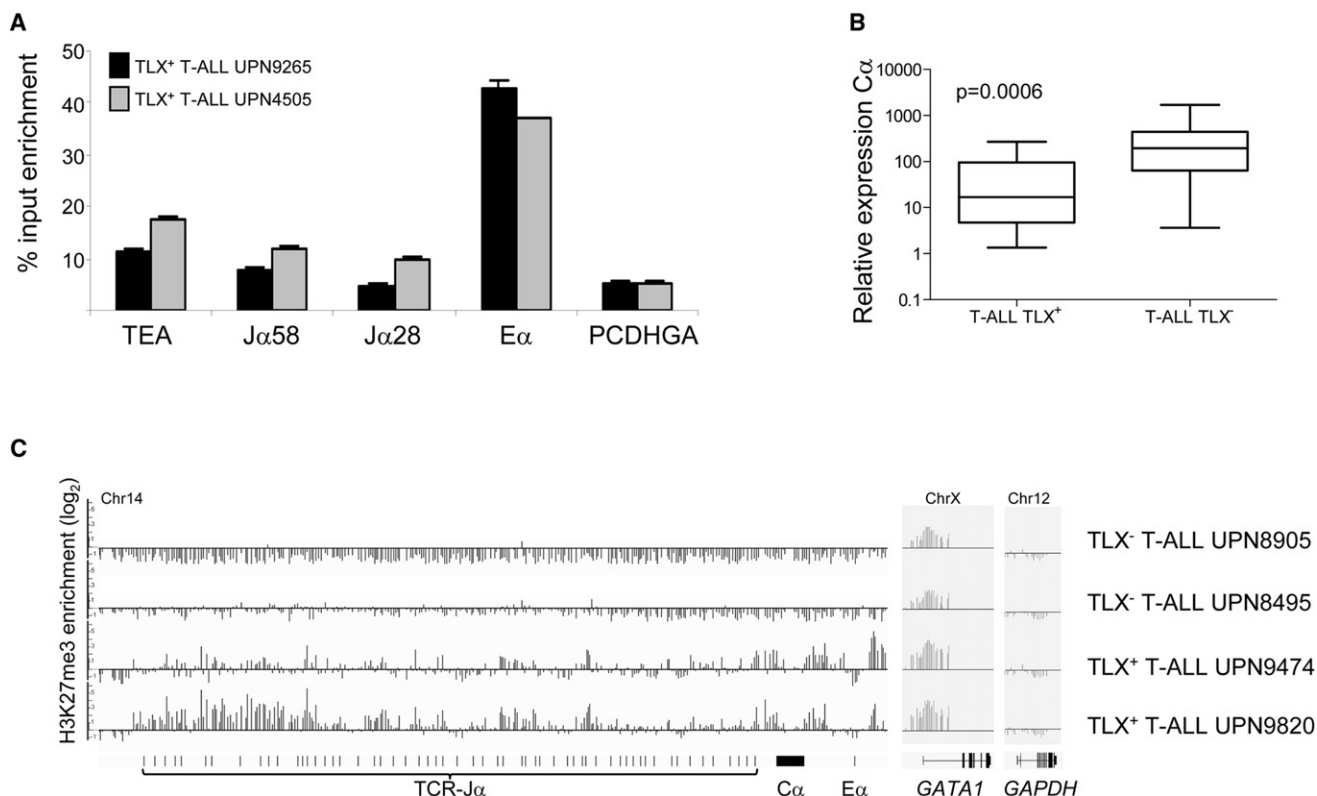


**Figure 1. TLX<sup>+</sup> T-ALLs Show Reduced Accessibility of the TCR $\alpha$  Locus**

(A) Graph showing formaldehyde-assisted isolation of regulatory elements (FAIRE) signals on two TLX<sup>+</sup> T-ALL primary cell samples (UPN, unique patient number), as assessed in using RT-qPCR and TEA, J $\alpha$ 58-, J $\alpha$ 28-, E $\alpha$ -, or PCDHGA (a gene not expressed in T cells)-specific primers. Data represent means of duplicate measurements whereby amplification signals were normalized to those of the corresponding input DNA with error bars to represent  $\pm$ SD.

(B) Box plots for relative TCR-C $\alpha$  gene expression normalized to housekeeping gene Abelson1 (ABL) in phenotypically matched TLX<sup>+</sup> (n = 23) and TLX<sup>-</sup> (n = 18) T-ALLs, as assessed by RT-qPCR.

(C) Plots of ChIP-on-chip signals for H3K27me3 relative enrichment in two TLX<sup>+</sup> and two TLX<sup>-</sup> T-ALL cell samples. Black horizontal lines represent the no-change lines. Black vertical bars indicate H3K27me3 peaks. The positions of the TCR-J $\alpha$ , C $\alpha$ , and E $\alpha$  genomic regions, as well as those of exons and upstream promoter sequences in the silent (GATA1) and expressed (GAPDH) control genes are indicated (exons depicted as vertical traits or black boxes). All four T-ALL samples harbor at least one unrearranged TCR $\alpha$  allele (not shown).

See also Figure S2.

the omission of ETS1 and, to a lesser extent, RUNX1, but not LEF1, diminished TLX1/TLX3-mediated E $\alpha$ -CAT repression (Figure 2E). We also found that serial diminution of transfected ETS1-expression vector led to a progressive decrease of TLX/TLX3-mediated repression (Figure 2F). Altogether, our data imply that TLX1/TLX3-mediated repression occurs mostly via ETS1.

We therefore carried out in vitro GST-pull-down assays and found that immobilized TLX1 and TLX3 retained the ETS1 FL protein but not LEF1 (Figure 3A). The ETS1 DNA binding domain (DBD) and the TLX1 and TLX3 HD-containing regions appeared to be most important for this interaction (Figure 3A). We further performed streptavidin precipitation experiments using HeLa cells transfected with expressing vectors encoding ETS1-HA-His, LEF1-HA, and TLX1- or TLX3-Flag-SBP tagged proteins. Precipitation of TLX1/TLX3 only retained ETS1 but not LEF1 (Figure 3B). To confirm an interaction between endogenous proteins, we carried out co-immunoprecipitation (Co-IP) using TLX1<sup>+</sup> ALL-SIL and TLX3<sup>+</sup> DND41 cell lines and anti-TLX1 or TLX3 monoclonal antibody (mAbs), which recovered both

ETS1 and the corresponding TLX in the precipitated material (Figure 3C). Finally, we investigated the subcellular localization of TLX1, TLX3, and ETS1 in TLX<sup>+</sup> T-ALL clinical samples by cell fractionation and immunostaining. Both analyses demonstrated that TLX1, TLX3, and ETS1 localize in the nucleus (Figures 4A and 4B). Moreover, both TLX<sup>+</sup> and TLX<sup>-</sup> T-ALL expressed similar amounts of ETS1 protein and RNA (Figure 4A and data not shown). Strikingly, the nuclear distribution of ETS1 was diffuse in TLX<sup>-</sup> patient leukemic cells and cell lines (Figure 4B) but was irregular in TLX<sup>+</sup> nuclei and overlapped significantly with that of the TLX proteins (Figure 4C; see figure legend for statistical information). Using ALL-SIL, we showed that, as anticipated, the nuclear distribution of ETS1 became more diffuse following TLX1 downmodulation (Figure 4D).

#### ETS1 Mediates TLX1 and TLX3 Recruitment to E $\alpha$ -Associated DNA Sequences

Given the data above in favor of an interaction between TLX1/TLX3 and ETS1 proteins impinging upon E $\alpha$  activity, we next tested whether TLX1/TLX3 directly interacts with the ETS1

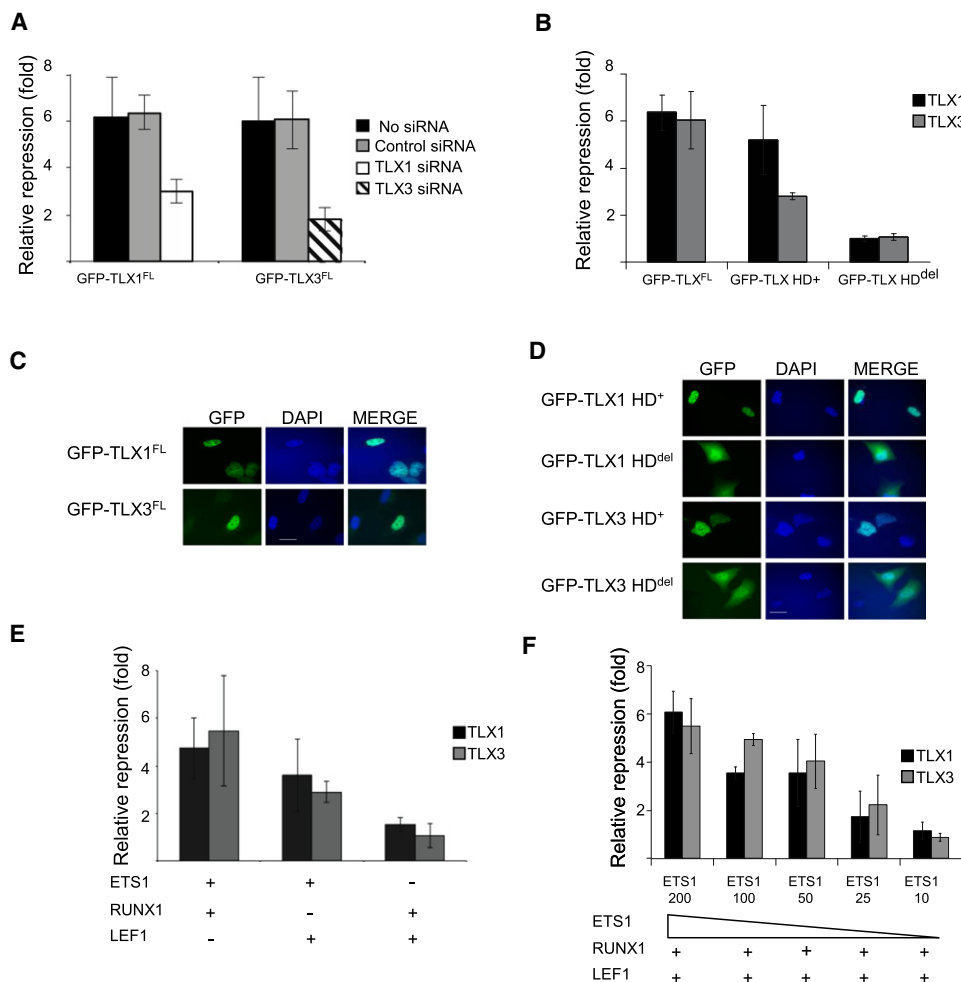


**Figure 2. TLX1 and TLX3 Repress E $\alpha$ -CAT Activity via Their Homeodomain**

(A) Graph showing E $\alpha$ -CAT fold repression in HeLa cells following transfection with GFP-TLX1<sup>FL</sup> or GFP-TLX3<sup>FL</sup> encoding vectors, with or without cotransfection of the indicated small interfering (si) RNAs. Data represent means of triplicate measurements whereby E $\alpha$ -CAT signals were normalized to those of control cells transfected with a GFP vector, with error bars to represent  $\pm$ SD.

(B) As in (A), but with HeLa cells transfected with GFP-TLX<sup>FL</sup> vectors alone, or with similar vectors carrying or lacking the corresponding TLX homeodomain (GFP-TLX HD<sup>+</sup> and GFP-TLX HD<sup>del</sup>, respectively).

(C and D) Examples of fluorescence microscopic analysis of GFP-TLX expression in transfected HeLa cells depicted in (A) and (B). White scale bar is 10  $\mu$ m.

(E) As in (A), but with HeLa cells transfected with GFP-TLX<sup>FL</sup> vectors, plus (+) or minus (-) additional vectors encoding the indicated ETS1, RUNX1, or LEF1 TFs.

(F) As in (E), but using decreasing amounts (200–10 ng) of ETS1-expression vector.

binding sequences (EBS) of human E $\alpha$ . Using electrophoretic mobility shift assays (EMSA) we observed no significant shift of the EBS probe when incubated with TLX1/TLX3 alone (Figure 5A, lanes 2–7). As expected, incubation with purified recombinant ETS1 led to a major shift of the labeled probe (Figure 5B, lane 1). Strikingly, the addition of TLX1 (lanes 2–4) or TLX3 (lanes 5–7) to ETS1 and EBS produced a dose-dependent super-shifted complex.

To ascertain E $\alpha$  occupancy by endogenous TLX1 and TLX3 in vivo, we performed ChIP assays using ALL-SIL (TLX1<sup>+</sup>), DND41 (TLX3<sup>+</sup>), and, as a control, RPMI-8412 (TLX<sup>-</sup>) cell lines. The ChIPed DNA was RT-qPCR amplified using E $\alpha$ -specific oligonucleotide primers and primers specific for the unrelated Actin gene promoter (not bound by either ETS1 or TLX TF; data not shown), used here as a mock control for data normali-

zation. As expected, anti-ETS1 enriched E $\alpha$ -associated sequences from all three cell lines (Figure 5C). In contrast, anti-TLX1 and anti-TLX3 enriched E $\alpha$ -associated sequences from only ALL-SIL and DND41, respectively, demonstrating in vivo recruitment of TLX1 and TLX3 onto E $\alpha$ . Using the DND41 and ALL-SIL cell lines, we verified that knockdown of ETS1 reduced E $\alpha$ -binding by both ETS1 and TLX1/TLX3 (Figure 5D). Taken together, these data indicate that TLX1 and TLX3 were recruited to E $\alpha$  via their interaction with ETS1 in TLX<sup>+</sup> leukemic cells.

#### TLX Downmodulation and Enforced TCR $\alpha\beta$ Expression Both Lead to Redifferentiation Linked with Massive Cell Apoptosis

Our results suggest that one of the major oncogenic functions of TLX1/TLX3 in T-ALL would be to block  $\alpha\beta$  T cell development by

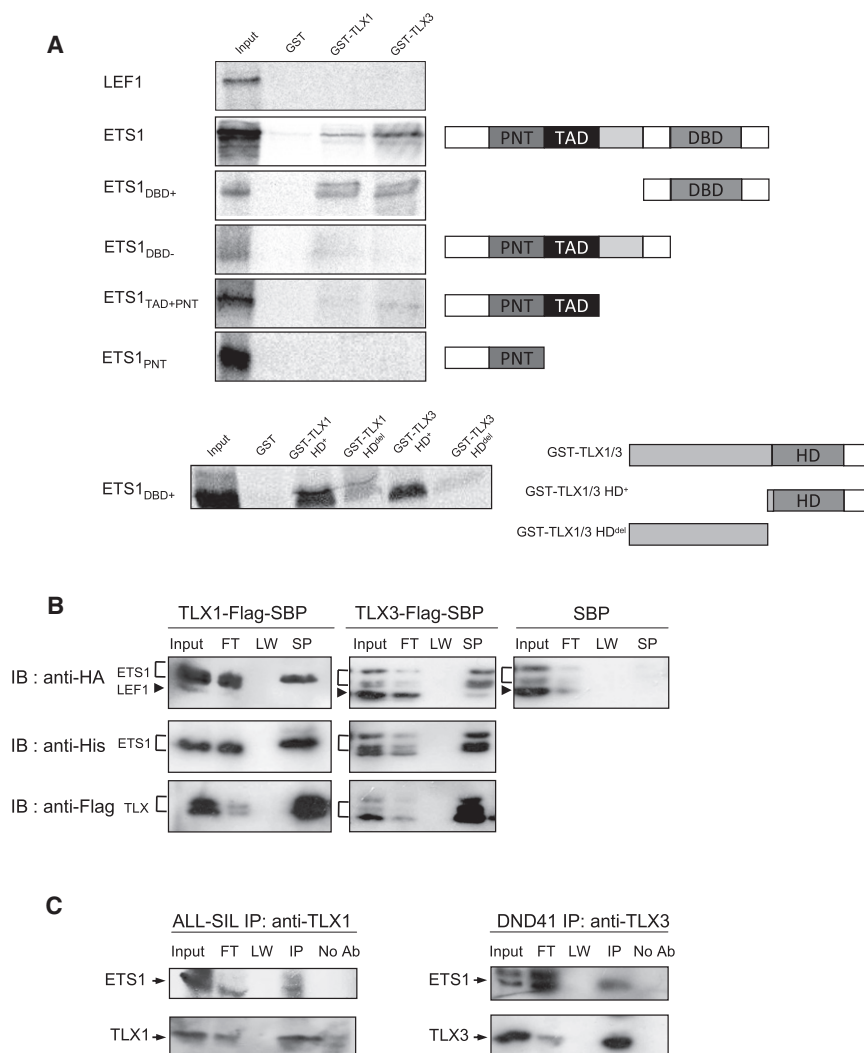


**Figure 3. TLX1 and TLX3 Interact with ETS1**

(A) GST, GST-TLX1, and GST-TLX3 pull-down of <sup>35</sup>S-labeled in vitro translated LEF1, ETS1, or truncated versions of ETS1: ETS1<sup>DBD+</sup>, ETS1<sup>DBD-</sup>, ETS1<sup>TAD+PNT</sup>, and ETS1<sup>PNT</sup>. The various versions of ETS1 are depicted on the right: PNT, pointed domain; TAD, transactivation domain; DBD, DNA binding domain. (Bottom) GST, GST-TLX<sup>HD+</sup>, and GST-TLX<sup>HDdel</sup> pull-down of <sup>35</sup>S-labeled ETS1<sup>DBD+</sup>. TLX and its truncated forms are depicted on the right: HD, homeodomain. The "Input" lanes correspond to 5% of the <sup>35</sup>S-labeled protein used for a pull-down experiment.

(B) Cell lysates from HeLa cells cotransfected with vectors expressing ETS1-HA-His, LEF1-HA, and TLX1(-or TLX3-) Flag-SBP were precipitated with streptavidin (SP) beads and then immunoblotted (IB) with either an anti-HA antibody (to reveal the fusion proteins ETS1-HA-His and LEF1-HA), an anti-His antibody (to reveal the ETS1-HA-His), or an anti-Flag antibody (to reveal TLX and to evaluate SP efficiency). Input represents 10% of cell lysate used for SP. FT, flow-through; LW, last wash.

(C) Cell lysates from ALL-SIL and DND41 cells were immunoprecipitated (IP) using anti-TLX1 (left) or anti-TLX3 (right) antibody followed by immunoblotting with indicated antibodies. The "Input" lanes correspond to 10% of cell extracts used in the Co-IP. No Ab, control IP experiment performed without antibody; FT, flow-through; LW, last wash.

inhibiting E $\alpha$  activity. To further explore this possibility, we knocked down TLX1 and TLX3 expression in ALL-SIL and DND41 cell lines, respectively. While the control cells grew normally, the knockdown TLX1/ALL-SIL and TLX3/DND41 cells demonstrated massive apoptosis (Figure 6A and 6B). Strikingly, both C $\alpha$  and TEA-C $\alpha$  transcripts, as markers of TCR-J $\alpha$  locus activation (Hernández-Munain et al., 1999; Monroe et al., 1999), were upregulated in the TLX knockdown cells (Figure 6C). Moreover, unlike transduced mock controls, the two TLX knockdown cells harbored V $\alpha$ -J $\alpha$  rearrangements, although with a restricted polyclonal pattern, as expected (Figure 6D). The knockdown cells further demonstrated a maturation shift, as shown by increased cell size and CD5 expression (Figure 6E). Most important, a small proportion of these cells became sTCR $\alpha\beta$ <sup>+</sup> (Figure 6F).

We then assessed whether such a redifferentiation process, including the triggering of cell death, could be induced by forced expression of sTCR $\alpha\beta$ , thus bypassing TLX/ETS1-mediated suppression of V $\alpha$ -J $\alpha$  rearrangement, in a TLX<sup>+</sup>/TCR<sup>-</sup> T-ALL cell line. TLX1<sup>+</sup> ALL-SIL cells were transduced using lentiviral multicistronic vectors enabling expression of GFP with or

without TCR $\beta$  and TCR $\alpha$  (Figure 6G, top). GFP<sup>+</sup> sTCR $\alpha\beta$ <sup>+</sup> ALL-SIL cells exhibited reduced viability and cell growth compared to GFP<sup>+</sup> sTCR $\alpha\beta$ <sup>-</sup> controls when cultured in the OP9-DL1 stromal-cell system (Figure 6G, bottom). This correlated with increased apoptosis of the sTCR $\alpha\beta$ <sup>+</sup> cells, as evidenced by propidium iodide (PI)/annexin V dual staining (Figure 6H; note that Jurkat cells carrying an identical sTCR $\alpha\beta$  were not affected). It is important to note that massive apoptosis was not observed when transduced cells were cultured in a stromal-cell-free standard culture system (Figures 6G and 6H). These data demonstrate the key role of TCR expression in mediating cell death in TLX<sup>+</sup> T-ALLs and strongly suggest that the apoptosis observed upon TLX inhibition is a consequence of redifferentiation.

Overall, ectopic expression of TLX1/TLX3 in cortical thymocytes appears to be required to maintain leukemic proliferation, survival, and failure to differentiate; and defect in TCR $\alpha\beta$  expression—via ETS1-mediated TLX recruitment onto E $\alpha$ —is a major mediator in oncogenic addiction, even after acquisition of a variety of additional genetic abnormalities.

Overall, ectopic expression of TLX1/TLX3 in cortical thymocytes appears to be required to maintain leukemic proliferation, survival, and failure to differentiate; and defect in TCR $\alpha\beta$  expression—via ETS1-mediated TLX recruitment onto E $\alpha$ —is a major mediator in oncogenic addiction, even after acquisition of a variety of additional genetic abnormalities.

### TCR $\alpha/\delta$ Translocations Occur 5' to TLX1 Leading to E $\alpha$ -Independent TLX1 Expression

While chromosomal translocations that lead to TLX3 deregulation in T-ALLs virtually always involve genomic partners other than TCR $\alpha/\delta$  (Bernard et al., 2001; Soulier et al., 2005), those leading to TLX1 deregulation predominantly involve TCR $\alpha/\delta$ .

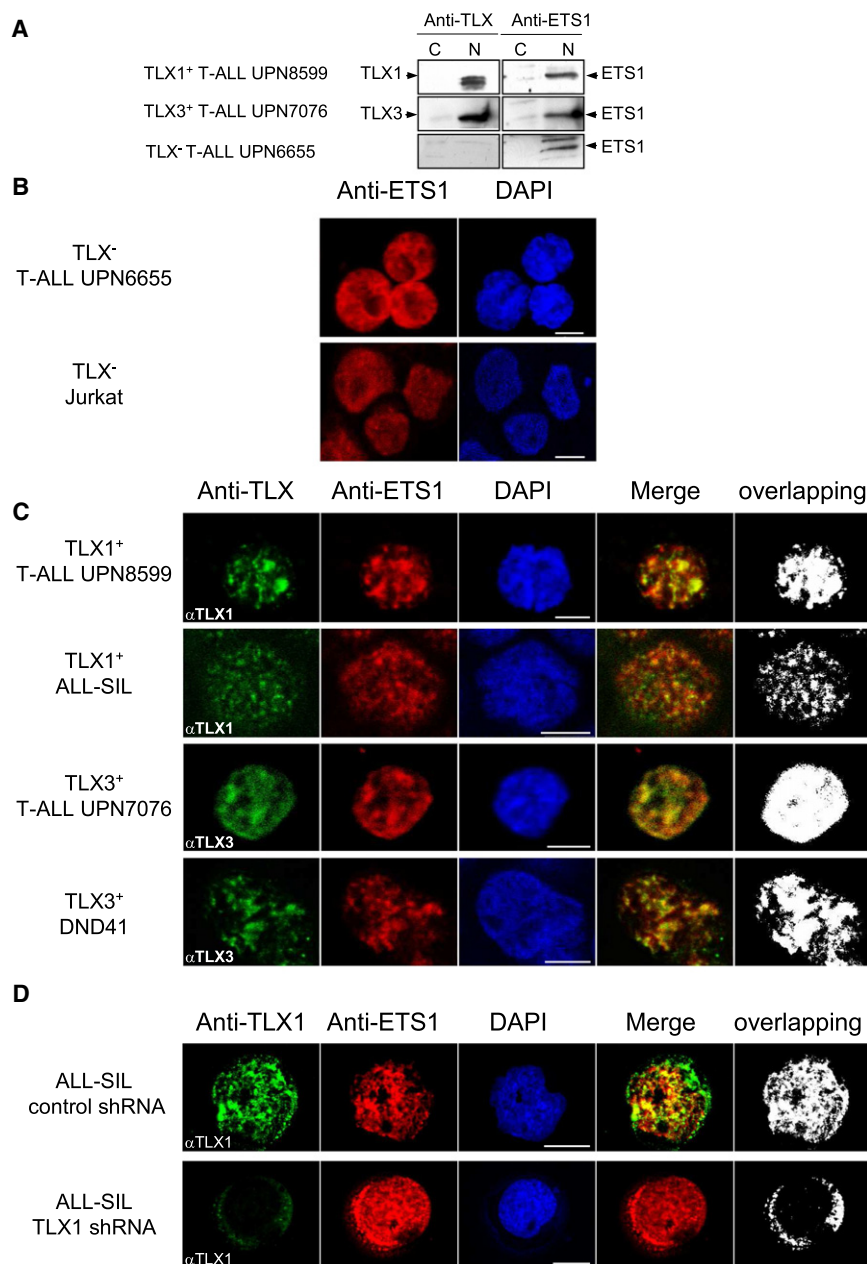


**Figure 4. TLX1, TLX3 and ETS1 Colocalize in TLX<sup>+</sup> T-ALL Blast Nuclei**

(A) Western blot analysis of cytoplasmic (C) and nuclear (N) extracts from TLX1<sup>+</sup>, TLX3<sup>+</sup>, and TLX<sup>-</sup> T-ALL cells. Blots were probed with anti-TLX and anti-ETS1 antibodies as indicated.

(B) Confocal microscopy analysis of TLX<sup>-</sup> T-ALL and cell line (Jurkat) labeled with the indicated fluorescent anti-ETS1 mAb (Alexa 647, red) or stained by DAPI.

(C) Confocal microscopy analysis of the TLX<sup>+</sup> T-ALL and cell lines ALL-SIL (TLX1<sup>+</sup>) and DND41 (TLX3<sup>+</sup>) labeled with the indicated fluorescent anti-TLX mAb (Alexa 488, green) and anti-ETS1 mAb (Alexa 647, red), or stained by DAPI. The merged images and overlapping areas (determined using ImageJ software) are also shown. Pearson's coefficients for the overlapping areas were as follows:  $r = 0.851$  (UPN480);  $r = 0.608$  (ALL-SIL);  $r = 0.929$  (UPN364); and  $r = 0.816$  (DND41). White scale bars are 5  $\mu$ m.

(D) As in (C), but the ALL-SIL cells were transduced with TLX1-specific (TLX1 small-hairpin [sh]RNA) or nonspecific (control shRNA) RNAs as indicated. White scale bars are 5  $\mu$ m.

However, if a critical oncogenic function of TLX1 is to repress E $\alpha$  activity, as supported by the data above, how could E $\alpha$  possibly provide sustained TLX1 expression if it is juxtaposed to and drives TLX1 expression? To get further insight into the mechanism of TLX1 transcriptional activation, we first analyzed its expression by RT-qPCR in 526 adult and pediatric T-ALLs and identified 61 cases as TLX1<sup>+</sup>. We then identified TLX1 translocation into either the TCR $\delta$  locus (35 cases) or the TCR $\beta$  locus (12 cases) in the 47 TLX1<sup>+</sup> cases with enough material for carrying out FISH- and/or ligation-mediated (LM) PCR analysis. All informative cases tested for allelic transcripts (12 TCR $\delta$ -TLX1 and 2 TCR $\beta$ -TLX1) demonstrated monoallelic TLX1 expression, in line with a "standard" regulatory element substitution mechanism of oncogene deregulation in cis. We mapped

the breakpoints from 8 out of 12 TCR $\beta$ -TLX1 alleles and 30 out of 35 TCR $\delta$ -TLX1 alleles (Figure S3). While all 8 breaks from TCR $\beta$ -TLX1 translocations mapped 3' to TLX1, all 30 breaks from TCR $\delta$ -TLX1 translocations mapped 5' to TLX1 (Figure 7A, top lane). Consequently, whereas TLX1 activation in TCR $\beta$ -TLX1 fusions was consistent with a classical scenario of TCR-gene-enhancer-mediated activation (in this case, the TCR $\beta$  gene enhancer E $\beta$ ; Figure 7A, middle lanes), the TCR $\delta$ -TLX1 translocations separated the TLX1 gene and E $\alpha$  element on the two derivative chromosomes (Figure 7A, bottom lanes), implying E $\alpha$ -independent activation and/or maintenance of TLX1 oncogenic expression.

To investigate whether TLX1 overexpression resulted from its juxtaposition

to a cis-regulatory element(s) within and/or upstream to the TCR $\delta$  promoter, we performed clonospecific RT-PCR across the breakpoints of both TCR $\delta$ -TLX1 and TCR $\beta$ -TLX1 translocations. Given the structure of these translocations, the detection of fusion transcripts in all the TCR $\delta$ -TLX1 samples, but not in the TCR $\beta$ -TLX1 samples (Figure 7B), was consistent with the presence of a positive regulatory element(s) within and/or upstream to the TCR $\delta$  locus that drives TLX1 overexpression.

#### E $\alpha$ Repression Results in a TLX1 Feed-Forward Repression Loop

Despite the obvious difference in the origin of TLX1 transcriptional activation in TCR $\beta$  versus TCR $\delta$  translocations, we observed no significant disparity in their levels of TLX1 expression



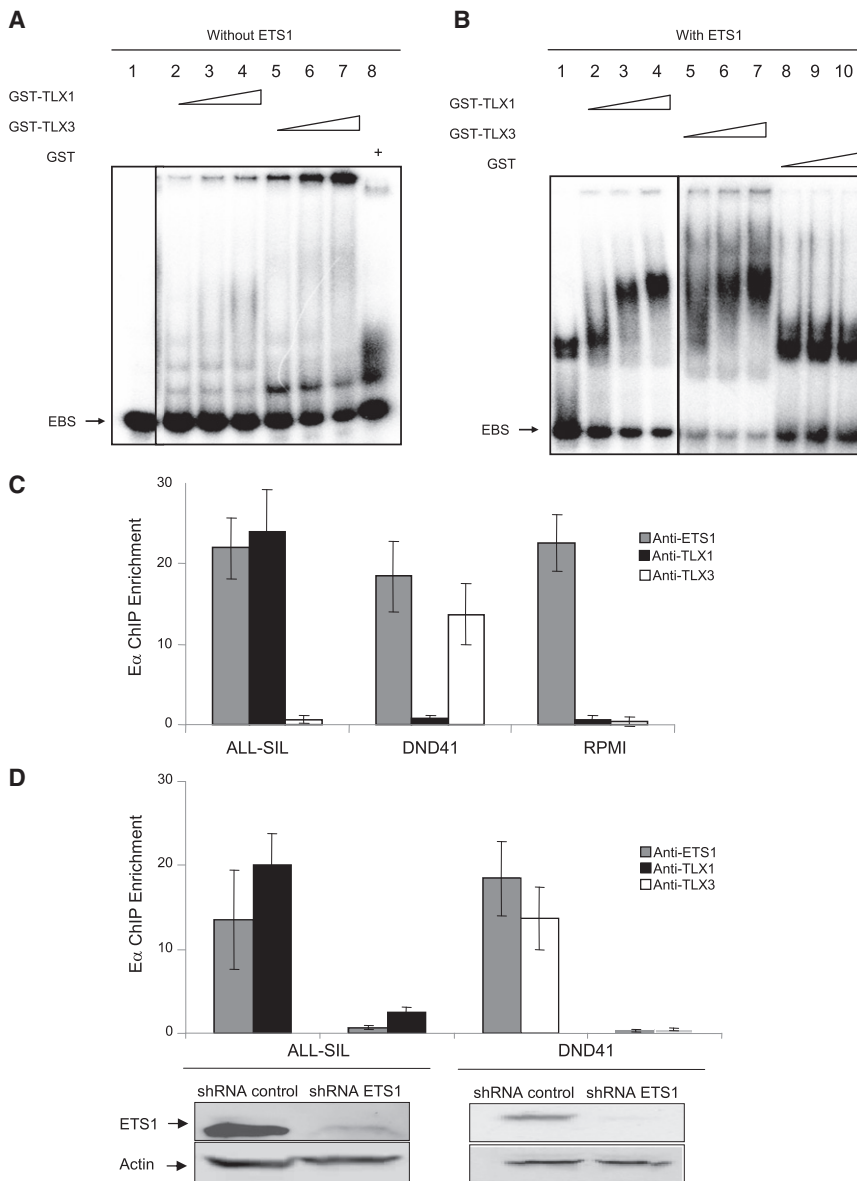


**Figure 5. ETS1 Mediates TLX1 and TLX3 Recruitment to E $\alpha$ -Associated DNA Sequences**

(A) EMSA of the  $^{32}$ P-labeled EBS oligonucleotide probe comprising core E $\alpha$  nucleotide sequences (Giese et al., 1995) with purified recombinant GST-TLX1 and GST-TLX3 proteins. Lane 1, free EBS probe; lanes 2–4 and lanes 5–7 EBS incubated with increasing amounts (10, 50, and 100 ng) of GST-TLX1 or GST-TLX3, respectively; lane 8, EBS incubated with 100 ng of GST.

(B) As in (A), but with the presence of 20 ng of purified recombinant ETS1 protein (lanes 1–7) and ETS1 with increasing amounts (10, 50, and 100 ng) of GST (lanes 8–10).

(C) Graphs of ChIP signals for E $\alpha$  from the ALL-SIL (TLX1 $^{+}$ ), DND41 (TLX3 $^{+}$ ), and RPMI (TLX $^{-}$ ) cell lines using anti-ETS1, anti-TLX1, and anti-TLX3 antibodies, as indicated. ChIPed DNA was qPCR amplified using E $\alpha$  and actin (negative-control)-specific oligonucleotide primers. Enrichment level was determined by comparison to a standard curve from input DNA. ChIPed signal enrichments correspond to the ratios between the E $\alpha$  signal and actin signal. IgG isotype control was performed to assess absence of nonspecific E $\alpha$  ChIP enrichment (not shown). Data represent means of triplicate measurements with error bars to represent  $\pm$ SD.

(D) As in (C), but with the ALL-SIL and DND41 cells transduced with ETS1-specific or nonspecific shRNAs. Shown beneath the graph are western blots for ETS1 or actin expression from mock transduced (shRNA control) and knockdown (shRNA ETS1) cells.

(data not shown). This may reflect oncogenic selection of only those rearrangements with sufficient/optimal *TLX1* expression. We also searched for possible differences in the stage of maturation arrest and/or kinetics of *TLX1* activation. TLX1 $^{+}$  T-ALLs are commonly arrested at a cortical TCR $\alpha\beta$  negative stage of maturation (Ferrando et al., 2002). In keeping with this, all TLX1 $^{+}$  T-ALL cases (whether *TCR $\delta$*  or *TCR $\beta$*  translocated) display a uniform cortical CD1a $^{+}$ /CD34 $^{neg}$  phenotype (Asnafi et al., 2003; Ferrando et al., 2002). Furthermore, sequence analysis demonstrated that both *TCR $\delta$*  and *TCR $\beta$*  translocations occurred at a similar stage of early thymic-cell differentiation with respect to rearrangement events, since all *TCR $\delta$* - and *TCR $\beta$* -*TLX1* junctions resulted from repair mistakes introduced during, respectively, a D $\delta$ 2-D $\delta$ 3 (or D $\delta$ 3-J $\delta$ 1) rearrangement, or a D $\beta$ -J $\beta$  rearrangement (Figure S3). These data further implied that *TLX1* oncogenic activation uniformly took place at an imma-

ture DN/CD1a $^{+}$ /CD34 $^{+}$  stage of thymic cell development, while cell maturation arrest occurred at a later (cortical) stage.

We therefore hypothesized that 3' *TCR $\delta$* -*TLX1* translocations do not undergo oncogenic selection because of a feed-forward inhibitory effect exerted by TLX1 itself, inducing autorepression of E $\alpha$  transcriptional activity. This would

infer that TCR $\alpha/\delta$  driven translocations with 3' *TLX1* breakpoints could occur but would fail to be selected within an oncogenic context. As several examples of potentially oncogenic TCR translocations have previously been reported in healthy thymus (Dik et al., 2007; Marculescu et al., 2003, 2006), we searched normal thymus for putative *TCR $\delta$* -*TLX1* translocations with breakpoints involving either side of *TLX1* (Figure 7C, top lanes). We set up a highly sensitive double-nested qPCR allowing the recovery of rare translocation events ( $10^{-8}$ – $10^{-9}$ ) and applied this assay to screen the DNA equivalent of  $10^9$  thymocytes from 10 healthy postnatal thymus. Even though no 5' type junction was observed, two 3' type junctions were reliably detected (Figure 7C, bottom lanes). This demonstrates that 3' type *TCR $\delta$* -*TLX1* translocations do occur in the normal thymus and are at least no less common than 5' translocations. The main difference between the 3' *TCR $\beta$* -*TLX1* translocations observed in T cell

leukemias and the 3' *TCR $\delta$ -TLX1* exclusively found in nonleukemic thymi consists in their association with the E $\beta$  or E $\alpha$  element, respectively. Given the aforementioned inhibition of E $\alpha$  activity by TLX1, these data support the intriguing possibility that deregulation of *TLX1*, when driven by E $\alpha$ , will lead not to oncogenic selection but rather to autonomous counterselection of the chromosomal translocation due to feed-forward repression (Figure 7D).

## DISCUSSION

HOX proteins in general, and TLX in particular, exert a repressive activity on transcriptional events during embryonic development (Mann et al., 2009; Merabet et al., 2005; Owens et al., 2003; Shen et al., 2001). Our study identifies TCR E $\alpha$  as a target for such a repressive activity upon ectopic expression in T cell development, offering molecular insight into the stage of maturation arrest and oncogenesis of TLX<sup>+</sup> T-ALLs.

The onset of V(D)J recombination is primarily regulated at the level of chromatin and access of the RAG1/RAG2 recombinase apparatus to its DNA targets, a process that depends on the activity of transcriptional enhancers in TCR and Ig loci, including E $\alpha$  and E $\delta$  in the TCR $\alpha/\delta$  locus (Krangel et al., 1998). Our data pinpoint a suppressive chromatin configuration around E $\alpha$  and a molecular explanation to the strong bias against V $\alpha$ -to-J $\alpha$  rearrangement observed in TLX<sup>+</sup> T-ALLs. The TCR $\alpha$  repressed structure appears to specifically affect the TEA/J $\alpha$ -containing region, since in cases where unrearranged TCR $\alpha/\delta$  alleles could be analyzed for H3K27me<sub>3</sub>, the proximal, 3' part of the TCR-V $\alpha$  locus behaved similarly in TLX<sup>+</sup> and TLX<sup>-</sup> blasts (Figure S2). Although proximal V $\alpha$  segments lie within the range of long-distance chromatin regulation by E $\alpha$ , an active, derepressed chromatin configuration would be expected at these sequences in early cortical thymocytes due to the activity of the nearby E $\delta$  (Hawwari and Krangel, 2005). In short, the aberrant TCR $\alpha/\delta$  recombination patterns seen in TLX<sup>+</sup> T-ALL faithfully mirror the chromatin opening function that exclusively relies on E $\alpha$ .

We have identified the ETS1 TF as a mediator, via protein-protein interaction, of this E $\alpha$ -suppressing function of TLX1/TLX3. There is precedent for inhibition of a cell-developmental pathway by ETS1, MafB-ETS1 interaction having been reported to result in a block to erythroid differentiation (Sieweke et al., 1996). The precise mechanisms for the repression by TLX remain to be elucidated, but our current data provide interesting clues. Recruitment of both TLX and ETS1 onto E $\alpha$  render unlikely a basic model whereby TLX sequesters ETS1 away from the enhanceosome; however, more complex, locally induced, opposing molecular switches dependent on the nature of ETS1-interacting TF partners could not be excluded (Sieweke et al., 1996). Likewise, our unpublished findings that TLX1/TLX3 still suppresses transcription on cell treatment with a histone deacetylase (HDAC) inhibitor suggest that HDAC is not involved. The creation of a distinct heterochromatin-promoting complex is plausible, since HOX proteins have been shown to fix polycomb (PcG) repressive components (Papp and Müller, 2006). Our finding of H3K27me<sub>3</sub> enrichment along E $\alpha$ -flanking genomic regions in TLX<sup>+</sup> T-ALL supports this, as H3K27me<sub>3</sub>, in addition to being a marker of repressive chromatin, is associated with activity of the PcG complex PRC2

(Sauvageau and Sauvageau, 2008). This suppressive function for TLX on E $\alpha$  activity via ETS1 does not exclude protein-protein interaction with and mediation of a suppressive effect by, other TFs, such as RUNX1 (Hollenhorst et al., 2009).

ETS1 plays an important role in cell developmental controls and neoplastic processes (Dittmer, 2003). TLX1/TLX3 overexpression would therefore be expected to deregulate multiple biological networks via its interaction with ETS1. The TLX1/TLX3-ETS1-mediated E $\alpha$  inhibition described here unlikely would explain the whole T-ALL oncogenic program induced by TLX1/TLX3, since E $\alpha$  deletion in mice has not been associated with the development of T cell leukemia (Sleckman et al., 1997) and transgenic TLX1-driven murine leukemias demonstrate a variety of somatic genetic abnormalities (De Keersmaecker et al., 2010). TLX1/TLX3-ETS1-mediated E $\alpha$  inhibition, however, likely accounts for the early cortical block in cell maturation around  $\beta$ -selection characteristic of these leukemias.

Inactivation of ETS1 impairs, but does not abolish, the development of DN3 thymic cell differentiation into DP cells and the defect appears to be specific to the  $\alpha\beta$  T cell lineage, as  $\gamma\delta$  T cells mature normally (Eyquem et al., 2004). In line with this, TLX<sup>+</sup> T-ALLs often express a TCR $\gamma\delta$ , albeit in conjunction with the cytoplasmic TCR $\beta$  chain. In this context, it is noteworthy that, despite the presence of ETS1 and RUNX binding sites within E $\beta$ , ETS1 deficiency did not affect E $\beta$  activity (Eyquem et al., 2004), pointing to different requirements for the activity of E $\beta$  and of E $\alpha$ . As mentioned, an alternative and non-mutually-exclusive candidate for mediation of the maturation arrest might be BCL11b, recently reported to be a direct target down-regulated by TLX1 (De Keersmaecker et al., 2010). Loss of BCL11b, a transcriptional repressor required for T lymphoid specification, leads, however, to a much earlier DN1/2 block (Ikawa et al., 2010; Li et al., 2000, 2004). Our data would suggest that abrogation of ETS1 activity on E $\alpha$  is more likely than loss of BCL11b to explain the cortical arrest seen in human T-ALLs. As in vivo confirmation of the capacity of TLX1 to inhibit E $\alpha$ -enhanceosome-driven transcription, we also show here that *TCR $\delta$ -TLX1* genomic products resulting from a t(10;14) translocation will lead to either a cell-maturation arrest and leukemogenesis or autoextinction of translocated clones, depending on the configuration of the translocation breakpoints. One interesting aspect of the autoextinction model is that in order to efficiently repress its own sustained expression *in-cis*, the TLX1 protein has to be produced prior to disrupting activity of the E $\alpha$  enhanceosome on the *TLX1-TCR $\delta$ /E $\alpha$*  translocated allele (Figure 7C). If so, it seems reasonable to assume that the same repression also occurs *in-trans* on the normal (nontranslocated) TCR $\alpha$  allele, leading to inhibition of TCR $\alpha$  rearrangement and a block in thymocyte differentiation. The fact that these cells do not undergo malignant transformation implies that sustained (and/or higher-level) TLX1 expression is required for leukemic transformation. Such a TLX1 "oncogene addiction" argues in favor of TLX1 being the initiating and causative oncogenic event in TLX1<sup>+</sup> T-ALL cases. This model obviously does not exclude oncogenic synergy with other abnormalities.

In line with a major role of ETS1/TLX-mediated repression of E $\alpha$  in this TLX-induced oncogenic addiction, knockdown of TLX1/TLX3 led to apoptosis, concomitant TCR $\alpha$  transcription and rearrangement, cell-maturation, and sTCR $\alpha\beta$ <sup>+</sup> expression

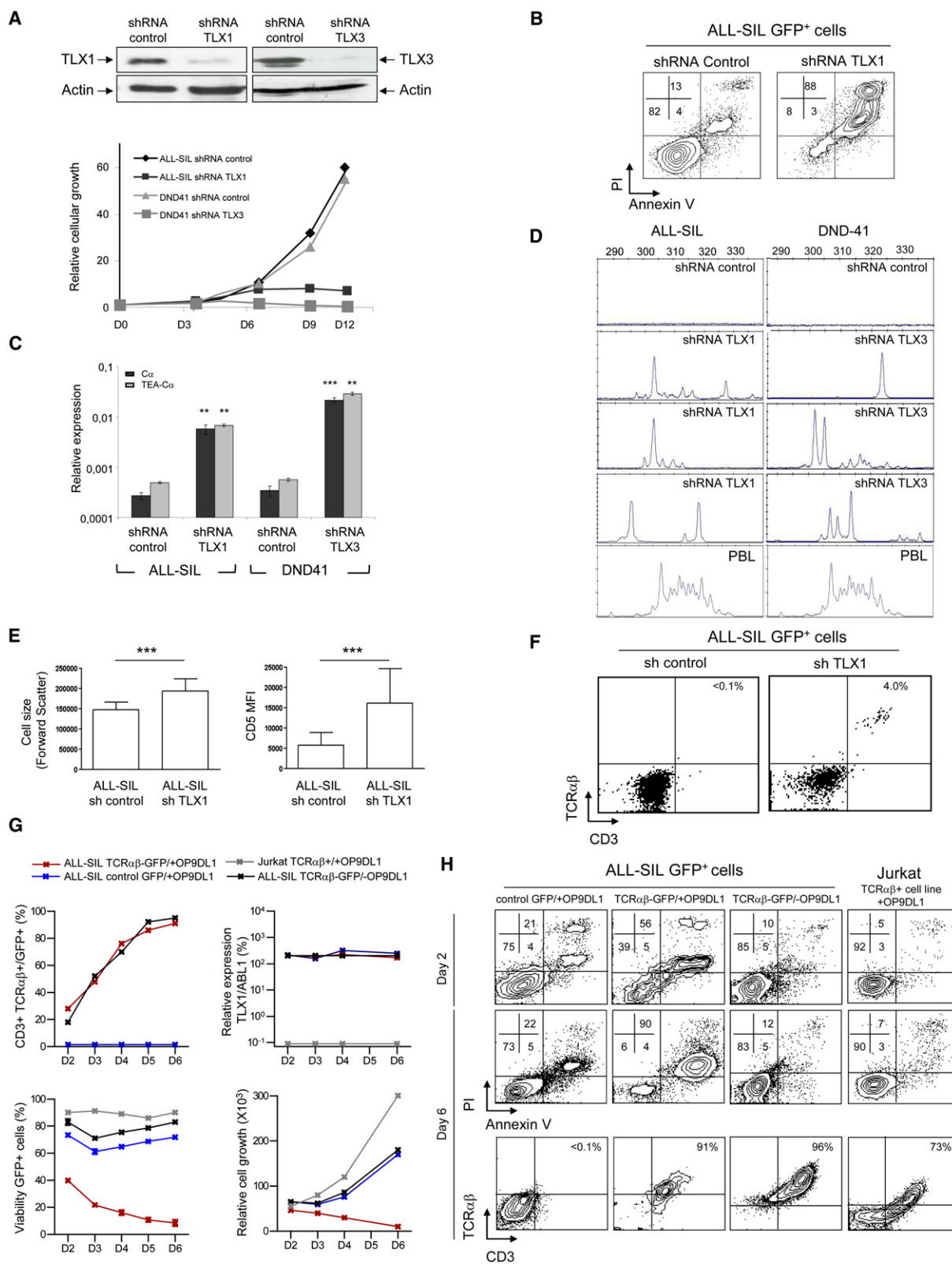


**Figure 6. Abrogation of the T Cell Maturation Block Induces Cell Death**

(A) Western blots for expression of TLX1 (top left), TLX3 (top right), and the actin control (bottom) in ALL-SIL and DND41 cells transduced with specific or nonspecific (control) shRNA. The graph shows cellular growth at days (D) 3, 6, 9, and 12 of cell culture.

in a significant proportion of cells. This implies that continuous TLX expression is required for maintenance of leukemic cell survival and blocked differentiation, and that both may be intricately linked. The fact that the apoptotic effect of TLX1 abrogation was mimicked by transducing a TCR $\alpha\beta$  transgene in TLX1/ALL-SIL cells in the presence, but not in the absence, of stroma supports these conclusions. Thus, as predicted from a bypass of the ETS1/TLX-mediated  $E\alpha$  inhibitory control, both enforced sTCR $\alpha\beta$  expression leading to exit from  $\beta$ -selection and TLX abrogation lead to a similar outcome (i.e., apoptosis). Different outcomes (cell death versus proliferation) depending on the presence or absence of OP9-DL1 stroma are likely to reflect a role for stromal (or other ligand) interaction in cell death following TCR $\alpha\beta$  expression and differentiation. In general, T cell responses require costimulation-engagement of the clonotypic TCR together with that of distinct coreceptors and cognate ligands. Our current findings offer a unique opportunity to explore such a partnership in TLX<sup>+</sup> T-ALL tumorigenesis in prospective studies.

Taken together, our results demonstrate that the maturation block observed in TLX<sup>+</sup> T-ALLs is in large part due to ETS1-mediated TLX recruitment to the  $E\alpha$  core, leading to repression of  $E\alpha$  and blocked  $V\alpha$ - $J\alpha$  rearrangement. Failure to express a TCR $\alpha$  gene arrests development of  $\alpha\beta$ -committed thymocytes around  $\beta$ -selection, when a variety of cell-proliferation signals are likely to be maintained, hence contributing to oncogenesis. This blockage can be overcome by TLX1/3 abrogation or by downstream TCR $\alpha\beta$  expression within an appropriate cellular context. These observations have fundamental consequences both for targeted therapy in TLX<sup>+</sup> T-ALLs and for the role of aberrant TCR expression in T lymphoid oncogenesis.

## EXPERIMENTAL PROCEDURES

Full Experimental Procedures and any associated references are available in the [Supplemental Experimental Procedures](#).

### Patient Analysis and Clinical Diagnosis

Diagnostic samples of peripheral blood or bone marrow from T-ALL patients included in the GRAALL or FRALLE protocols were investigated. Approval was obtained from institutional review boards of institutions participating in this study; the full list of participating centers is given in [Supplemental Experimental Procedures](#). The age cut-off between pediatric and adult cases was 18 years. All samples contained  $\geq 80\%$  blasts. Informed consent was obtained according to the declaration of Helsinki. DNA and RNA extraction and identi-

fication of TCR $\delta$ , TCR $\gamma$ , and TCR $\beta$  clonal rearrangement were identified as described ([Asnafi et al., 2003](#)).

### CAT-Reporter Assays

CAT-transactivation assays were performed as described ([Giese et al., 1995](#)).

### Streptavidin Precipitations and Immunoprecipitations

HeLa cells were cotransfected using expression vectors for ETS1-*HA-His*, LEF1-*HA*, and either TLX1-SBP-Flagx3 or TLX3-SBP-Flagx3, or the empty expression vector SBP-Flagx3 as a control. ALL-SIL (TLX1<sup>+</sup>) and DND41 SIL (TLX3<sup>+</sup>) cells were used for protein IPs. Nuclear extracts were prepared and incubated with streptavidin agarose beads or with anti-TLX1 (16F6) or anti-TLX3 (10A5) mAbs, respectively, covalently linked to protein G agarose beads. After washes, precipitated proteins were detected by western blot analysis.

### Fluorescence and Immunofluorescence Analyses

For EGFP fluorescence analysis, HeLa cells plated on coverslips were transiently transfected with EGFP-fusion constructs and further cultured for 48 hr. Imaging was performed using a Zeiss (LSM-510) confocal microscope. For immunofluorescence analysis, cell lines or primary blast cells ( $1 \times 10^5$ ) were cytospun onto glass slides. Images were obtained on a Leica TCS SP5 confocal laser scanning microscope and merged using Leica LAS AF software.

### Chromatin Immunoprecipitation

ChIPs from the ALL-SIL, DND41, and RPMI cell lines or from T-ALL samples were performed according to the Agilent protocol version 10.0 (<http://www.chem.agilent.com>), using anti-TLX1 (16F6), anti-TLX3 (10A5), anti-H3K27me3 (05851, Abcam), and anti-ETS1 (sc-350, C-20X, Santa Cruz) mAbs.

### TLX1 and TLX3 Knockdown

MISSION TRC shRNA Target Set vectors for TLX1 (TRCN0000014995), TLX3 (TRCN0000018030), and ETS1 (TRCN0000231917) were purchased from Sigma. Knockdown of the corresponding endogenous RNA transcripts was performed by transduction of the ALL-SIL and DND41 cell lines.

### Screening for TCR-TLX1 junctions

Screening for 3' type t(10;14)(q24;q11) translocations was performed using pooled thymocytes from 10 healthy children undergoing cardiac surgery.

### ACCESSION NUMBER

The ChIP-on-chip data have been deposited at ArrayExpress (<http://www.ebi.ac.uk/arrayexpress/>) with the accession number E-MEXP-3527.

### SUPPLEMENTAL INFORMATION

Supplemental Information includes one table, three figures, and Supplemental Experimental Procedures and can be found with this article online at [doi:10.1016/j.ccr.2012.02.013](#).

(B) Flow cytometric analysis of TLX1<sup>+</sup> ALL-SIL cells following transduction with retroviruses encoding the GFP protein and either control (nonspecific) or TLX1-specific shRNAs. GFP<sup>+</sup>-transduced cells were gated for analysis of AnnexinV/PI staining.

(C) RT-qPCR quantification of  $C\alpha$  and TEA- $C\alpha$  transcripts in ALL-SIL/DND41 following shRNA (TLX-specific versus mock control) transduction.  $C\alpha$  and TEA- $C\alpha$  transcript levels are shown relative to those of ABL control transcripts (\*\* $p$  value  $\leq 0.01$ ; \*\*\* $p$  value  $\leq 0.001$ ), with error bars to represent  $\pm$ SD.

(D) Multiplex RT-PCR analysis of  $V\alpha$ - $J\alpha$ - $C\alpha$  rearrangements from ALL-SIL (left) and DND41 (right) cDNA, following mock control (top) or TLX-specific (second to fourth panel pairs) shRNA transduction and 9 days of cell culture. Normal TCR $\alpha\beta$  rearranged repertoires give a Gaussian distribution of variable length  $V\alpha$ - $J\alpha$ -rearranged PCR fluorescent products, as found in normal PBLs (bottom). Abrogation of TLX1/TLX3 allows a variety of  $V\alpha$ - $J\alpha$  rearrangements.

(E) Histograms of forward scatter and CD5 mean of fluorescence of GFP<sup>+</sup> ALL-SIL cells assessed by flow cytometry, following shRNA transduction. Error bars represent  $\pm$ SD. \*\*\* $p \leq 0.001$ , Student test.

(F) Flow cytometric analysis of GFP<sup>+</sup> ALL-SIL cells for CD3 and TCR $\alpha\beta$  surface expression.

(G) Kinetics of CD3 and TCR $\alpha\beta$  surface expression (top left), and cell viability and growth (bottom), analyzed for GFP<sup>+</sup> cells in the indicated cell lines, with or without transduction of TCR $\alpha\beta$  cDNAs and with or without OP9-DL1 stromal culture conditions. RT-qPCR analysis for TLX1 transcription in Jurkat and ALL-SIL cells is also shown (top right).

(H) Top and middle cytographs are as in (B), but with the ALL-SIL cells treated as in (G). Bottom cytographs are as in (F), but with the ALL-SIL cells treated as in (G). Jurkat cells are shown as TCR $\alpha\beta$ <sup>+</sup> TLX1<sup>−</sup> controls cultured in identical conditions.



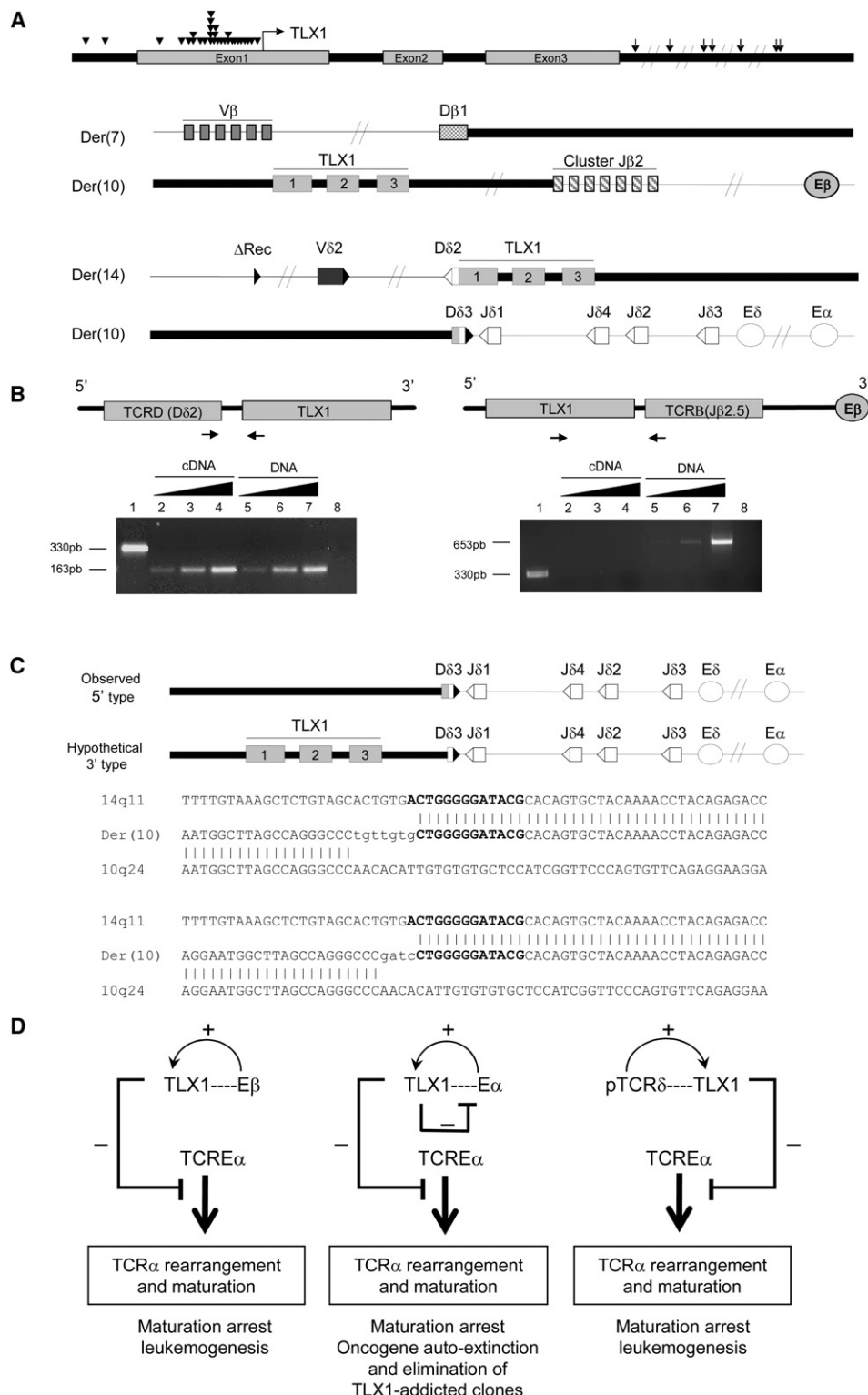


**Figure 7. Molecular Analysis of TCR $\beta$ -TLX1 and TCR $\delta$ -TLX1 Translocations**

(A) Top lane, schematic representation of the TLX1 locus (10q24). Arrowheads and arrows indicate the relative positions of breakpoints in TCR $\beta$ - and TCR $\delta$ -TLX1 translocations, respectively; middle and bottom lanes, representations of TCR $\beta$ - and TCR $\delta$ -TLX1 typical translocations. Thick and thin lines depict the 10q24 and 7q34 chromosomal regions, respectively (sequences of the TCR-TLX breakpoint junctions are reported in Figure S3).

(B) TCR $\delta$ -TLX1 translocations, but not TCR $\beta$ -TLX1 translocations, generate TCR-TLX fusion transcripts. Fusion sequences resulting from TCR $\delta$ -TLX1 translocations (left) or TCR $\beta$ -TLX1 translocations (right) are depicted and PCR primers indicated for 150 ng of cDNA amplified using TLX1-specific primers (lane 1), 15,

## ACKNOWLEDGMENTS

We thank participants in the LALA-94, GRAALL-2003/05, FRAALLE-93/2000, Dutch Childhood Oncology Group (DCOG) (project OC2001/003), and COG ALL (project #2002-09) study groups for collecting and providing biological samples and data sets. Samples were collected and processed by the AP-HP "Direction de Recherche Clinique" Tumor Bank at Necker-Enfants Malades. We are grateful to: V. Lheritier for her help in collecting clinical samples; Dr. M. Pierres (CIML) for the generation of anti-TLX1/3 mAbs; the Paris-Descartes Institute for Research at Necker-Enfants Malades (IRNEM) Cell Imaging and Cell sorting platforms; Dr. R. Grosschedl (University of Munich, Germany) for the gift of materials for TCR $\alpha$ enhCAT reporter assays; and Dr. Emmanuelle Six for cell culture assistance.

S.D. was supported by grants from the Ministère de l'Enseignement Supérieur et de la Recherche, the Fondation pour la Recherche Médicale (FRM), and the Société Française d'Hématologie (SFH). J.Z.-C. was supported by a fellowship from the Agence Nationale de la Recherche (ANR). J.B. was supported by the National Cancer Institute of Canada (NCIC), Terry Fox Foundation (TFF) award. A.W.L. and W.A.D. were supported by the Dutch Cancer Society, Grant EMCR 2002-2707. S.L.N. was supported by the Institut National du Cancer (INCa-DHOS) and a grant from the Association pour la Recherche sur le Cancer (ARC). This work was supported by grants from ARC, the Fondation de France/Comité Leucémie and Enfants et Santé, in association with the Société Française de Lutte contre les Cancers et Leucémies de l'Enfant et de l'Adolescent (SFCE). Work in the P.F. laboratory is supported by institutional grants from Inserm and CNRS, and by grants from the Commission of the European Communities, the ANR, INCa, and the Fondation Princesse Grace de Monaco. Work in the BN laboratory is supported by institutional grants from Inserm and CNRS, and grants from INCa and the Fondation de France.

S.D., S.L.N., D.P.B., L.L., E.Va., J.C.Z., P.V., and S.S. performed cellular and molecular biology experiments; W.A.D. and A.W.L. provided material and data; E.Ve. and F.L.C. provided lentiviral shRNAs; J.B., C.M., and I.R. contributed to LM-PCR and FISH analysis; A.P., N.I., H.D., and O.H. provided clinical materials and data; S.D., S.L.N., D.P.B., B.N., E.A.M., P.F., and V.A. analyzed data and wrote the manuscript; D.P.B., B.N., E.A.M., P.F., and V.A. oversaw conceptual development of the project, analyzed data, and wrote the manuscript.

Received: April 2, 2010

Revised: January 3, 2012

Accepted: February 13, 2012

Published: April 16, 2012

## REFERENCES

- Aifantis, I., Raetz, E., and Buonomi, S. (2008). Molecular pathogenesis of T-cell leukaemia and lymphoma. *Nat. Rev. Immunol.* 8, 380–390.
- Asnafi, V., Beldjord, K., Boulanger, E., Comba, B., Le Tutour, P., Estienne, M.H., Davi, F., Landman-Parker, J., Quartier, P., Buzyn, A., et al. (2003). Analysis of TCR, pT  $\alpha$ , and RAG-1 in T-acute lymphoblastic leukemias improves understanding of early human T-lymphoid lineage commitment. *Blood* 101, 2693–2703.
- Asnafi, V., Beldjord, K., Libura, M., Villarese, P., Millien, C., Ballerini, P., Kuhlein, E., Lafage-Pochitaloff, M., Delabesse, E., Bernard, O., and Macintyre, E. (2004). Age-related phenotypic and oncogenic differences in T-cell acute lymphoblastic leukemias may reflect thymic atrophy. *Blood* 104, 4173–4180.
- Bassing, C.H., Tillman, R.E., Woodman, B.B., Canty, D., Monroe, R.J., Sleckman, B.P., and Alt, F.W. (2003). T cell receptor (TCR)  $\alpha/\delta$  locus enhancer identity and position are critical for the assembly of TCR  $\delta$  and  $\alpha$  variable region genes. *Proc. Natl. Acad. Sci. USA* 100, 2598–2603.
- Bernard, O.A., Busson-LeConiat, M., Ballerini, P., Mauchauffé, M., Della Valle, V., Monni, R., Nguyen Khac, F., Mercher, T., Penard-Lacronique, V., Pasturaud, P., et al. (2001). A new recurrent and specific cryptic translocation, t(5;14)(q35;q32), is associated with expression of the Hox11L2 gene in T acute lymphoblastic leukemia. *Leukemia* 15, 1495–1504.
- Cauwelier, B., Dastugue, N., Cools, J., Poppe, B., Herens, C., De Paepe, A., Hagemeijer, A., and Speleman, F. (2006). Molecular cytogenetic study of 126 unselected T-ALL cases reveals high incidence of TCR $\beta$  locus rearrangements and putative new T-cell oncogenes. *Leukemia* 20, 1238–1244.
- De Keersmaecker, K., Real, P.J., Gatta, G.D., Palomero, T., Sulis, M.L., Tosello, V., Van Vlierberghe, P., Barnes, K., Castillo, M., Sole, X., et al. (2010). The TLX1 oncogene drives aneuploidy in T cell transformation. *Nat. Med.* 16, 1321–1327.
- Degos, L. (1992). All-trans-retinoic acid treatment and retinoic acid receptor  $\alpha$  gene rearrangement in acute promyelocytic leukemia: a model for differentiation therapy. *Int. J. Cell Cloning* 10, 63–69.
- Dik, W.A., Pike-Overzet, K., Weerkamp, F., de Ridder, D., de Haas, E.F., Baert, M.R., van der Spek, P., Koster, E.E., Reinders, M.J., van Dongen, J.J., et al. (2005). New insights on human T cell development by quantitative T cell receptor gene rearrangement studies and gene expression profiling. *J. Exp. Med.* 201, 1715–1723.
- Dik, W.A., Nadel, B., Przybylski, G.K., Asnafi, V., Grabarczyk, P., Navarro, J.M., Verhaaf, B., Schmidt, C.A., Macintyre, E.A., van Dongen, J.J., and Langerak, A.W. (2007). Different chromosomal breakpoints impact the level of LMO2 expression in T-ALL. *Blood* 110, 388–392.
- Dittmer, J. (2003). The biology of the Ets1 proto-oncogene. *Mol. Cancer* 2, 29.
- Eyquem, S., Chemin, K., Fasseu, M., and Bories, J.C. (2004). The Ets-1 transcription factor is required for complete pre-T cell receptor function and allelic exclusion at the T cell receptor  $\beta$  locus. *Proc. Natl. Acad. Sci. USA* 101, 15712–15717.
- Ferrando, A.A., Neuberg, D.S., Staunton, J., Loh, M.L., Huard, C., Raimondi, S.C., Behm, F.G., Pui, C.H., Downing, J.R., Gilliland, D.G., et al. (2002). Gene expression signatures define novel oncogenic pathways in T cell acute lymphoblastic leukemia. *Cancer Cell* 1, 75–87.
- Giese, K., Kingsley, C., Kirshner, J.R., and Grosschedl, R. (1995). Assembly and function of a TCR  $\alpha$  enhancer complex is dependent on LEF-1-induced DNA bending and multiple protein-protein interactions. *Genes Dev.* 9, 995–1008.
- Giresi, P.G., Kim, J., McDaniell, R.M., Iyer, V.R., and Lieb, J.D. (2007). FAIRE (Formaldehyde-Assisted Isolation of Regulatory Elements) isolates active regulatory elements from human chromatin. *Genome Res.* 17, 877–885.
- 75, or 150 ng of cDNA (lanes 2–4, respectively) and 1, 10, or 100 ng of genomic DNA (lanes 5–7, respectively) amplified using *TCR-TLX1* hybrid primers. The absence of genomic DNA contamination in the cDNA fractions was tested by qPCR using albumin-specific primers (lane 8).
- (C) Schematic representations of the observed 5' (Der[14]) and hypothetical 3' (Der[10]) types of *TCR $\delta$ -TLX1* translocations. The nucleotide sequences of two 3' type *TCR $\delta$ -TLX1* junctions amplified from healthy thymi are shown; N regions and D $\delta$ -specific nucleotides are indicated in bold and lowercase letters, respectively.
- (D) Model of how TLX1 addiction may drive autoselection of chromosomal translocations via *trans* repression of the *E $\alpha$*  enhanceosome. (Left) In t(7;10) translocation, TLX1 ectopic expression is driven by the TCR $\beta$  gene enhancer (E $\beta$ ), leading to *E $\alpha$*  repression and inhibition of *TCR $\alpha$*  gene rearrangement. (Right) An identical scenario occurs when TLX1 ectopic expression is driven by TCR $\delta$  regulatory elements, i.e., in a subset of t(10;14) in which TLX1 and *E $\alpha$*  are segregated on different derivative chromosomes. (Middle) In a distinct subset of t(10;14), TLX1 segregates on der(10) and is linked to *E $\alpha$* . *E $\alpha$* -driven TLX1 expression leads to *E $\alpha$*  repression and the extinction of its own expression. This form of t(10;14) can be found in the thymus from hematologically healthy individuals, but not in T-ALL samples, implying that the resulting unsustained/cyclic TLX1 expression may not be sufficient for full leukemic transformation.

See also Figure S3.

- Hawwari, A., and Krangel, M.S. (2005). Regulation of TCR  $\delta$  and  $\alpha$  repertoires by local and long-distance control of variable gene segment chromatin structure. *J. Exp. Med.* 202, 467–472.
- Hernández-Munain, C., Sleckman, B.P., and Krangel, M.S. (1999). A developmental switch from TCR delta enhancer to TCR  $\alpha$  enhancer function during thymocyte maturation. *Immunity* 10, 723–733.
- Ho, I.C., Yang, L.H., Morle, G., and Leiden, J.M. (1989). A T-cell-specific transcriptional enhancer element 3' of C  $\alpha$  in the human T-cell receptor  $\alpha$  locus. *Proc. Natl. Acad. Sci. USA* 86, 6714–6718.
- Ho, I.C., Bhat, N.K., Gottschalk, L.R., Lindsten, T., Thompson, C.B., Papas, T.S., and Leiden, J.M. (1990). Sequence-specific binding of human Ets-1 to the T cell receptor  $\alpha$  gene enhancer. *Science* 250, 814–818.
- Holland, P.W., Booth, H.A., and Bruford, E.A. (2007). Classification and nomenclature of all human homeobox genes. *BMC Biol.* 5, 47.
- Hollenhorst, P.C., Chandler, K.J., Poulsen, R.L., Johnson, W.E., Speck, N.A., and Graves, B.J. (2009). DNA specificity determinants associate with distinct transcription factor functions. *PLoS Genet.* 5, e1000778.
- Ikawa, T., Hirose, S., Masuda, K., Kakugawa, K., Satoh, R., Shibano-Satoh, A., Kominami, R., Katsura, Y., and Kawamoto, H. (2010). An essential developmental checkpoint for production of the T cell lineage. *Science* 329, 93–96.
- Krangel, M.S., Hernandez-Munain, C., Lauzurica, P., McMurry, M., Roberts, J.L., and Zhong, X.P. (1998). Developmental regulation of V(D)J recombination at the TCR  $\alpha/\delta$  locus. *Immunol. Rev.* 165, 131–147.
- Li, A., Rue, M., Zhou, J., Wang, H., Goldwasser, M.A., Neuberg, D., Dalton, V., Zuckerman, D., Lyons, C., Silverman, L.B., et al; Dana-Farber Cancer Institute ALL Consortium. (2004). Utilization of Ig heavy chain variable, diversity, and joining gene segments in children with B-lineage acute lymphoblastic leukemia: implications for the mechanisms of VDJ recombination and for pathogenesis. *Blood* 103, 4602–4609.
- Li, R., Pei, H., and Watson, D.K. (2000). Regulation of Ets function by protein-protein interactions. *Oncogene* 19, 6514–6523.
- Look, A.T. (1997). Oncogenic transcription factors in the human acute leukemias. *Science* 278, 1059–1064.
- Mann, R.S., Lelli, K.M., and Joshi, R. (2009). Hox specificity unique roles for cofactors and collaborators. *Curr. Top. Dev. Biol.* 88, 63–101.
- Marculescu, R., Vanura, K., Le, T., Simon, P., Jäger, U., and Nadel, B. (2003). Distinct t(7;9)(q34;q32) breakpoints in healthy individuals and individuals with T-ALL. *Nat. Genet.* 33, 342–344.
- Marculescu, R., Vanura, K., Montpellier, B., Roulland, S., Le, T., Navarro, J.M., Jäger, U., McBlane, F., and Nadel, B. (2006). Recombinase, chromosomal translocations and lymphoid neoplasia: targeting mistakes and repair failures. *DNA Repair (Amst.)* 5, 1246–1258.
- Mauvieux, L., Villey, I., and de Villartay, J.P. (2003). TEA regulates local TCR-Jalpha accessibility through histone acetylation. *Eur. J. Immunol.* 33, 2216–2222.
- McMurry, M.T., and Krangel, M.S. (2000). A role for histone acetylation in the developmental regulation of VDJ recombination. *Science* 287, 495–498.
- Merabet, S., Pradel, J., and Graba, Y. (2005). Getting a molecular grasp on Hox contextual activity. *Trends Genet.* 21, 477–480.
- Monroe, R.J., Sleckman, B.P., Monroe, B.C., Khor, B., Claypool, S., Ferrini, R., Davidson, L., and Alt, F.W. (1999). Developmental regulation of TCR  $\delta$  locus accessibility and expression by the TCR  $\delta$  enhancer. *Immunity* 10, 503–513.
- Owens, B.M., Zhu, Y.X., Suen, T.C., Wang, P.X., Greenblatt, J.F., Goss, P.E., and Hawley, R.G. (2003). Specific homeodomain-DNA interactions are required for HOX11-mediated transformation. *Blood* 101, 4966–4974.
- Papp, B., and Müller, J. (2006). Histone trimethylation and the maintenance of transcriptional ON and OFF states by trxG and PcG proteins. *Genes Dev.* 20, 2041–2054.
- Pui, C.H., Relling, M.V., and Downing, J.R. (2004). Acute lymphoblastic leukemia. *N. Engl. J. Med.* 350, 1535–1548.
- Roberts, C.W., Shutter, J.R., and Korsmeyer, S.J. (1994). Hox11 controls the genesis of the spleen. *Nature* 368, 747–749.
- Roberts, J.L., Lauzurica, P., and Krangel, M.S. (1997). Developmental regulation of VDJ recombination by the core fragment of the T cell receptor  $\alpha$  enhancer. *J. Exp. Med.* 185, 131–140.
- Sauvageau, M., and Sauvageau, G. (2008). Polycomb group genes: keeping stem cell activity in balance. *PLoS Biol.* 6, e113.
- Shen, W.F., Krishnan, K., Lawrence, H.J., and Largman, C. (2001). The HOX homeodomain proteins block CBP histone acetyltransferase activity. *Mol. Cell. Biol.* 21, 7509–7522.
- Shirasawa, S., Arata, A., Onimaru, H., Roth, K.A., Brown, G.A., Horning, S., Arata, S., Okumura, K., Sasazuki, T., and Korsmeyer, S.J. (2000). Rnx deficiency results in congenital central hypoventilation. *Nat. Genet.* 24, 287–290.
- Sieweke, M.H., Tekotte, H., Frampton, J., and Graf, T. (1996). MafB is an interaction partner and repressor of Ets-1 that inhibits erythroid differentiation. *Cell* 85, 49–60.
- Sleckman, B.P., Bardon, C.G., Ferrini, R., Davidson, L., and Alt, F.W. (1997). Function of the TCR  $\alpha$  enhancer in  $\alpha\beta$  and  $\gamma\delta$ T cells. *Immunity* 7, 505–515.
- Soulier, J., Clappier, E., Cayuela, J.M., Regnault, A., Garcia-Peydro, M., Dombret, H., Baruchel, A., Toribio, M.L., and Sigaux, F. (2005). HOXA genes are included in genetic and biologic networks defining human acute T-cell leukemia (T-ALL). *Blood* 106, 274–286.
- Spicuglia, S., Payet, D., Tripathi, R.K., Rameil, P., Verthuy, C., Imbert, J., Ferrier, P., and Hempel, W.M. (2000). TCRalpha enhancer activation occurs via a conformational change of a pre-assembled nucleoprotein complex. *EMBO J.* 19, 2034–2045.
- Spits, H. (2002). Development of  $\alpha\beta$  T cells in the human thymus. *Nat. Rev. Immunol.* 2, 760–772.
- von Boehmer, H., Aifantis, I., Azogui, O., Feinberg, J., Saint-Ruf, C., Zober, C., Garcia, C., and Buer, J. (1998). Crucial function of the pre-T-cell receptor (TCR) in TCR  $\beta$  selection, TCR  $\beta$  allelic exclusion and  $\alpha\beta$  versus  $\gamma\delta$  lineage commitment. *Immunol. Rev.* 165, 111–119.